Investigation of the mechanism of action of ursodeoxycholic acid on normal or inflamed epithelia *in vivo* and on the intestinal epithelial cells *in vitro*

Inaugural-Dissertation
to obtain the academic degree
Doctor rerum naturalium (Dr. rer. nat.)

submitted to the Department of Biology, Chemistry and Pharmacy
of Freie Universität Berlin

by

Santosh Krishna Subramanian

Born in Tiruchirappalli, India.

Submission: December 2010.

Time period : 17th February 2007 to 21st December 2010

Supervisor : Prof.Dr.Christoph Hanski

Institute : Department of Gastroenterology
Charité Campus Benjamin Franklin
Berlin, Germany.
Director: Prof.Dr.M.Zeitz

1st Reviewer: Prof. Dr. B. Wittig

2nd Reviewer: Prof. Dr. C. Hanski

Date of defense: 29.04.2011

Table of contents

1 Acknowledgements

I dedicate this doctoral work to certain important people who either directly or indirectly enabled me to do this Ph.D. First and foremost I consider myself very fortunate to get the doctoral training under the guidance and mentorship of Professor Dr.Christoph Hanski. He identified my potentials and analysed my lacunae. He greatly influenced and improved my research-perspective, personality, language, writing skills and hence altogether my competitiveness as a scientist.

I thank Prof.Dr.Wittig for accepting to review my doctoral work.

I thank Dr.Mandar Bhonde for introducing me to Prof.Dr.Christoph Hanski.

I thank Marie Luise Hanski for her immense contribution to my doctoral work. She helped me with my experiments, gave important suggestions and criticisms and was of moral support at various times. I thank Brittta Jebautzke who has helped me with different experiments. Not to forget her wonderful laughter. I thank Roser Peiro Jordan and Bhavesh Choudhary who were good collegues and friends. The long discussions with them in lab often led to critical thinking. They were part of our brainstorming sessions where their suggestions gave important inputs in my work. I thank Wan for her timely and ever-ready help.

I thank Prof.Dr.Loddenkemper and Dr.Kuban for their expert technical help. I thank Sandra Bauer and the members of research group of Dr. Fechner for the timely help with experimental resources. I thank René for his help with the fluorescence microscope.

My wife Kavita has been with me at all times and bearing with me during hours of stress. She bucked me up and pardoned me for spending several weekends in the lab. Her role in my life before, during and after PhD is beyond what I can write in words. I thank my father, mother and brother Venkatesh for their good wishes, prayers and constant support. My brother indirectly gave me the strength that he is there with our parents and could take the responsibility to be of support to our parents in my absence. I thank all my relatives and in-laws and specially Mr. & Mrs. S.D.Bala & Mr. & Mrs. N.Subramaniam for their special roles in my scientific career. I thank my friends in Berlin specially Raghu, Smitha, Bhavesh, Ruby, Dr.Khandare, Shyam, Katya, Tulsi, Omkar, Rashmi, Ranjit, Ashwini and others who were all integral part of my life during this PhD.

Funding and financial support

I thank DFG for funding the project. I thank Dr.Falk Pharma GmbH for donating UDCA and for providing the conference-attendance grants twice during my doctoral study. I thank Berliner Krebbsgesellschaft for giving me the scholarship during the last year of my Ph.D and also for providing conference-attendance grants thrice during my doctoral study. I also extend my thanks to Dr.Daum for the timely financial support in the last year of my Ph.D.

2 Abbreviations

ACF	Aberrant crypt foci
Adv-	Adenovirus
AOM	Azoxymethane
AP-1	Activator protein-1
BrdU	Bromo-deoxyuridine
β-galactosidase	Beta-galactosidase
C/EBPβ	CCAAT/enhancer-binding protein beta
CA	Cholic acid
cDNA	Complementary DNA
Cdx2	Causal type homeobox type-2 gene
CIP1	CDK-interacting protein 1
Cox	Cyclooxygenase
Cre	Cyclization recombination
DAPI	4',6-diamidino-2-phenylindole
DCA	Deoxycholic acid
DNA	Deoxyribonucleic acid
dn	Dominant negative
DSS	Dextran sodium sulphate
EGF	Epithelial growth factor
EGFR	Epithelial growth factor receptor
EphA2	Epinephrin A2
ERK	Extracellular regulated kinase
FACS	Fluorescence activated cell sorting
FAP	Familial adenomatous polyposis
G1	Gap-phase 1
G2	Gap-phase 2
Gbp2	Guanylate binding protein-2
GFP	Green fluorescent protein
GSH	Glutathione
h	Hours
HBSS	Hank's balanced salt solution
HisH3	Histone H3
HMG	High mobility box
HNPCC	Hereditary non-polyposis colorectal cancer
IEC-6	Intestinal epithelial cell 6
IGF-1	Insulin-like growth factor-1
IGF-1R	Insulin-like growth factor-1-receptor
IL-1β	Interleukin 1-beta
IFN-γ	Interferon gamma
Irs-1	Insulin receptor substrate-1
LOH	Loss of heterozygosity
MAPK	Mitogen activated Protein Kinase
ml	Milli litres
min	Minutes
Mdm-2	Minichromosome maintenance
MEK	Methyl ethyl ketone

min	Minutes
mGbp2	murine Guanylate binding protein-2
MTT	3-(4,5-Dimethylthiazol-2-yl)-2,5-diphenyltetrazolium bromide
NER	Nuclear excision repair
NF-κB	Nuclear factor k B
NIH3T3	National institute of health 3T3- (Cell line)
Pb(II)	Lead
PBC	Primary biliary cirrhosis
PCNA	Proliferating cell nuclear antigen
PI3K	Phospho-inositol-3 kinase
PKC	Protein Kinase C
PSC	Primary Sclerosing cholangitis
RA	Retinoic acid
Rb	Retinoblastoma
RIN	RNA integrity number
RNA	Ribonucleic acid
ROS	Reactive oxygen species
rRNA	Ribosomal RNA
RT-PCR	Reverse transcriptase - polymerase chain reaction
SDS	Sodium dodecyl sulphate
sec	Seconds
Ser10	Serine-position 10
siRNA	Small interfering RNA
SOCS3	Suppressor of cytokine signalling – 3
S-phase	Synthesis-phase
TCF4	T-cell factor-4
TGF	Transforming growth factor
TOP-FOP	Reporter assay for TCF4 targets
UC	Ulcerative colitis
UDCA	Ursodeoxycholic acid
Wnt	Wingless / Int1

3 Summary

The original objective of this work was to clarify the mechanism of the chemopreventive action of ursodeoxycholic acid (UDCA) in a DSS-colitis mice model. The secondary question was how UDCA acts upon the normal epithelium. Both DSS-colitis mice and normal mice were fed with diet containing UDCA at different concentrations for 86 days and 21 days respectively. The RNA from colonic epithelial cells was used for a microarray experiment to identify proliferation-associated genes. The changes in gene expression were confirmed by real time RT-PCR. The effect on proliferation was assayed by immunohistochemical staining of the colonic sections for Ki-67-expression and BrdU incorporation. The mechanism was investigated in detail in an *in vitro* model using IEC-6 cell line.

DSS-colitis increased the crypt length and the number of proliferating cells per crypt. The treatment of DSS-colitis mice with UDCA decreased the crypt length and the number of proliferating epithelial cells per crypt. Proliferation promoting genes like Gbp2 were identified which were upregulated in DSS-colitis mice and were brought to normal expression levels by UDCA treatment. Treatment of normal mice with UDCA did not change the crypt length but resulted in a decrease of the number of proliferating cells per crypt and decrease in the expression of many pro-proliferative genes like Tcf4, Gbp2, Klf5, Irs-1, Il-15, Ghr and Flot2.

UDCA treatment of colon cancer cells decreased proliferation and caused differential expression of genes identified in mice. The changes in gene expression in colon cancer cells were different from that observed in the mice. By contrast, proliferation of the nontransformed intestinal epithelial cell line IEC-6 was dose dependently inhibited by UDCA and the genes upregulated or downregulated in mice were similarly regulated in IEC-6 cell line. In IEC-6 cell line, Irs-1 mRNA and protein expression was strongly suppressed which decreased proliferation.

UDCA treatment of IEC-6 cells caused high and persistent phosphorylation of ERK which was associated with an inhibition of EGF- or IGF-1-induced proliferation, a slow progress through the cell cycle, decreased uptake of BrdU, transcriptional

suppression of Irs-1 and transcriptional upregulation of p21 mRNA and protein expression. Furthermore suppression of ERK1 but not of ERK2 or inhibition of phosphorylation of ERK1/ERK2 by pharmacological inhibitors, led to an increase in expression of Irs-1 and decrease in expression of p21. The inhibition of ERK-phosphorylation or suppression of ERK1 protein but not ERK2 protein abrogated the antiproliferative effects of UDCA.

It was concluded that UDCA inhibits the proliferation of normal intestinal epithelial cells by causing high and persistent ERK phosphorylation wherein an ERK1-dependent transcriptional suppression of Irs-1 and upregulation of p21 contributes to the decrease of cell proliferation.

4 Zusammenfassung

Zielsetzung:

In den Vorarbeiten der AG Hanski wurde die Inhibition der kolitisbedingten Kolonkarzinogenese durch Gabe von Ursodesoxycholsäure (UDCA) im murinen Modell der DSS-Kolitis festgestellt.

Das Ziel der vorliegenden Arbeit war es, die Mechanismen der Wirkung von UDCA auf intestinale Zellen *in vivo* und *in vitro* zu untersuchen.

Vorgehensweise:

DSS-Kolitis-Mäuse sowie normale Mäuse wurden 3 Monate bzw. 3 Wochen mit einer Standarddiät mit oder ohne UDCA Supplementierung (0,4%) gefüttert. Die Kolonepithelzellen wurden isoliert, die Genexpression wurde einer Affymetrix-Array Analyse unterzogen. Die Validierung der Genexpressionsveränderungen erfolgte mit RT-PCR. Die Proliferation *in vivo* wurde durch den immunhistochemischen Nachweis des Ki-67 Proteins bzw. des eingebauten BrdUs verfolgt. Die *in vivo* detektierten potenziellen Mechanismen wurden anhand von humanen Kolonkarzinomzelllinien sowie einer nichttransformierten intestinalen Rattenzelllinie IEC-6 im Detail untersucht.

Ergebnisse:

Die anhaltende DSS-Kolitis bewirkte die Erhöhung der Anzahl der proliferierenden Zellen pro Krypte und eine Kryptenverlängerung. Die dreimonatige UDCA-Behandlung von DSS-Kolitis-Mäusen reduzierte die Anzahl der proliferierenden Zellen pro Krypte und die Kryptenlänge. Die dreiwöchige Behandlung der normalen Mäuse hatte ebenfalls eine Inhibition der epithelialen Proliferation jedoch ohne Kryptenverlängerung zur Folge. Mehrere Gene, wie Gbp2, Socs3, CcnK, die potenziell an Proliferation beteiligt sind, werden bei der Entzündung überexprimiert und durch die Behandlung mit UDCA auf ein niedrigeres Niveau gebracht. Im normalen Gewebe bewirkt die UDCA Behandlung ebenfalls die Suppression von

potenziell an der Proliferation beteiligten Genen wie Tcf4, Gbp2, Klf5, Irs-1, Il-15, Ghr und Flot2. Die detaillierte Untersuchung der Rolle von zwei Genen, Gbp2 sowie TCF4 in humanen Kolonkarzinomzellen brachte jedoch keine schlüssigen Ergebnisse zu ihrer Beteiligung an der UDCA-vermittelten Proliferationsinhibition. Dies wurde u.a. darauf zurückgeführt, dass das Gesamtgenexpressionsprofil der humanen Kolonkarzinomzelllinien nach UDCA Behandlung von dem murinen Genexpressionsprofil unterschiedlich war.

Demgegenüber entsprachen die UDCA-bedingten Genexpressionsveränderungen in der nichttransformierten intestinalen Rattenzelllinie IEC-6 den Veränderungen die im murinen Kolonepithel beobachtet wurden. Diese Zelllinie eignete sich somit sehr gut als Modell zur detaillierten Untersuchung der Wirkungsmechanismen der UDCA *in vitro.*

UDCA inhibierte in der IEC-6 Zelllinie das proproliferative Signal von EGF sowie von IGF-1. Dies war mit einer starken und anhaltenden Phosphorylierung der ERK1/ERK2 Kinasen sowie mit der Suppression des Irs-1 Proteins verbunden, das an der Vermittlung des IGF-1 Signals beteiligt ist.

Durch Anwendung von ERK Inhibitoren sowie durch die selektive Suppression von ERK1 bzw. ERK2 mittels siRNA konnte gezeigt werden, dass die antiproliferative Wirkung von UDCA durch ERK1 und nicht durch ERK2 vermittelt ist. Dauerhaft phosphoryliertes ERK potenziert die Transkription des $p21^{WAF1/cip1}$ Proteins, das zur Proliferationsinhibition beiträgt. Darüber hinaus supprimiert die hochphosphorylierte ERK1 Kinase die Transkription des Irs-1 Proteins, wodurch das proproliferative IGF-1- Signal inhibiert wird.

Schlussfolgerung:

Zusammenfassend ist die durch UDCA Behandlung ausgelöste hohe und anhaltende ERK1 Phosphorylierung die entscheidende Veränderung, welche die transkriptionellen Alterationen von Regulatormolekülen (p21 Hochregulation, Irs-1 Suppression) auslöst und Zellzyklusverlangsamung sowie die Inhibition der EGF- und IGF-1-Signalwege zur Folge hat.

5 Introduction

5.1 Etiology of colon cancer

Colon cancer is one of the leading causes of death in the industrialized world. In Europe colorectal cancer is the second most common cause of cancer deaths (2008) (1) . According to National Cancer Institute (NCI), the estimated new cases of colon cancer in the United States in 2010 are 102,900 (colon cancer) and 51,370 deaths (colon and rectal cancer combined). Colon carcinoma can develop sporadically or due to hereditary predisposition or as a result of specific conditions like colitis.

5.1.1 Sporadic colon carcinogenesis

Sporadic colon cancer is the most common of all types of colon cancer. Almost 80 % of colorectal cancer cases are sporadic in nature.

5.1.1.1 The adenoma-carcinoma sequence

The hyperproliferation of normal epithelia can be the beginning of a step-by-step process leading to colon cancer. The different stages have been characterized by morphological features.

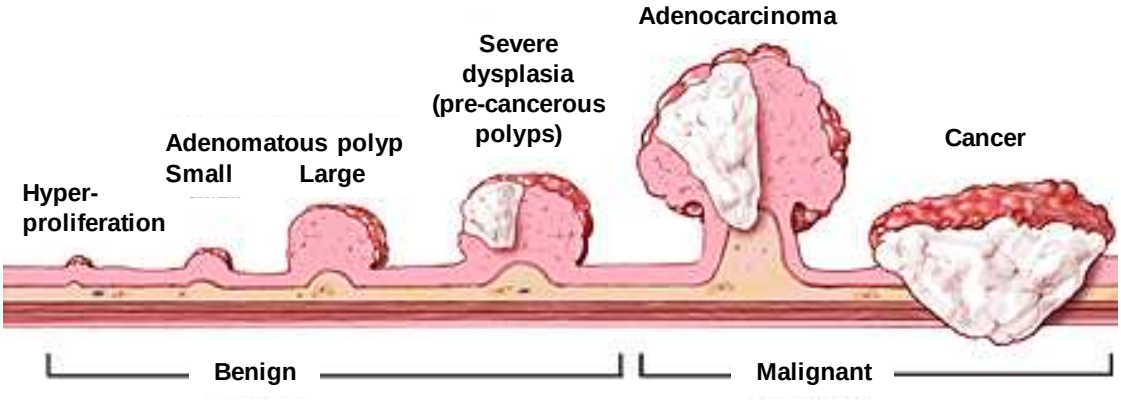

Fig. 1. Different pathomorphological stages in colon carcinogenesis: Adenoma-carcinoma sequence. (From: www.hopkinscoloncancercentre.org)

Hyperproliferation of the epithelia can lead to the formation of small polyps (early adenoma), then to large adenomatous polyps (intermediate adenoma), followed by

severe dysplasia. When the dysplastic lesion passes the muscularis mucosa, it becomes by definition an adenocarcinoma. This process of gradual morphological changes leading to cancer is commonly referred as the adenoma – carcinoma sequence (Fig. 1.).

5.1.1.2 Different mutations mark the different stages of carcinogenesis

The mutations which occur at the different steps of the adenoma-carcinoma sequence were studied in detail by Vogelstein et al. In their ground-breaking publication (2), they suggested that the epithelium is transformed to adenoma and then to carcinoma due to accumulation of mutations (Fig. 2) (2-4).

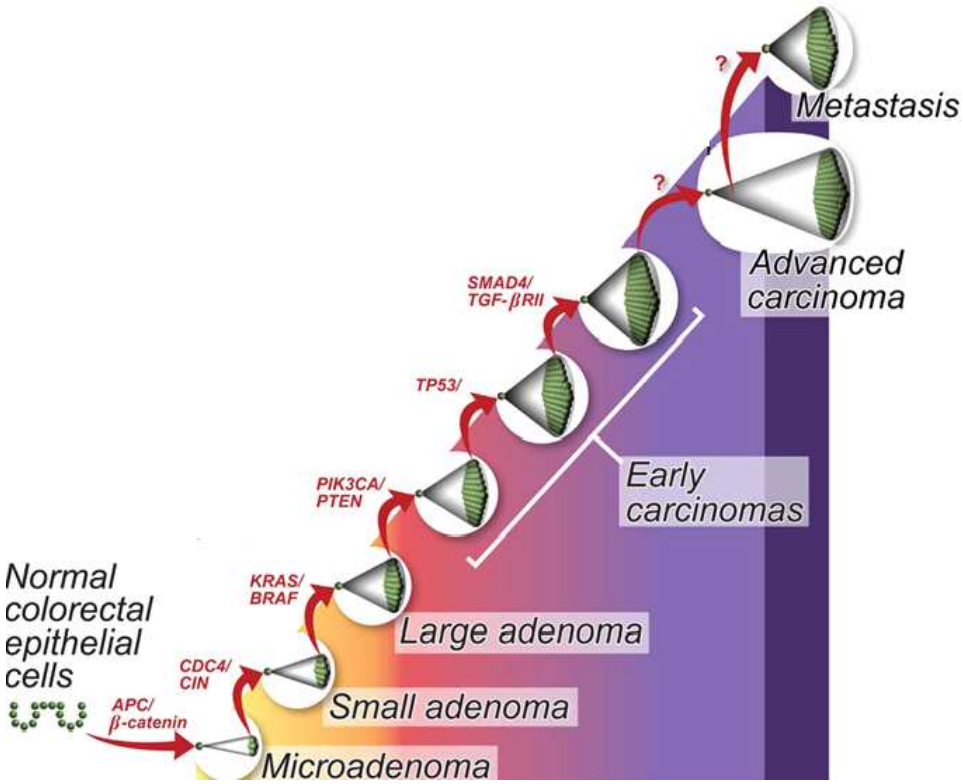

Fig. 2. Mutations which mark the different stages of colon carcinogenesis (4)

The sequence of genetic events, colloquially named “Vogelgram” accompanying the adenoma-carcinoma sequence has been repeatedly updated (4). The mutation observed in the adenomatous polyposis coli (APC) gene belongs to the early mutations. APC-protein recruits β-catenin to axin and GSK3β, which then

phosphorylates β–catenin. Phosphorylated β–catenin is ubiquitinated and degraded. A mutation in APC-gene or in β-catenin-gene itself causes stabilisation of β-catenin which is then free to enter the nucleus and interact with the Lef-Tcf family of transcription factors which further transcribe proproliferative genes constitutively. These mutations mark the beginning of the conversion of normal epithelium to an aberrant crypt focus (ACF) or a microadenoma. APC is a tumour suppressor gene whose germ-line mutations are also responsible for hereditary familial adenomatosis polyposis (FAP) syndrome (5, 6). Activating mutation in Cdc4 gene commonly follows the APC/ β-catenin mutations. Cdc4 regulates the G1 to S-phase transition during the cell cycle by inactivating cdk-inhibitors. Mutated Cdc4 marks the stage where chromosomal instability is observed, which has been assumed to be facilitating mutations. Mutations in the K-ras or B-raf genes follow the APC/Cdc4 mutations as small adenomas develop into large adenomas. These mutations cause constitutive activation of Ras-Mapk pathway paving way to uncontrolled cell proliferation. Mutations in the PI3K gene appear after K-ras/B-raf mutations. PI3K mutation is also a type of constitutively active mutations whereby the PI3K-AKT pathway is constitutively activated. Mutation in the p53 gene is a late event in this sequence which is followed by mutations in TGF β and SMAD4 (4).

B. Vogelstein and K.W.Kinzler (7) have generalized the description of the process of colon carcinogenesis as being caused by three main types of events:

1. **Suppressive mutations in tumour-suppressor genes.**
(e.g Mutations in APC or p53)
2. **Activating mutations in oncogenes.**
(e.g Mutations in K-ras and B-raf)
3. **Mutations in genome stability genes.**
(e.g Mutations in genes of DNA repair pathways like hMLH1, hMSH2)

5.1.1.3 The *wnt*-APC/β-catenin/Tcf4 pathway

APC, a key controller of the canonical *Wnt* / β-catenin signalling pathway (8), sequesters β-catenin in the cell membrane and prevents its entry into the nucleus. APC protein also facilitates the interaction of β–catenin and GSK3β, which leads to ubiquitin-mediated degradation of β–catenin. If APC gene is mutated then β-catenin

may translocate to the nucleus and interact with members of the T-cell factor (Tcf) family of transcription factors and activate transcription of proproliferative genes (8) like c-myc (9) and cyclin D1 (10). The same pathway regulates many genes whose transcription is associated with inflammation e.g COX-2 (11), NOS2 (12), VEGF(13), MMP-2 and MMP-9 (14). In the absence of the wnt signal or β-catenin, Tcf4 forms a complex with Groucho protein and the signal of *wnt* pathway is abrogated.

A B

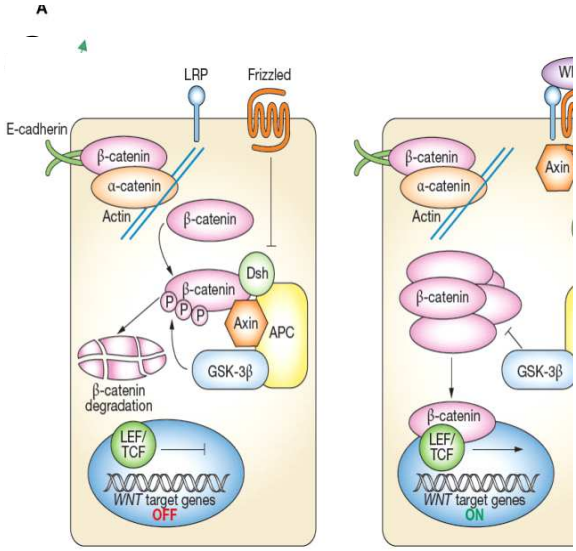

Fig. 3. Canonical *wnt* signaling pathway A.: *wnt* pathway inactive; B.: *wnt* pathway active (15) ; C.: Colonic crypt showing regions of β-catenin/Tcf4 activity (16).

Fig. 3A. shows schematically how in the absence of *wnt* ligand the wnt pathway is inactive. β-catenin is sequestered in the cytoplasm and eventually degraded by the action of APC, GSK3β and other proteins. The Lef/Tcf transcription factors are not activated. Fig. 3B. shows the activation of *wnt*-pathway by *wnt*-ligand and stabilization of β-catenin, which enters the nucleus and binds to the Lef / Tcf transcription factors which then transcribe the proproliferative genes (15). Fig. 3C. shows a colonic crypt containing both normal or APC / β-catenin mutated epithelial cells. The epithelial cells in the upper part of the crypt are differentiated (no β-catenin / Tcf4 signalling) and in the bottom of the crypt they are proliferating (active β-catenin/Tcf4 signalling). The cells with mutated APC or β-catenin exhibit a constitutive activation of the *wnt*-pathway and are assumed to have a crypt progenitor like phenotype which initiates carcinogenesis (17).

5.1.1.4 The role of p53 mutation in carcinogenesis

Mutations in the tumour suppressor gene p53 are associated with the development of sporadic colon cancer. p53 normally controls cell division through action on the normal cell cycle and regulates the repair of damaged DNA, thereby preventing the emergence of abnormal and/or cancerous cells. A mutation in the p53 gene is associated with tumour progression and metastasis. A hereditary mutation in p53 gene is associated with Li-Fraumeni Syndrome. (18-20).

5.1.1.5 The K-ras-B-raf-MAP Kinase pathway

Mutations in the K-ras gene follow the mutations in APC gene (Fig. 2.). K-ras mutations are found in 40-65% of colorectal cancers. They activate downstream signals involving Raf/MAPK and PI3K pathways, leading to constitutive stimulation of proliferation (21).

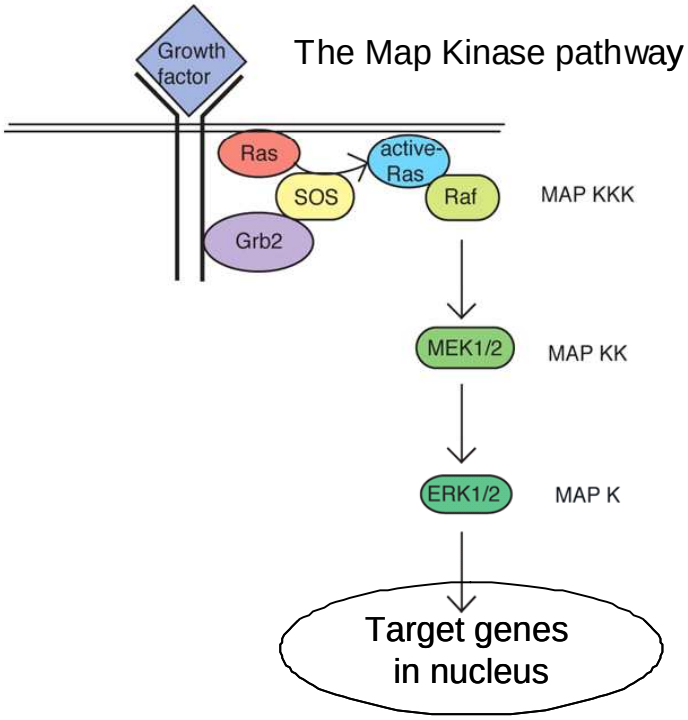

Fig. 4. The Mitogen activated protein kinase (MAPK) pathway.

Mitogen-activated protein (MAP) kinase was first discovered as a protein kinase which was activated in response to a mitogenic stimulus such as growth factors. In

response to growth factors the corresponding surface receptors, which are tyrosine receptor kinases, phosphorylate the downstream kinases. The pathway operates as a cascade of phosphorylation events with each preceeding kinase phosphorylating the subsequent kinase starting from receptor tyrosine kinases to Ras-Raf-Mek1/2 and ERK1/2 (22). The activated ERK1/2 then regulates the expression of transcription factors and genes related to several different pathways.

5.1.1.5.1 Role of EGF/EGFR or IGF-1/IGF-1R in colon cancer

The presence of K-ras mutations in the colorectal tumours was found to be predictive for lack of clinical response of these tumours to antibodies against the epidermal growth factor receptor (EGFR). Mutated K-ras gene keeps the Ras/Raf/MAPK pathway constitutively active. Hence inhibiting EGFR, which is upstream of K-ras in the signalling cascade, does not stop the constitutive MAPK signalling. The importance of epithelial growth factor signaling in colon cancer is also indicated by the fact that EGFR signaling is upregulated already in aberrant crypt foci (23).

EGFR activity also contributes to tumour promotion in a mice model of azoxymethane-DSS colitis induced colon cancer (24). Inhibition of EGFR by tyrosine kinase inhibitor Gefinitib led to inhibition of azoxymethane-induced hyperproliferation, abberent crypt foci and microadenoma formation in mice model of AOM induced carcinogenesis (25).

5.1.1.5.2 Phosphorylation and cellular localisation of ERK1/ERK2

Growth factors promote rapid nuclear translocation and activation of ERK1 and ERK2 during the entire G1 period and the decline of ERK-activity during the S-phase. The dephosphorylation of MAP kinases is controlled by the MAP kinase phosphatases (MKP1-3). MAP kinases in return also phosphorylate MKP1-3 as an autoregulatory loop (26, 27). Upon mitogenic stimulus the cytoplasmic ERK is rapidly phosphorylated and is transported to the nucleus (28). It has also been shown that upon EGF stimulation, ERK is rapidly phosphorylated and it oscillates

between the nucleus and the cytoplasm with an oscillation frequency of 15 min (29).

5.1.1.5.3 Role of ERK kinases in cell proliferation

ERK1 and ERK2 kinases play a key role in cell proliferation, cell differentiation and cell death. In primary human keratinocytes, loss or either ERK1 or ERK2 had no effect on proliferation but simultaneous inhibition of both kinases inhibited cell division and proliferation associated with G2M-arrest (30)

In NIH3T3 fibroblasts it has been shown that ERK activity is required for proliferation (31). Specifically, ERK1 ablation had no effect on proliferation whereas ERK2 ablation, markedly slowed down proliferation. The positive contribution of ERK1 to cell proliferation was identified only when ERK2 expression was completed inhibited. Cells could not proliferate when both kinases were ablated (31). Inhibition of ERK phosphorylation by U0126 reduced soft agar colony formation of liver cancer cells and decreased size of hepatoma xenografts in nude mice. In liver cells, siRNA mediated suppression of ERK2 and not of ERK1 inhibited proliferation as shown by inhibition of DNA synthesis *in vitro* and *in vivo* (32).

5.1.1.5.4 Antiproliferative effects of high and persistent ERK-phosphorylation

The brief activation of ERK kinase brought about by growth factors is proproliferative whereas the persistent ERK phosphorylation is antiproliferatory (33). In human prostate cancer cell line PC-3, persistent phosphorylation of ERK caused by constitutively active-MEK1 overexpression inhibited proliferation (34). ERK activation induced growth arrest, Rb (retinoblastoma) hypophosphorylation, E2F1 down-regulation, c-Myc suppression and/or p21 protein up-regulation in the human tumor lines LNCaP, U251, and TT. These changes were abrogated by suppression or ablation of ERK1 and ERK2 (35). In MCF-10 breast cancer cell

line, persistent ERK phosphorylation caused G1-arrest (36). Treatment of human hepatoma cells with cpd-5 (inhibitor of cdc25A phosphatase) caused persistent phosphorylation of ERK which suppressed proliferation (37). Treatment of human colon cancer cell line HCT116 with selenomethionine induces high and persistent ERK phosphorylation leading to cell cycle arrest and subsequent inhibition of cell proliferation (38).

5.1.2 Hereditary colon cancer

The mutations mentioned in point 5.1.1.2 are germline mutations which could be inherited by the subsequent generations. Different hereditary disorders are closely associated with the development of colon cancer.

5.1.2.1 Familial adenomatous polyposis

Familial adenomatous polyposis (FAP) is phenotypically characterized by occurrence of numerous polyps in the colon. FAP is caused by a genetically inherited mutation in the APC gene (39). If a sporadic mutation occurs in the APC gene in a germ cell and the following generations inherit the mutation, they are genetically predisposed to colon cancer.

5.1.2.2 HNPCC or Lynch syndrome

Hereditary nonpolyposis colorectal cancer (HNPCC), originally described by Lynch et al. in 1970 (40) is a syndrome genetically characterised by mutations in DNA mismatch repair genes. Their dysfunction leads to microsatellite instability (MSI) which is a hallmark of HNPCC. Lack of DNA repair function leads to the retention of mutated DNA sequences (39). Microsatellites are short stretches of repetitive DNA sequences whose length is not reproducibly maintained in mismatch repair defective cells. Presence of varied lengths of the microsatellite in a PCR based assay is a sign of malfunctioning DNA repair machinery of the cell.

Individuals with HNPCC have about an 80% lifetime risk for developing colon cancer. Two-thirds of these cancers occur in the proximal colon (41).

5.1.2.3 Li-Fraumeni Syndrome

An autosomal dominant hereditary syndrome due to a mutation in p53 tumour-suppressor gene is known as Li-Fraumeni syndrome. p53 mutations predispose patients to cancer, although colon cancer is much less prevalent as compared to breast or brain cancer or soft-tissue sarcomas (42, 43).

5.1.3 Colitis-associated colon cancer

Chronic inflammation of the colonic epithelium involves a hyperproliferative process of regeneration which is assumed to facilitate mutations. Mutations of the same kind as during the sporadic colon carcinogenesis, contribute to the development of cancer. The sequence of mutations which occur during chronic inflammation is different from that observed in sporadic carcinogenesis (44).

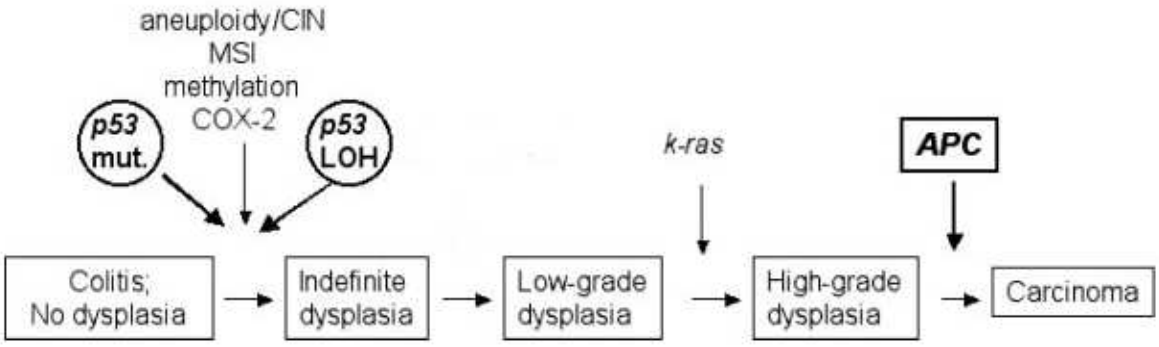

Fig. 5. Sequence of mutations during the development of colitis-associated colon cancer (44)

Chronic colitis is associated with the occurance of mutations in the p53 and DNA repair genes leading to an inability to repair damaged DNA. This is associated with indefinite dysplasia. As dysplasis progresses from low grade to high grade, mutations in the K-ras gene are common. The mutation in the APC gene occurs late in colitis-associated carcinogenesis and marks the conversion of severe dysplastic lesions to carcinoma (44). The patients suffering from ulcerative colitis have a high risk of

developing colon cancer (45). Chronic inflammation or colitis is characterized by the activation of cytokines like IL-6, proinflammatory molecules like cyclooxygenase (COX-2), nitric oxide synthase (iNOS / NOS2), and matrix metalloproteinases (MMPs). They promote carcinogenesis by increasing proliferation signals and excessive immune response leading to hyperproliferation and angiogenesis (46).

5.1.3.1 Importance of NF-κB - IL-6 - STAT3 signalling in colitis associated cancer

Infectious agents and proinflammatory cytokines activate NF-κB which contributes to tumourigenesis. Karin and Greten et al. have shown in a DSS-colitis mice model how epithelial cells and myeloid cells differentially respond to IKKβ deletion, in the process of tumourigenesis. Deletion of IKKβ in epithelial cells resulted into decrease of tumour incidence without influencing tumour size. Deletion of IKKβ in myeloid cells resulted into decreased tumour size (assumed to be due to a decrease in the growth promoting cytokines released by myeloid cells lacking IKKβ) (47).

Enzymes like TACE (TNF-alpha converting enzyme) which is activated in inflammatory conditions, cleave IL-6 receptors from cell surfaces (shedding). As a result, soluble IL-6-receptor binds to IL-6 and transactivates target immune cells. This enhances proliferation of cell types which even lack the IL-6 receptor (48). The release of IL-6 is a NF-κB dependent process. Deficiency of IL-6 decreased the number, size and frequency of tumours in an AOM-DSS-colitis mice model. In a DSS-colitis model IL-6 was shown to enhance epithelial cell proliferation via activation of STAT3. Knockdown of IL-6 or of STAT3 protected mice from developing tumours during DSS-colitis (49).

5.2 Colon cancer chemoprevention

There are different strategies of chemoprevention of colon cancer, focused on the aetiology of the disease and on molecules which play a role in the process of carcinogenesis. For example, infection with *Helicobacter pylori* causes chronic inflammation of the stomach and predisposes to stomach cancer. Antibiotic treatment

aimed at eradication of *H.pylori* is immediately prescribed upon detection. On the other hand chemoprevention is achieved by antiinflammatory drugs, antiproliferative drugs or by specific inhibition of pathways and molecules involved in carcinogenesis.

5.2.1 Use of NSAIDs and selective cyclooxygenase inhibitors

Inhibition of COX (cyclooxygenase isoforms Cox1 or Cox2), which are induced by mitogenic and proinflammatory stimuli (50) is one of the most common antiinflammatory treatment used in cancer chemoprevention. Non-steroidal anti-inflammatory drugs (NSAIDs) suppress prostaglandin synthesis by inhibition of COX. Treatment with NSAIDs decreases adenoma and carcinoma incidences in high risk families and also in patients with a history of chronic colitis (51-55). In murine models of colon cancer, either genetic deletion or pharmacological inhibition of COX suppresses the development of tumour (56-58).

5.2.2 iNOS inhibitors

Inducible nitric oxide synthase (iNOS) is an enzyme involved in synthesis of NO (nitric oxide). NOS is induced in chronic inflammation. NO damages DNA and induce mutations directly or indirectly via its reactive species. Hence iNOS inhibitors are also potential drugs against inflammation-associated cancer (59-62). Omeprazol, a proton pump inhibitor, has been shown to decrease iNOS and COX2 expression, decrease NO levels and decrease tumour incidence in a mice model of colitis (63).

5.2.3 5-Aminosalicylic acid (5-ASA)

5-Aminosalicylic acid also known as Mesalamine or Mesalazine is a drug of choice in chemoprevention of colorectal cancer in patients with inflammatory bowel disease (IBD). Mesalamine induces mucosal healing and is very effective in inducing remission in patients with IBD and has been shown to prevent colon cancer (64-66). A meta-analysis of 48 studies links 5-ASA chemopreventive properties to interference with cell cycle progression, scavenging of reactive oxygen species

(ROS), inhibition of nitric oxide synthase (NOS), TNF-alpha/TGF-beta signaling, *wnt* signaling and anti-bacterial properties (67).

5.2.4 Ursodeoxycholic acid (UDCA)

Factors contributing to colon carcinogenesis are high epithelial proliferation rate in the inflamed region and the resulting increased accumulation of mutations as well as the disturbed regulation of cell death and proliferation. Intestinal bile acids contribute to the homeostatic regulation of proliferation and apoptosis of the colonic epithelium. Ursodeoxycholic acid (UDCA) is a tertiary bile acid which is metabolized by intestinal bacteria from the primary bile acid, cholic acid (68). Tertiary bile acids are generally stable and are not further metabolized. Conjugation of UDCA to glutamic acid (UDCA-Glu) reduces its intestinal absorption or biotransformation and facilitates increased colonic delivery of UDCA. This has a potential application since most of the tumours appear in the distal colon (69).

5.2.4.1 Use of UDCA in colon cancer chemoprevention in patients

A chemopreventive effect of UDCA was recently demonstrated in patients with primary sclerosing cholangitis (PSC), which accompanies 2–7% cases of ulcerative colitis (UC) and increases the risk for developing colon cancer 3- to 5-fold (70). Two retrospective studies showed that patients with PSC and UC, who were treated with UDCA to improve the liver function, have a significantly lower risk of colitis-associated cancer than the non-treated group (71, 72). Whether UDCA treatment has also a protective effect in patients with UC alone, in whom the treatment with UDCA is not a standard therapy, has not been investigated.

Primary biliary cirrhosis (PBC) patients with colorectal cancer, who were treated for 46 months with UDCA, had significantly lower probability of colorectal adenoma recurrence after resection. UDCA also decreased colonic epithelial cell proliferation as seen by a decrease in % of cells expressing Ki-67 protein (73-75). On the other hand Ochsenkuhn et al. reported that UDCA did not influence colonic epithelial cell proliferation after UDCA treatment for 6 months (76).

In a phase III clinical trial with patients who had colorectal adenoma removed, UDCA treatment caused a statistically significant reduction in recurrence of adenomas with high-grade dysplasia (77).

5.2.4.2 Effects of UDCA *in vivo* in rodent models of colon cancer

Deoxycholic acid (DCA) stimulates the proliferation of the colonic epithelial cells and promotes colon carcinogenesis in the azoxymethane (AOM) rat model of colon carcinogenesis.

UDCA treatment decreased the incidence of tumors with mutant K-ras and prevented the development of tumors with activated wild-type Ras in an azoxymethane (AOM) rat model (78).

In DSS-colitis+AOM mice model of colitis-associated colon carcinogenesis, the addition of ursodeoxycholic acid (UDCA) to the diet decreases the prevalence of tumours (79, 80) and multiplicity of adenomas and adenocarcinomas (81). The decrease in tumour incidence was associated with decreased expression of Cox-2 in the tumour tissue and downregulation of C/EBPβ expression (78, 82), decreased cyclin D1 expression, return to normal levels of E-cadherin protein expression (79) and a decrease in the % of PCNA expressing epithelial cells within the adenocarcinoma (81).

In a DSS-colitis mice model without AOM, UDCA decreases prevalence of dysplasia from 88% to 40% and squamous carcinoma from 54% to 20% compared to non-UDCA-treated. UDCA did not affect adenoma occurence but completely inhibited occurence of adenocarcinoma (83). UDCA treatment also decreases prevalence of tumors in MIN mice (84).

5.2.4.3 Effects of UDCA *in vitro* in colon cancer cells

Treatment with UDCA inhibited the proliferation of HCT116 colon cancer cell line (85, 86). Long term treatment decreased telomerase expression and led to senescence which was independent of p53 or p21 expression or Rb-phosphorylation status (85). The decrease in proliferation was associated with increase of cytokeratin-18 and E-

cadherin expression which are markers of differentiation. In HT-29 cells UDCA treatment decreased proliferation by causing G2M arrest (87) and the decrease in proliferation has also been attributed to caveolin-mediated degradation of EGFR (85-88).

Unlike UDCA, DCA is a tumour promoting bile acid which promotes apoptosis in colon cancer cells. The apoptosis caused by DCA could be abrogated by suppressing or inhibiting the ERK1/ERK2 kinase (89). In HCT116, UDCA pretreatment decreased DCA induced apoptosis (90, 91), which could be attributed to increase of AKT-phosphorylation (92) and inhibition of fragmentation of mitochondria (93). UDCA has also been show to inhibit Protein kinase C (PKC) translocation from cytosol to the plasma membrane (94), IL-1β expression, AP-1 DNA binding, NF-kB activation (90), p38 and Raf-kinase activity (91) and EGFR expression (91). In HCA-7 cell line UDCA decreased the DCA induced expression of Cox-2 and C/EBPβ which was p38 dependent. The kinase activity of Ras and p38 were suppressed by UDCA (82). p38, Raf, C/EBPβ and AP-1 transcription factors are proproliferative molecules whereas IL-1β, NF-κB, Cox-2 are proinflammatory molecules. The interference in their functions could be involved in the mechanism of chemoprevention by UDCA.

5.2.4.4 Effects of UDCA on primary hepatocytes and hepatoma cell lines

Since UDCA is used for treatment of primary sclerosing cholangitis and primary biliary cirrhosis, the molecular effects of UDCA have also been studied in primary rat hepatocytes. UDCA prevents TGF-β -induced apoptosis in hepatocytes (95-97). UDCA reduces p53 transcriptional activity via modulation of Mdm-2/p53 interaction, thereby resulting in less Bax expression and attenuation of Bax mediated apoptosis (98, 99). Treatment of hepatocytes with UDCA suppressed proproliferative-genes like Apaf-1, cyclin D1, cadherin 1, HMG-box containing protein 1 and the genes of the proapoptotic E2F-1/p53/Apaf-1 pathway (100).

UDCA switches oxaliplatin or cisplatin or carboplatin-induced necrosis to apoptosis via inhibition of ROS production and activation of the p53-caspase 8 pathway in HepG2 hepatocarcinoma cell line (101). UDCA inhibited reactive oxygen species

produced due to excessive iron in HepG2 cells. This antioxidant action of UDCA was mediated by an increase in the expression of Glutathione synthase via the activation of the PI3K/Akt/Nrf2 pathway (102).

UDCA does not enter the colon cancer cell lines (HCT116 and HT29) (86). On the other hand in hepatocytes UDCA is transported to the nucleus via the glucocorticoid receptors (95, 103). This could be the reason why the hepatocytes have a different response to UDCA than the colon cancer cell lines.

5.3 The crosstalk between MAP-kinase & PI3-kinase pathways

It has been shown in NIH3T3 fibroblasts that Ras activates both Raf and PI3-kinase (PI3K) (104). Constitutive Raf signaling activates MEK1 which either directly or via ERK activate EphA2. Activated EphA2 inhibits Ras which leads to decreased PI3K activation and hence less AKT activation leading to cellular arrest (104). Another aspect of the crosstalk between these two pathways is seen in the resistance to MEK-kinase inhibition in colon cancer cells which have both constitutively active K-ras and PI3K mutations (105). In these cells, when PI3K was suppressed, the cells were sensitive to MEK inhibitor U0126 as compared to mock transfected cells (105).

5.4 Irs-1 and proliferation

Insulin receptor substrate 1 (Irs-1) is an intracellular protein which transduces the signal of insulin, insulin-like growth factors and growth hormone (106). It has been shown to transcriptionally activate the expression of proproliferative genes like rRNA, cMyc and cyclin D1 (107). Irs-1 is constitutively activated in breast cancers, leiomyomas, rhabdosarcomas, liposarcomas and adrenal cortical carcinomas (108).
In breast cancer cells isolated from primary tumours, the blockade of the constitutive Irs-1 signaling by overexpression of dominant-negative Irs-1 protein proliferation decreased cell growth and inhibited colony formation in soft agar culture (108).

Irs-1 overexpression in MCF-7 breast cancer cells induces loss of estrogen requirements for growth as compared to the mock-transfected clones (109).

Treatment of MCF7 cells with retinoic acid (RA) results in decrease of proliferation and downregulation of Irs-1 protein. Irs-1 overexpressing clones of MCF7 were less sensitive to RA as compared to empty-vector transfected clones (110).

Only Irs-1 expressing clones of T47D-YA breast cancer cells proliferated in response to IGF-1 compared to mock transfected clones confirming that Irs-1 transduces the signal of IGF-1 (111). Irs-1 has been shown to be targeted by MicroRNA 145 which leads to suppression of proliferation in colon cancer cells (112, 113).

Overexpression of Irs-1 is considered procarcinogenic *in vivo*. Transgenic mice overexpressing Irs-1 showed progressive mammary hyperplasia, tumorigenesis, and metastasis. Irs-1 was also found to be associated with β-catenin (114).

6 Objectives

6.1 What is the mechanism of chemopreventive action of ursodeoxycholic acid (UDCA) in murine colitis-associated colon carcinogenesis ?

6.1.1 What is the effect of DSS-colitis on epithelial cell proliferation and how is it altered in the presence of UDCA?

6.1.2 Expression of which genes is altered by DSS-colitis and normalised after UDCA treatment?

The first part of the work has lead to the following subsequent questions:

6.2 What is the mechanism of antiproliferative action of UDCA in intestinal epithelial cells *in vivo* and *in vitro*?

6.2.1 What is the effect of UDCA treatment on proliferation of the normal intestinal cells *in vivo*?

6.2.2 Which proliferation associated genes are differentially expressed after UDCA treatment in the normal mice colonic epithelium?

6.2.3 What is the effect of UDCA treatment on proliferation of intestinal epithelial cells *in vitro*?

6.2.3.1 What was the effect on colon cancer cell lines?

6.2.3.2 What was the effect on nontransformed intestinal epithelial cell line IEC-6?

6.2.3.3 Which signaling pathways are affected by UDCA which could explain its antiproliferative property?

7 Materials and Methods

7.1 Experiments with mice

7.1.1 Animal handling, water and diet

CBL57/6J mice were given autoclaved water *ad libitum*. The feed was a standard AIN-76 (American Institute of Nutrition-76) diet supplemented with 90 mg / kg of iron. For treating the mice with different concentration of UDCA, 0.04, 0.08, 0.2 or 0.4 % UDCA was added to the same diet. All mice were kept in an animal house with proper amenities and the standard principles of animal care were followed.

7.1.2 DSS-water cycle

For the colitis experiment 0.7% DSS was added to the drinking water and was given to the mice *ad libitum* for 7 days followed by 10 days of normal autoclaved tap water. The mice were given 5 cycles of DSS / normal water before sacrificing.

7.1.3 BrdU incorporation in mice

10 mg / ml BrdU in PBS was sterile filtered. 100 µg BrdU per gram weight of the mice was injected intraperitoneally. The mice were sacrificed 2 h after BrdU injection.

7.1.4 Isolation of murine colonic epithelial cells

The following buffers were used for isolation of the colonic epithelial cells, HBSS without Ca^{2+} and Mg^{2+} (Biochrom Berlin, Germany) and HBSS with 0.5 µM EDTA. Carbogen (95% O_2 + 5% CO_2) was passed through all the solutions for oxygenation and finally the pH was adjusted to 7.5.

The colon was dissected out from the mice and the lumen was washed with warm HBSS. 4 cm from the distal end was defined as colon. The dissected colon was kept at 37℃ in HBSS. The distal end of the cut colon was slided onto a hooked needle and tied with tooth floss. The colon was inverted by gently rolling the colon on the

needle. The tooth floss was pulled off and the inverted colon was released into warm HBSS. The inverted colon was slided onto a steel wire and one end was tied with a thread. Using a sharp-edged forceps the colon was stretched along its length on the steel wire and then the other end was also tied with a thread. This steel wire was immersed into pre-warmed HBSS without Ca^{2+} and Mg^{2+} containing 5 mM EDTA and was incubated for 30 min. Then it was transferred into another tube with normal HBSS and the wire was attached to a vibrator. The whole crypts and loose epithelial cells were shaken off into warm HBSS using 20 bursts of vibration. Bursts are intermittent number of shakes given by switching on and off the vibrator, with one burst lasting 20 sec. The cells were centrifuged for 10 min at 2000 x g and the pellet was resuspended in HBSS with Ca^{2+} and Mg^{2+} and filtered using a nylon filter with pore size of 30 µm, fitted in a funnel. The cells were washed with HBSS containing Ca^{2+} and Mg^{2+} without phenol red. The cells from the filter were transferred to a tube with fresh HBSS with Ca^{2+} and Mg^{2+} and centrifuged at 2 000 x g for 10 min.

7.1.5 Immunohistochemistry: preparation of sections and staining

The longitudinally dissected colon was spread on a Whatman filter paper. This was immersed in a solution of 0.4 % formaldehyde (Merck, Darmstadt, Germany). The embedding, sectioning and staining with respective antibodies were carried out in the Institute of Pathology, Charité Campus Benjamin Franklin, in collaboration with Prof. Dr. Christoph Loddenkemper.

7.2 Molecular Biology

7.2.1 RNA isolation, purification and quality control

7.2.1.1 Extraction of RNA

The isolated cell pellet was weighed and 1 ml of Trizol (TRI Reagent) (Sigma, St.Louis, Mo, USA) per 100 mg of wet weight of the cells was added and mixed by pipetting up and down several times until the solution was clear. The solution was incubated at room temperature for 5 min and transferred to a 2 ml sterile centrifuge

tube. 200 µl of chloroform was added per ml of Trizol reagent used and mixed vigorously by inverting the tube several times for 15 sec. The tube was let to stand 2 min in RT until phase separation was visible. The tubes were then centrifuged at 12000 x g for 15 min at 4 ℃. From now onwards all the steps were carried out on ice. After centrifugation the top aqueous layer was carefully transferred into fresh centrifuge tubes without touching the intermediate layer. 500 µl of isopropyl alcohol per initial ml of Trizol used, was added to this aqueous layer and mixed well by inverting several times. This mixture was incubated for 1 hour at -20℃ and then centrifuged at 12 000 x g for 10 min at 4℃.

The pellet was washed twice with 1 ml of ice-cold 70% ethanol, made in DEPC (Sigma, München, Germany) treated water. The pellet was dried at RT for 10 min and then dissolved in 100 µl of DEPC-treated sterile RNase-free water. For proper solubilisation it was incubated further at 56℃ for 5 min and then pipetted up and down several times.

7.2.1.2 DNase-1 treatment

1 µl (10 units) of RNase-free-DNase-I (Roche, Mannheim, Germany) and 5 µl of 2.5 mM $MgCl_2$ (MBI Fermentas, St.Leon-Rot, Germany) were added to the isolated RNA and incubated at 37℃ for 30 min. After this step 3 00 µl of buffer “RLT” from the RNeasy RNA purification kit (Qiagen, Hilden, Germany) was added to it and mixed well.

7.2.1.3 Purification of RNA

250 µl of ethanol was added to the RNA in RLT buffer and mixed well by pipetting up and down several times. This mixture was transferred to a RNeasy spin column and centrifuged at 8 000 x g for 15 sec at RT. The columns were washed twice with 500 µl of RPE buffer (Qiagen) and dried by centrifuging without the buffer at 12 000 x g for 1 min. RNA was eluted with 50 µl of DNase/RNase-free water.

7.2.1.4 Determination of RNA concentration

The absorbance of RNA was measured at 260 nM and at 280 nM using a Nanodrop spectrophotometer (ND-100) (Peqlab, Erlangen, Germany) and the ratio of absorbance at 260 nm to absorbance at 280 nm was calculated. An absorbance of 1 at 260 nM is equivalent to 50 µg / ml RNA and the ratio above 1.9 indicates minimal protein contamination.

7.2.1.5 Visualizing RNA

The agarose gel apparatus (Mini SUB DNA CELL), comb and the lid (Bio-Rad, München, Germany) were rinsed with 0.1 % SDS (Roth, Karlsruhe, Germany) solution and washed with DEPC treated water and dried. The 50x-Tris-acetate-EDTA buffer (50x-TAE) was diluted with DEPC-treated water. 3% Agarose gel (Qualex Gold DNase / RNase free) (AGS, Heidelberg, Germany) was casted in 1x-TAE buffer with 50 ng / ml ethidium bromide. 250 ng of the RNA were loaded per well and the gel was run at 50 V for 45 min. After the completion of electrophoresis the gel was photographed using the UV-illuminator (Biometra, Gottingen, Germany).

7.2.1.6 Determination of RNA quality (RIN)

RIN (RNA integrity number) is a measure of integrity and quality of RNA. This value was obtained by analyzing RNA on a LabChip on the Agilent Bioanalyzer 2100 (Agilent Technologies Inc., CA, USA). The values for all the RNA preparations were above 9. RIN value of 9 and above out of a maximum of 10 indicates an excellent quality of RNA preparation which is a prerequisite for a microarray experiment.

7.2.2 Microarray experiment

7.2.2.1 Microarray probe preparation, labeling and hybridization

The amplification and labeling of the RNA samples were carried out according to the manufacturer's instructions (Affymetrix, CA, USA) as follows: Between one to three micrograms from each sample were converted into double-stranded cDNA using

SuperScript transcriptase (Life Technologies, CA, USA). Biotin-labeled complementary RNA (cRNA) was prepared from double-stranded cDNA by *in vitro* transcription using the GeneChip RNA transcript labeling kit (Affymetrix, CA, USA). The lebelled cRNA was cleaned using the RNeasy columns (RNeasy, Qiagen, Hilden, Germany), the biotin-labeled cRNA was fragmented by heating at 94 ℃ for 35 min. 10 µg of each cRNA sample was hybridized for 16 hours at 45℃ to an Affymetrix mouse 430A 2.0 GeneChip array. Chips were stained with streptavidin-phycoerythrin using the GeneChip fluidics station 450.

7.2.2.2 Scanning and chip evaluation

The hybridization and chip evaluation was carried out by LFGC, Charité. Briefly, Affymetrix GeneChip® Mouse Genome 430A-2 arrays were scanned at 1.56-µm resolution using the Affymetrix GeneChip System confocal scanner 3000. Image intensities of the hybridization patterns obtained by laser scanning were stored in raw data files. Raw data were analyzed with the Affymetrix GeneChip Operating Software 1.4 (GCOS). The detection p-value of a transcript determines the detection call, which indicates whether the transcript is reliably detected ($p<0.05$; present) or not detected (absent). To enable the comparison between chips, the data in each chip were normalized to a global intensity of 500.

7.2.2.3 Evaluation of microarray raw data

For comparison of the fold changes in the pivot table the following threshold values were applied: signal $\geq$ 50, present calls in both signals (P), ($p \leq 0.05$). For the downregulated genes the fold change was < 0.6 and signal log ratio < -1.52. For the upregulated genes the fold change was > 1.52 and the signal log ratio > 0.6, i.e the genes which were 1.52 fold up or down regulated in comparison to the treated group were further investigated. For the nomenclature and identification of the genes using the Affymetrix ids, the Netaffyx program in the Affymetrix website was used and the data was saved as a MS-Excel file.

7.2.3 Real-time PCR

Real-time RT-PCR was used for the validation of the array data using the RNA samples which were used for the arrays. The RNA isolated from IEC-6 and from human colon cancer cell lines with or without UDCA treatment for 3 days was also tested.

7.2.3.1 cDNA synthesis

The RNA was transcribed to cDNA using 5 µg of RNA in a reaction as follows:

RNA (1 µg / µl)	**=**	**5 µl**
Oligo $(dT)_{18}$ primer (0.5 µg / µl)	**=**	**1 µl**
(MBI Fermentas, St.Leon-Rot, Germany)		
5x RT buffer	**=**	**8 µl**
(Gibco BRL, CA, USA)		
dNTP mix (10 mM each)	**=**	**2 µl**
(MBI Fermentas, St.Leon-Rot, Germany)		
RiBo Lock	**=**	**1 µl**
(Promega, NJ, USA)		
RNase-free water	**=**	**33 µl**
Total reaction volume	**=**	**50 µl**

RNA and Poly dT primer and RNase-free water were mixed in a tube and heated at 70℃ for 5 min and chilled in ice for 1 min. Then 5 x reaction buffer, dNTPs and RiBo lock were added and incubated at 37℃ for 5 min and then finally 1 µl of RT-enzyme M-MLV-RT (Gibco BRL, Invitrogen Corporation, CA, USA) was added and incubated for 1 hour at 37 ℃. The RT-enzyme was inactivated by incubating the samples at 70℃ for 1 min.

7.2.3.2 RT-PCR

The 2x SYBR GREEN Master mixes (Applied Biosystem, CA, USA) was used to carry out the real time PCR in a reaction volume of 10 µl in the StepOnePlus Real-time

PCR system (Applied Biosystem, USA). Different annealing temperatures were optimised for different genes in question. All the reactions were carried out for 40 cycles followed by the standard melting curve.

7.2.3.3 Data analysis

The real time data were analysed using the Step One software (Applied Biosystems, CA, USA) The amounts of mRNA after treatment relative to those prior to treatment were calculated as $R=2^{-\Delta\Delta Ct}$ (i.e., $2^{-(\Delta CTafter\ -\Delta Ctprior)}$) for each sample.

7.2.4 Bacterial transformation

The E.coli TOP-10 bacteria were used for transformation with plasmids.

7.2.4.1 Competent cell preparation

Single colony of the TOP-10 bacteria was grown in LB broth as a preculture and then subcultured in 200 ml of LB broth (Invitrogen, CA, USA) medium and grown until O.D 0.5 at 600 nm. The culture was centrifuged in a sterile centrifuge tube, washed once with ice cold 0.1 M $CaCl_2$ solution, again resuspended in 0.1 M $CaCl_2$ solution, incubated on ice for 30 min and then finally centrifuged**.** The pellet was suspended in 5 ml of sterile ice cold 0.1 M $CaCl_2$ +15% glycerol solution and stored as 100 µl aliquots in - 70 °C deep freezer.

7.2.4.2 Transformation

20 µl of the suspension of competent bacterial cells were mixed with 5 to 10 ng of the plasmid and kept on ice for 20 min. A heat shock was given at 42°C for 1 min and then the suspension was immediately cooled on ice. 100 µl of LB medium were added to it and incubated at 37°C for 1 h. The transformation mix was plated on LB-Agar (Invitrogen, CA, USA) plates containing the antibiotic either Ampicillin (Sigma-Aldrich, München, Germany) or Kanamycin (Serva, Heidelberg, Germany) depending on the antibiotic resistance marker of the plasmid.

7.2.4.3 Storage of transformed bacteria

The overnight grown bacteria were mixed with sterile 50% glycerol in LB broth in 1:1 ratio, vortexed and stored in - 70 °C deep freezer.

7.2.5 Plasmid isolation

The plasmid was isolated from 2 ml (*Miniprep)* or from 200 ml (*Midiprep)* of bacterial culture using the plasmid purification kit (Qiagen, Hilden, Germany) as per the standard protocol.

7.2.6 Luciferase assay

7.2.6.1 Tcf4-promoter based reporter

$0.1x10^6$ HCT116 cells were seeded in a 12 well plate. The following day the cells were cotransfected with pGL3-hTCF4-luci plasmid (2.5 µg) and the pRL-TK renilla plasmid (50 ng) using the Fugene transfection reagent. The transfections were done in medium containing 10% FCS. All transfections were done in duplicates. The next day, cells were treated with 400 µM UDCA for 48 h. The assay was made using the Dual Luciferase reporter assay kit (Promega, Mannheim, Germany) as described in point No 7.2.6.5.

7.2.6.2 TOP-FOP: Tcf4 luciferase reporter assay

The TOP-FOP assay allows measuring the transcriptional activity of Tcf4. Similar to the pGL3-hTCF4-luci experiments, HCT116 cells were transfected either with pTOP-flash (containing repeated binding sites of Tcf4 found on promoters of target genes) plasmid or pFOP-Flash (scrambled Tcf4 target sequences) plasmid along with pRL-TK (Renilla-luciferase coding plasmid) for normalization of transfection efficiency. Lipofectamine 2000 was used for transfection. Treatment was with 400 µM UDCA for 48 h. 100 µl of the passive lysis buffer (Dual-Luciferase reporter assay kit), was

added directly to the wells and shaken on a plate shaker for 15 min. Then the lysate was transferred to a 1.5 ml cup and centrifuged at 12 850 x g for 1 min.

7.2.6.3 Irs-1 reporter assay

$2x10^6$ IEC-6 cells were transfected with 20 µg of the Irs-1 reporter plasmid pGL2-Irs-1, kindly provided by Dr. M. Schubert (115) containing the full-length Irs-1 promoter region from -2338 bp upstream of Irs-1 transcription start site, cloned into pGL2-vector, using the Amaxa Nucleofector device (Lonza AG, Cologne, Germany). The cells were centrifuged and the pellet was resuspended in 100 µl of Buffer-V, prewarmed at 37°C (Amaxa Buffer-V kit). For cotransfections with pSuper-EGFP or pSuper-ERK1 or pSuper-ERK2 plasmids, 20 µg of plasmids were used. 2 µg of pSV-β–Galactosidase plasmid were used for normalization of transfection efficiency. One day after transfection the transfected cells were reseeded in a 12 well plate with duplicate wells for each measurement. The next day they were treated with 600 µM UDCA for another 48 hours. The cells were trypsinised and lysed using 50 µl of the passive lysis buffer (Dual-Luciferase reporter assay kit), (Promega, Mannheim, Germany) instead of 100 µl buffer recommended for a 12 well plate. Lysing in low volume lysis buffer is a critical step in getting reproducible and high fluorescence values for each measurement using IEC-6 cells.

7.2.6.4 p21 reporter assay

p21 reporter experiments were carried out using the plasmid p21-0-luc, kindly provided by Dr. Wafik. S. El-Deiry (116), which contains the p21 promoter region from -2326 bp to +16 bp upstream of the p21 transcription initiation site. IEC-6 cells were transfected with the p21 reporter plasmid and the β-galactosidase-coding plasmid and treated with 600 µM UDCA in the presence or absence of 0.2 µM PD0325901 and handled as in 7.2.6.3.

7.2.6.5 Measurement of luciferase activity

20 µl of the supernatant (lysate) were mixed with 50 µl of firefly luciferase substrate and the luminescence was read immediately in a Luminometer (LUMAT LB 9501, Berthold, Germany) with a 10 sec measurement time. To this sample 50 µl of the renilla luciferase substrate, dissolved in Stop-and-Glow buffer were added and measured again, with a measurement time of 10 sec. The Stop-and-Glow buffer quenches the firefly luciferase and allows a quick measure of renilla luciferase in the same sample.

7.2.6.6 Measurement of β-Galactosidase activity

For detection of β-Galactosidase activity the chemiluminescent reporter assay kit, Galacto-Light Plus (Tropix, Ma, USA) were used. 10 µl of the lysate were incubated with the substrate for 1 h, then 100 µl of the extraction buffer was added and the luminescence was read in a luminometer with 5 sec measurement time.

7.3 Cell biology

7.3.1 Preparation of UDCA solution

196 mg of UDCA (Sigma, Germany) was dissolved in 3.5 ml of distilled water with 500 µl of 1 M NaOH and vortexed vigorously for 5 min. When the solution was clear, the volume was made up to to 5 ml with distilled water. If any particulate matter was still visible then 2 to 3 µl of 1 M NaOH was added and vortexed again. The solution thus obtained was 100 mM sodium salt of UDCA. The solution was sterile filtered and stored at RT.

7.3.2 Measurement of cell proliferation

The effect of UDCA on the proliferation of cells in vitro was determined by the following three methods.

7.3.2.1 Total cell count

The cell line in question was seeded in the respective medium and the following day treated with different agents for 3 days. Then the cells were trypsinised and counted by trypan blue exclusion method.

Trypan Blue dye exclusion assay: 50 µl of cell suspension in PBS was mixed with 50 µl of 2x-concentrated Trypan Blue solution and loaded onto the haemocytometer. The total cells which lie in the four quardrants of the chamber were counted, and the cell number was determined with the following formula: **(Total cells in 4 quadrants / 2) x 0.01= Total cell number in millions per ml of the suspension**

The blue cells were considered to be dead.

7.3.2.2 MTT assay

Cells were seeded in a 96 well plate in 100 µl volume. For IEC-6 cell line, 500 cells and for HCT116 1000 cells per well were seeded and treated with UDCA after 1 day. 3 days after treatment 25 µl of the MTT (3-(4, 5-Dimethylthiazol-2yl)-2, 5 diphenyltetrazoliumbromide) solution (5 mg/ml in PBS) was added to the wells and incubated for 2 h. After 2 h, 100 µl of MTT extraction buffer were added and mixed well by pipetting up and down. The plate was further incubated for 1 hour at 37 ℃ and then the extinction was measured in an ELISA plate reader (DYNATECH MR 5000, Ruckersdorf, Germany) at 550 nm.

7.3.2.3 Determination of formazan normalization factor for MTT assay

As described in the results point number 7.4.2, it was necessary to determine how the treatment with different UDCA concentrations affected the MTT result per well. To check if different UDCA concentrations caused the production of different amounts of Formazan per cell, IEC-6 cells were seeded in 22 cm^2 dishes and treated with different concentrations of UDCA. 3 days after treatment, both UDCA-treated and nontreated cells were harvested and were seeded in a 96 well plate with 10 000 and

20 000 cells per well, in triplicates. MTT assay was performed as described. Since equal number of cells must have equal formazan per well, a higher optical density in UDCA treated cells than the nontreated cells would mean that UDCA treatment increases formazan produced per cell. The mean absorbance corresponding to each UDCA concentration was divided through the mean absorbance of nontreated cells to get a factor which was applied to normslize the values of MTT which could then be used as a measure of cell number.

7.3.2.4 BrdU incorporation

The cells were treated with 10 µM BrdU for 30 min and then trypsinised and counted. $1x10^6$ cells were taken per sample in ice cold PBS and centrifuged. The pellet was dispersed in 70% ethanol in PBS at -20℃ and stored at -20℃. The % of cells incorporating BrdU was determined by FACS.

7.3.3 Flourescence activated cell sorting (FACS)

7.3.3.1 Propidium iodide staining

The ethanol-fixed cells were washed once with PBS and resuspended in 800 µl of 0.1 %Triton X-100 in PBS, containing 20 µg/ml of propidium iodide and 200 µg/ml of RNase A. The samples were incubated for 30 min at RT in the dark and taken for FACS measurement. The FACS determination was carried out by Marie-Luise Hanski.

7.3.3.2 BrdU staining

The ethanol-fixed samples were washed once with PBS and then with 0.5% BSA in PBS. The cell pellet was resuspended in 100 µl of 2 M HCl and incubated for 20 min at RT. 1 ml of 0.5% BSA in PBS was directly added to the tubes and centrifuged. The cell pellet was resuspended in 500 µl of 0.1 M sodium tetraborate ($Na_2B_4O_7$) pH 8.5, incubated for 2 min at RT and then washed with 0.5% BSA in PBS. The pellet was resuspended in 500 µl of 0.5% Triton X-100 in PBS and incubated for 10 min at RT

and again washed with 0.5 % BSA in PBS. The cell pellet was resuspended in 60 µl of FITC labelled anti-BrdU antibody (Flow kit) (BD-Pharmingen, CA, USA) diluted 1:3 in 0.25% Triton X-100 + 0.5 % BSA in PBS and incubated for 30 min at RT. For the isotype control the cells were resuspended in FITC labelled anti-mouse IgG antibody (BD Pharmingen CA, USA). After the incubation the cells were washed twice with 0.5% BSA in PBS. The pellet was resuspended in 50 µg / ml propidium iodide (Sigma, Manheim, Germany) solution in PBS.

7.3.3.3 FACS instrumentation and evaluation

The cellular DNA content of 20 000 events per sample was determined by flow cytometry using the BD FACSCalibur^{TM} (Becton, Dickinson and company, CA, USA) equipped with a pulse code processor for doublet discrimination module and analysed using the CellQuest^{TM} software (Becton-Dickinson, CA, USA). For quantitative analysis, the histograms of DNA distributions were reanalyzed using the ModFitLT^{TM} software (Verity Software House, Topsham, USA).

7.3.4 Determination of senescence

0.04 x10^6 IEC-6 cells were seeded in a 9.6 cm^2 dish and the following day treated with UDCA (400 µM for HCT116 and 600 µM for IEC-6). After 3 days of treatment the cells were washed with PBS and fixed with 2% formamide + 0.2 % glutaraldehyde in PBS for 5 min at RT. The protocol as published by Hirose *et al.* (117) was used. The dishes were washed twice with PBS and incubated overnight at 37℃ in fresh 5-bromo-4-chloro-3-indolyl-b-D-galactopyranoside solution (1 mg/ml 5-bromo-4-chloro-3-indolyl-b-D-galactopyranoside, 5 mM potassium ferrocyanide, 5 mM potassium ferricyanide, 150 mM NaCl, and 2 mM $MgCl_2$ in 40 mM citric acid/sodium phosphate buffer (pH 6.0)). The next day the dishes were washed with PBS and photographed under the microscope (Olympus BX60 (Optocal Co.GmbH, Hamburg, Germany).

7.3.5 Visualisation of nuclei by DAPI staining

IEC-6 cells were treated with 600 µM UDCA for 3 days and cytospins were made with 10 000 cells per slide and dried at RT. The slides were immersed in methanol (-80℃) for 5 min and then washed with PBS. A circle was drawn around the cells using a DakoPen. DakoPen makes a hydrophobic circle around the cells beyond which aqueous solutions do not pass, and hence the liquid stays within the circle. 100 µl of 1 µg / ml DAPI in PBS was added inside the circle and incubated in dark. The slides were washed twice with PBS and mounted with Fluoromount G (Southern Biotechnology Associates, AL, USA) and covered with glass coverslip. The photographs were taken under the Olympus BX60 microscope (Optocal Co.GmbH, hamburg, germany) and images were processed using the image processing software – "Cell" (Soft imaging Systems, Münster, Germany).

7.3.6 Transient transfections

IEC-6 cells were either transfected using Lipofectamine 2000 (Invitrogen, USA) reagent or by using the Amaxa Nucleofector (Lonza Cologne AG, Germany). HCT116 cells were transfected by using Lipofectamine 2000 reagent.

7.3.6.1 Adeno virus mediated overexpression

IEC-6 cells were seeded at a density of $0.045x10^6$ cells per cm^2 in a 9.8 cm^2 dish and transduced with 1, 2.5 or 10 MOI (multiplicity of infection) of Adv-Irs-1 or Adv-GFP. MOI could be defined as the number of virus particles infecting or transducing 1 cell. 2.5 MOI was chosen for cell count experiments. Next day, cells were replated and then treated with UDCA the day after seeding. Cell number and expression was checked 3 days after UDCA treatment. For p21 overexpression 50, 100 or 200 MOI of adenovirus was used to transduce $0.2x10^6$ cells seeded in a 22 cm^2 dish and cell number and expression was checked after 2 days.

7.3.6.2 Lipofectamine 2000

0.5 x 10^6 cells per 9.8 cm^2 dish or 0.1 x 10^6 cells per well in a 12 well plate were seeded a day prior to transfection in DMEM medium containing 10% FCS. The following mixtures were made and incubated for 5 min:

Solution A	**Plasmid**	**OptiMem**
12 well plate	1.6 µg	100 µl
9.8 cm^2 dish	4 µg	250 µl
Solution B	**Lipofectamine 2000**	**OptiMem**
12 well plate	4 µl	100 µl
9.8 cm^2 dish	10 µl	250 µl1

Solution A and B were mixed and incubated for 20 min. The dishes were washed with DMEM without FCS and 2 ml DMEM without FCS was added. After 20 min the transfection mix was added to the dishes, swirled and incubated at 37℃ for 4 h. The dishes were washed with DMEM + 10% FCS and 2 ml of DMEM + 10% FCS were added.

7.3.6.3 Amaxa Nucleofection

2x10^6 IEC-6 cells were used per transfection. 20 µg of plasmid DNA were mixed with buffer-V preincubated at 37℃ (Amaxa nucleofection kit (Lonza AG, Cologne, Germany)). The cells were dispersed in this mixture, taken in a 0.5 cm cuvette and electroporated in the Amaxa instrument using the program X-005. Immediately after pulsing, the cells were transferred to a 22 cm^2 dish with prewarmed DMEM+10% FCS medium and incubated for 24 h.

7.3.7 Generation of stable clones

Stable clones of HCT116 cells overexpressing human Gbp2 were generated by transfecting cells with the plasmid pEGFP-C2-mGbp2 using the Lipofectamine 2000

reagent as described in 7.3.6.2 . The next day the cells were harvested and seeded in a 58 cm^2 dish with 10 000, 20 000 or 50 000 cells per dish in DMEM+10% FCS+1 mg/ml G418. After two weeks, single isolated colonies expressing GFP were picked under the UV-microscope and were transferred to 96 well plate. The clones were expanded and screened by western blotting for high expressors.

For obtaining clones of IEC-6 cells overexpressing constitutively active MEK1 kinase (CA-MEK1), IEC-6 cells were transfected with pEGFP-N1-MEK1-CA using Amaxa protocol as mentioned in 7.3.6.3 and the cells were cloned by dilution cloning. 0.5, 1 or 2 cells of the transfectants were seeded per well in a 96 well plate with DMEM medium containing 10% FCS+1 mg/ml G418. The wells which had only one green colony i.e. a colony arising from a single transformed and MEK1-GFP expressing cell were further expanded and screened by western blotting for high and moderate expression of MEK1.

7.3.8 Suppression of ERK1 or ERK2 protein

Suppression of ERK1 or ERK2 or both in IEC-6 cells was done by transfecting IEC-6 cells with either pSuper-ERK1 or pSuper-ERK2 or both pSuper-ERK1 and pSuper-ERK2 plasmids (31) using the Amaxa protocol as described in 7.3.6.3. The suppression of ERK protein was checked 4 days after transfection, by western blotting. For suppression of ERK in reporter experiments with pGL2-Irs-1, 20 µg plasmid of either pSuper-ERK1 or pSuper-ERK2 or pSuper-EGFP was used along with 2 µg of pSV-βGalactosidase normalisation plasmid with a total of 42 µg of plasmids per transfection.

7.3.9 Inhibition of ERK phosphorylation

Phosphorylation of ERK1/ERK2 was inhibited by using inhibitors of MEK1 kinase, which phosphorylates ERK. IEC-6 cells were treated with either 10 µM of U0126 (Calbiochem, Merck, Darmstadt, Germany) or 0.25 µM of PD0325901 (Cayman Chemicals, Michigan, USA) for 3 days. Inhibition of ERK phosphorylation was checked by western blotting.

7.3.10 Suppression of Irs-1 protein

To suppress Irs-1 protein in IEC-6, $0.4x10^6$ cells were seeded in 9.8 cm^2 dish in DMEM + 10% FCS and transfected with 40 nM siRNA (mouse-Irs-1) (Santa cruz, Massachusetts USA), using 4 µl of the Lipofectamine 2000 reagent as described in 7.3.6.2 . P1-siRNA (40 nM) (Invitrogen, CA, USA) was used as a control siRNA to monitor the effects of transfection. 24 h after transfection the cells were reseeded into 22 cm^2 dish for the cell count experiments. Suppression of Irs-1 protein was checked by Western blotting 24 h after transfection.

7.3.11 Preparation of cell lysate and western blotting

For preparation of cell lysate either of the following two methods was followed:

7.3.11.1 Using lysis buffer without SDS ("Sato buffer")

This procedure was used only for those samples where phosphorylation of proteins was not in question, for e.g. Tcf4. The cells were trypsinised, washed with PBS and counted. 80 µl of 1x Sato buffer (118) was used per $1x10^6$ cells and mixed well by pipetting up and down. The samples were incubated for 20 min in ice, vortexed once and then centrifuged at 17 900 x g at 4℃ and the supernatant was stored at -80 ℃. Protein concentration was determined by Bradford method.

7.3.11.2 Cell lysis in 1x-sample buffer ("Laemmli buffer")

This procedure was used when phosphorylation of ERK kinase was investigated. The medium was discarded and the dishes were washed with ice-cold PBS containing phosphatase inhibitors (12 mM β-glycerophosphate and 1 mM sodium orthovanadate). The cells were scrapped in the presence of 120 µl of 1x Laemmli buffer per 1×10^6 cells. The lysates were treated with 1 µl of benzonase (10 units per ml) per 100 µl of lysate to reduce viscosity due to DNA, boiled for 5 min and stored at

– 20 ℃. Here cell number was determined to normsli ze the amount of protein per well.

7.3.11.3 Protein estimation by Bradford method

1 µl or 2 µl of the samples lysed with the “Sato buffer” were diluted in 800 µl water. 200 µl of the Bradford reagent (Protein assay reagent, Bio-Rad Laboratories GmbH, Germany) were added and mixed. In parallel 0, 20, 40, 60, 80 and 100 µg/ml BSA was also pipetted to generate a standard curve. After 30 min of incubation the samples were vortexed again and the absorbance was measured at 595 nM in a spectrophotometer (Ultrospec 2000) (Pharmacia Biotech, Freiburg, Germany) and plotted using MS-Excel.

7.3.12 Polyacrylamide gel electrophoresis and Western blotting

All the protein samples (20 µg / well) were separated on a 10% SDS polyacrylamide gel (Mini-Protean-II apparatus, Bio-Rad) and electroblotted (Mini Trans-Blot Cell apparatus, (Bio-Rad, München, Germany) onto a PVDF membrane (Immobilon-P) (Millipore, MA, USA). The membranes were blocked for 1 hour in 5% dry fat milk + 0.1%Tween-20 in TBS. The membranes were incubated overnight in the respective primary antibodies followed by 1 h of secondary antibodies with intermittent washes with 0.1% Tween-20 in TBS. Detection was carried out using the SuperSignal West Pico (Pierce, Rockford, IL, USA) substrate. The Chemiluminescence was detected and captured using the Fujifilm Chemiluminescence documentation system, and analysed using the Multigauge program (Fujifilm Europe GmbH, Düsseldorf, Germany).

7.3.13 Immunofluorescence staining of IEC-6 cells

0.03 x 10^6 IEC-6 cells were seeded in 9.8 cm^2 dishes in DMEM + 10 % FCS and treated with UDCA for 3 days. After 3 days, the dishes were washed with ice cold PBS and fixed with 4% paraformaldehyde prepared in PBS, for 10 minutes. The dishes were washed once with TBS (Tris buffered saline-buffer) and then cold

methanol stored in – 20 ℃ was added to the dishes and kept for 5 min. The dishes were washed with TBS + 0.1% Triton X-100 and then with TBS without Triton X-100. A circle was made using a clean cotton swab on which a hydrophobic circle was made using a Dako Pen. The unspecific binding of the antibody was blocked with 5% donkey serum in TBS + 0.1% Triton X-100, followed by wash and then 100 µl of the anti-phospho p44/42 MAP Kinase antibody at 1:1000 dilution in 3 % BSA in TBS was added. The dishes were incubated at 4℃ O/N.

Next day, dishes were washed once with TBS + 0.1% Triton X-100 and then with TBS alone, and 100 µl of donkey anti-rabbit Cy3-conjugated secondary antibody (Dianova, Hamburg, Germany) at a dilution of 1:400 in 3% BSA in TBS was added and incubated in dark for 45 min. The dishes were washed once with TBS + 0.1% Triton X-100 and then with TBS alone. 100 µl of DAPI solution (0.5 µg / ml in TBS) was added and the dishes were incubated in dark for 15 min. The dishes were washed once with TBS and the cells were coated with Fluoromount G (Southern Biotechnology Associates, Birmingham AL, USA) and covered with glass coverslip. The slides were photographed under the Olympus BX60 microscope (Optocal Co.GmbH, Hamburg, Germany) and the images were processed using the image processing software – “Cell” (Soft imaging Systems, Münster, Germany).

Table 1. List of plasmids used.

Plasmid name	Application	Provided by
pGL3-hTcf4-luci	Tcf4 promoter based luciferase reporter	Dr.Kurt Engeland, Univ. of.Leipzig, Germany
pTOP-flash	Tcf4 binding elements based reporter	Dr.Bert Vogelstein John Hopkins University, USA
pFOP-flash	Control for pTOP-flash	Dr.Bert Vogelstein
pRL-TK	Renilla luciferase expression, normalization of transfection efficiency in reporter experiments	Commercial, Promega corporation, USA.
pSV-β–galactosidase	β-galactosidase expression , normalization of transfection efficiency in reporter experiments	Commercial, Promega corporation, USA.
pFLAG-hTcf4	Tcf4 overexpression	Dr. Hans Clevers University Medical Centre, Utrecht, Netherlands
pFLAG-ΔN-hTcf4	Dominant negative Tcf4 overexpression	Dr. Hans Clevers
pEGFP-C2-mGbp2	Overexpression of murine Gbp2	Dr. V. Pfeffer The University of Tennessee, Knoxville, USA
pEGFP-N1-MEK1-CA	Overexpression of constitutively active MEK1	Dr. Rony Seger The Weizmann Institute of Science, Rehovot, Israel
pSuper-EGFP	For mock transfection of cell lines in pSuper based experiments	Dr.M.Trüss, Charité, CVK, Berlin , Germany
pSuper-ERK1	Suppression of ERK1	Dr. Philippe Lenormand Université de Nice Sophia Antipolis, Nice, France
pSuper-ERK2	Suppression of ERK2	Dr. Philippe Lenormand
pGL2-Irs-1	Luciferase reporter of Irs-1	Dr. M. Schubert University of Cologne, Germany

Table 2. List of primary antibodies used

Antigen name	Mol. wt. (kDa)	Raised in	Company	Cat No.	Concentration (µg / ml)
Akt-1	60	Goat	Santa Cruz	Sc-1618	200
Akt-phospho (Ser 473)	60	Rabbit	New England Biolabs	927-1S	50
BrdU	-	Mouse	Sigma	B2531	Ascites fluid
c-myc tag	-	Mouse	Santa Cruz	Sc-40	200
c-myc tag	-	Rabbit	Abcam	Ab-9106	1000
Flottilin-2	42	Mouse	BD Transduction lab	610383	250
γ-tubulin	48	Mouse	Sigma	T-6557	Ascites fluid
GBP2 (N-17)	67	Goat	Santa Cruz	10581	200
GHR (H-300)	85	Rabbit	Santa Cruz	20747	200
His-tag	-	Mouse	Qiagen	34610	100
IL-15 (L-20)	15	Goat	Santa Cruz	Sc-1296	200
Irs-1	187	Rabbit	Upstate Millipore	06-248	270
Ki-67	340	Rat	Dako	M7249	-
KLF5 (BTEB2)	57	Rabbit	Santa Cruz	22797	200
KLF5	57	Rabbit	Abcam	Ab 24331	1000
MAPK (p44/42) protein	44/42	Rabbit	Cell signalling	9102	10
Phospho MAPK(p44/42)	44/42	Rabbit	Cell signalling	9101S	110
MEK1/2 protein	45	Rabbit	Cell signalling	9122	108
p21	21	Rabbit	Santa cruz	Sc-397	200
TCF4	72+57	Rabbit	Cell signalling	2566	32

Table 3. List of secondary antibodies used

Against	Raised in	Conjugated with	Company	Cat.no.	Concentration (µg / ml)
Rabbit IgG(H+L)	Goat	Peroxidase	Dianova	111-035-003	800
Mouse (IgG+IgM)	Goat	Peroxidase	Dianova	115-035-044	800
Goat (IgG)	Donkey	Peroxidase	Santa cruz	Sc-2020	400
Rabbit	Donkey	Cy3	Dianova	711-165-152	1500

8 Results

8.1 What are the effects of UDCA on the colonic epithelium of mice with DSS-colitis?

8.1.1 Set-up of the experiment: mice with colitis

To understand the effect of UDCA on proliferation of the colonic epithelial cells under the conditions of DSS-colitis, the following experimental setup was used. The CBL57/6J mice were divided into five groups with 24 mice each and were named and fed as follows:

Nontreated **:** AIN-76 diet + water

Green **:** AIN-76 diet + 0.7% DSS in water

Yellow **:** AIN-76 diet with 0.08 % UDCA + 0.7% DSS in water

Orange **:** AIN-76 diet with 0.2 % UDCA + 0.7% DSS in water

Red **:** AIN-76 diet with 0.4 % UDCA + 0.7% DSS in water

Mice were given autoclaved water with 0.7% DSS for one week and then water without DSS for 10 days. Mice were sacrificed at the end of the fifth DSS / water cycle i.e. on the 86^{th} day from the start of the experiment. In 18 mice per group, the colon was prepared for immunohistochemical staining. In the Green and Red group alone the remaining six mice were sacrificed and the colonic epithelial cells were processed for the Affymetrix microarray analysis. The mRNA from two mice was pooled and used per chip. Three chips per group were used.

8.1.2 Effect of DSS-colitis on colonic crypt length and proliferation

To find out the effect of DSS-colitis on the length of colonic crypts and on the proliferation of crypt epithelial cells, the total number of epithelial cells per crypt and the total number of Ki-67 expressing cells per crypt was compared between the nontreated mice and the mice with DSS-colitis.

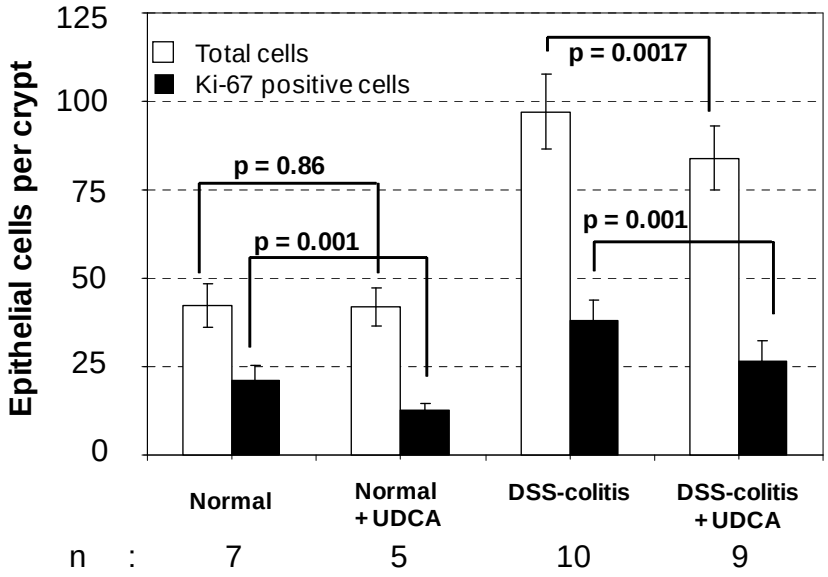

Fig. 6. Effect of UDCA treatment on proliferation of colonic epithelial cells in normal mice or in mice with DSS-colitis.
The epithelial cells per crypt and cells expressing Ki-67 were counted. Mean values ± SD of 25 crypts per mice. p-value was calculated by Student's t-test. Evaluated by three observers.

DSS-colitis caused an increase in the number of epithelial cells per crypt from 42 ± 6 cells in normal mice to 97 ± 10 cells in DSS-colitis mice. The number of Ki-67 expressing epithelial cells also increased from 20 ± 4 to 36 ± 6 (Fig. 6). Thus it was concluded that DSS-colitis increases colonic epithelial cell proliferation. The effect of UDCA treatment on proliferation of colonic epithelial cells in normal mice has been mentioned in 8.2.2.

8.1.3 Effect of UDCA on proliferation of inflamed epithelium

To find out the effect of UDCA treatment on epithelial cell proliferation and crypt length in the inflamed epithelium, the total number of epithelial cells per crypt and Ki-67 expressing cells was compared between DSS-colitis mice and DSS-colitis mice treated with 0.4% UDCA. The total number of cells per crypt decreased from 97 to 82 ($p = 0.0017$) and the number of Ki-67 expressing cells decreased from 36 to 26 ($p = 0.001$) (Fig. 6). Thus after treatment with UDCA there was a significant decrease in epithelial cell proliferation in DSS-colitis mice.

8.1.4 Genes which are differentially expressed due to DSS-colitis

To identify the proliferation-associated genes differentially expressed due to DSS-colitis, the genes which were up- or down-regulated in DSS-colitis mice as compared to the normal mice were shortlisted. The evaluation criteria were: signal intensity > 50, fold change >1.52 and p value < 0.05.

8.1.4.1 Genes upregulated by DSS-colitis

There are 143 genes which are upregulated in the DSS-colitis mice as compared to normal mice. Among these 143 genes (listed as supplementary Table 11.), the genes whose increased expression would enhance cell proliferation have been identified and listed.

Table 4. Proliferation-promoting genes upregulated in DSS-colitis mice.
Selection of genes whose expression is upregulated in DSS-colitis mice compared to that in normal mice. The evaluation criteria were: signal intensity > 50, fold change >1.52 and p value < 0.05. Fold change is the ratio of signal intensity of genes in mice with DSS-colitis to the signal intensity in normal mice.

Affymetrix id	Gene Symbol	Gene Name	Fold Change
1424688_at	Creb3l3	cAMP responsive element binding protein 3-like 3	3,01
1427711_a_at	Ceacam1	CEA-related cell adhesion molecule 1	2,63
1448573_a_at	Ceacam10	CEA-related cell adhesion molecule 10	6,54
1424830_at	Ccnk	cyclin K	3,46
1435906_x_at	Gbp2	guanylate nucleotide binding protein 2	3,05
1419043_a_at	Iigp1	interferon inducible GTPase 1	6,79
1425862_a_at	Pik3c2a	phosphatidylinositol 3-kinase, C2 domain containing, alpha polypeptide	2,22
1451969_s_at	Parp3	poly (ADP-ribose) polymerase family, member 3	3,77
1421646_a_at	Pias3	protein inhibitor of activated STAT 3	2,43
1417333_at	Rasa4	RAS p21 protein activator 4	2,88
1425929_a_at	Rnf14	ring finger protein 14	1,88
1448377_at	Slpi	secretory leukocyte peptidase inhibitor	4,53
1416576_at	Socs3	suppressor of cytokine signaling 3	3,25
1419132_at	Tlr2	toll-like receptor 2	5,67
1421908_a_at	Tcf12	transcription factor 12	2,03
1418099_at	Tnfrsf1b	tumor necrosis factor receptor superfamily, member 1b	2,62

There were 16 proproliferative genes whose expression increased in the mice with DSS-colitis as compared to the normal mice (Table 4.). These were the potential candidate genes responsible for the increase in the proliferation of colonic epithelial cells in mice with DSS-colitis.

8.1.4.2 Genes downregulated by DSS-colitis

169 genes (Supplementary Table 12.) were downregulated in the DSS-colitis mice as compared to the normal mice. Out of these 169 genes suppressed in DSS-colitis, only suppression of Chek1, which is an antiproliferative gene, could have contributed to the increase of proliferation observed in mice with DSS-colitis (Table 5.).

Table 5. Proliferation-inhibiting genes downregulated in DSS-colitis mice
Selection of genes whose expression is downregulated in DSS-colitis mice compared to normal mice. The evaluation criteria were: signal intensity > 50, fold change >1.52 and p value < 0.05. Fold change is the ratio of signal intensity in DSS-colitis mice to the signal intensity in normal mice.

Affymetrix id	Gene Symbol	Gene Name	Fold Change
1449708_s_at	Chek1	checkpoint kinase 1 homolog (S. pombe)	0,37

Since not many antiproliferatory genes were downregulated in mice with DSS-colitis, it was concluded that they are not responsible for the increase in the colonic epithelial cell proliferation in DSS-colitis mice.

8.1.5 Effect of UDCA treatment on gene expression in DSS-colitis mice

To identify the genes whose expression was changed in mice with DSS-colitis after UDCA treatment, the expression of genes in the DSS-colitis mice was compared with that of DSS-colitis mice treated with 0.4% UDCA. Genes which fulfilled the criteria: signal intensity > 50, fold change >1.52 and p value < 0.05 were shortlisted.

8.1.5.1 Genes upregulated in DSS-colitis+UDCA mice vs. DSS-colitis

153 genes (Supplementary Table 13.) were upregulated by UDCA treatment of mice with DSS-colitis. The genes whose expression inhibits proliferation were shortlisted (Table 6.).

Table 6. Proliferation-inhibitory genes upregulated in DSS-colitis mice by UDCA treatment.
Genes whose expression in DSS-colitis mice treated with UDCA is higher than in DSS-colitis mice were selected. The evaluation criteria were: signal intensity > 50, fold change >1.52 and p value < 0.05. Fold change is the ratio of signal intensity in DSS-colitis mice+UDCA to the signal intensity in DSS-colitis mice.

Affymetrix id	Gene symbol	Gene Name	Fold change
1415773_at	Ncl	Nucleolin	1.55
1416664_at	Cdc20	cell division cycle 20 homolog (S. cerevisiae)	1.55
1415878_at	Rrm1	ribonucleotide reductase M1	1.61
1427742_a_at	Klf6	Kruppel-like factor 6	1.65
1420931_at	Mapk8	mitogen-activated protein kinase 8	1.69
1416157_at	Vcl	Vinculin	1.72
1448377_at	Slpi	secretory leukocyte peptidase inhibitor	2.13

Among these 6 antiproliferatory genes Klf6 has been previously investigated and shown to inhibit proliferation by inhibition of transcription of other proproliferative genes and inhibition of cyclin-Cdk complexes by direct binding (119). Klf6 has also been reported to be mutated in gastric cancer (120).

8.1.5.2 Genes downregulated in DSS-colitis+UDCA mice vs. DSS-colitis mice

57 genes (Table 14.) were downregulated in DSS-colitis mice by UDCA treatment. From these 57 genes, the genes whose suppression would have an antiproliferatory effect were shortlisted (Table 7.).

Table 7. Genes downregulated in mice with DSS-colitis by UDCA treatment.
Selection of genes whose expression is downregulated in mice with DSS-colitis treated with UDCA compared to DSS-colitis mice. Genes fulfilling the criteria: signal intensity > 50, fold change >1.52 and p value < 0.05 were shortlisted. Fold change is the ratio of signal intensity in DSS-colitis mice+UDCA to the signal intensity in DSS-colitis mice.

Affymetrix id	**Gene symbol**	**Gene Name**	**Fold change**
1419042_at	Iigp1	interferon inducible GTPase 1	0.44
1419235_s_at	Helb	helicase (DNA) B	0.59
1424218_a_at	Creb3l4	cAMP responsive element binding protein 3-like 4	0.60
1435906_x_at	Gbp2	guanylate binding protein 2	0.56
1455462_at	Adcy2	adenylate cyclase 2	0.57

8.1.5.3 Genes upregulated in DSS-colitis mice and returning to normal expression level in DSS-colitis mice treated with UDCA

The original hypothesis was that DSS-colitis changes the expression of carcinogenesis-relevant genes and that the chemopreventive action of UDCA is based on its ability to act upon these genes and bring their expression to a normal level. Hence it was decided to identify those genes which are upregulated in mice with DSS-colitis but whose expression returns to normal upon treatment with UDCA.

The genes upregulated in DSS-colitis mice (related to those in normal mice) were compared with the genes upregulated in DSS-colitis+UDCA mice (related to those in normal mice). The genes which were found to be upregulated only in DSS-colitis mice and not in DSS-colitis+UDCA mice were listed.

Table 8. Proliferation-associated genes upregulated in DSS-colitis mice which return to normal level upon UDCA treatment.

The list of genes whose expression is upregulated in DSS-colitis mice and the list of genes whose expression is upregulated in DSS-colitis+UDCA mice were compared. The genes which were upregulated in DSS-colitis but either not upregulated or less upregulated in DSS-colitis mice treated with UDCA, were shortlisted. The evaluation criteria were: signal intensity > 50, fold change >1.52 and p value < 0.05. In this table only genes which enhance cell proliferation are listed.

Affymetrix id	Gene Symbol	Gene Name
1450387_s_at	Ak3l1	adenylate kinase 3 alpha-like 1
1452351_at	Parp4	Poly (ADP-ribose) polymerase family, member 4
1424830_at	Ccnk	cyclin K
1424688_at	Creb3l3	cAMP responsive element binding protein 3-like 3
1418240_at	Gbp2	guanylate nucleotide binding protein 2
1419042_at	Iigp1	interferon inducible GTPase 1
1422574_at	Mxd4	Max dimerization protein 4
1417333_at	Rasa4	RAS p21 protein activator 4
1425929_a_at	Rnf14	ring finger protein 14
1416576_at	Socs3	suppressor of cytokine signaling 3
1416975_at	Stam2	signal transducing adaptor molecule (SH3 domain and ITAM motif) 2

Amongst the genes which were upregulated in DSS-colitis, expression of 80 genes returned to the normal level after UDCA treatment (Table 15.). Out of these 80 genes, the proliferation-promoting genes have been listed in Table 8. The return to the

normal level of these genes could be responsible for the antiproliferative effect of UDCA.

8.1.6 Validation of the microarray data of the DSS-colitis mice

To test the correctness of the data obtained in the microarray experiment real time RT-PCR was performed using the same RNA as in the microarray experiment with gene specific primers for Gbp2, SOCS3, CcnK and Mxd4 (Table 8.).

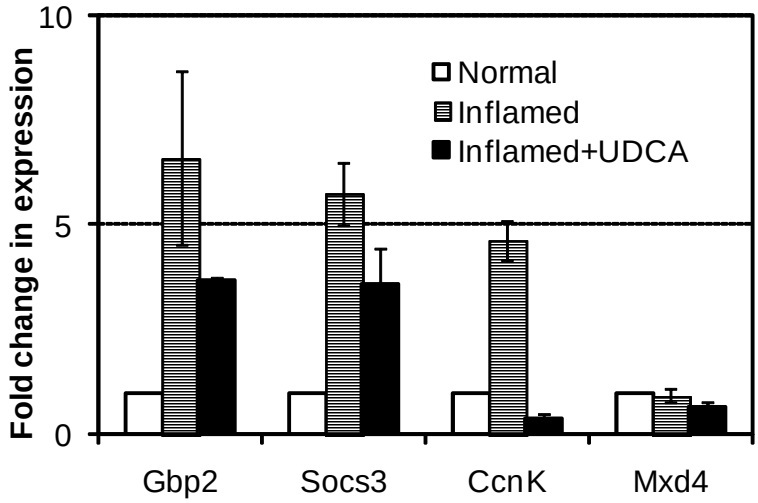

Fig. 7. Validation of the results of Affymetrix arrays of DSS-colitis mice
Validation of microarray data by real time RT-PCR using gene-specific primers against four genes from Table 8. PCR was performed twice from two different cDNA preparations from the RNA used for the arrays. Mean values of 4 PCRs ± SD.

The results of the arrays were confirmed for Gbp2, Socs3 and Cyclin-K but not for Mxd4. Based on literature data (121, 122), Gbp2 appeared to be the best candidate gene among the other genes. Therefore it was investigated in detail in an *in vitro* system. (Point 8.3.5).

8.2 What are the effects of UDCA treatment on the normal colonic epithelial cells *in vivo*?

8.2.1 Set up of the experiment

The CBL57/6J mice were divided into 5 groups with 12 mice each and were fed for 3 weeks with a diet containing UDCA at increasing concentrations. Each group was fed as follows:

Nontreated **:** AIN-76 diet

UDCA (0.002%) **:** AIN-76 diet + 0.002 % UDCA

UDCA (0.004%) **:** AIN-76 diet + 0.004 % UDCA

UDCA (0.04%) **:** AIN-76 diet + 0.04 % UDCA

UDCA (0.4%) **:** AIN-76 diet + 0.4 % UDCA

At the end of 3 weeks, the colons of 6 mice per group were processed for immunohistochemistry. From the remaining 6 nontreated mice and 6 mice of the 0.4% UDCA group, RNA was isolated and purified. RNAs of 2 mice were pooled and used for the Affymetrix array experiment. Thus 3 chips for the nontreated mice and 3 for the UDCA-treated mice were used.

8.2.2 Inhibition of proliferation of normal colonic epithelial cells by UDCA

To investigate if UDCA influenced the proliferation of intestinal epithelial cells, Ki-67 expression and BrdU incorporation were compared between the nontreated and the UDCA-treated groups of mice.

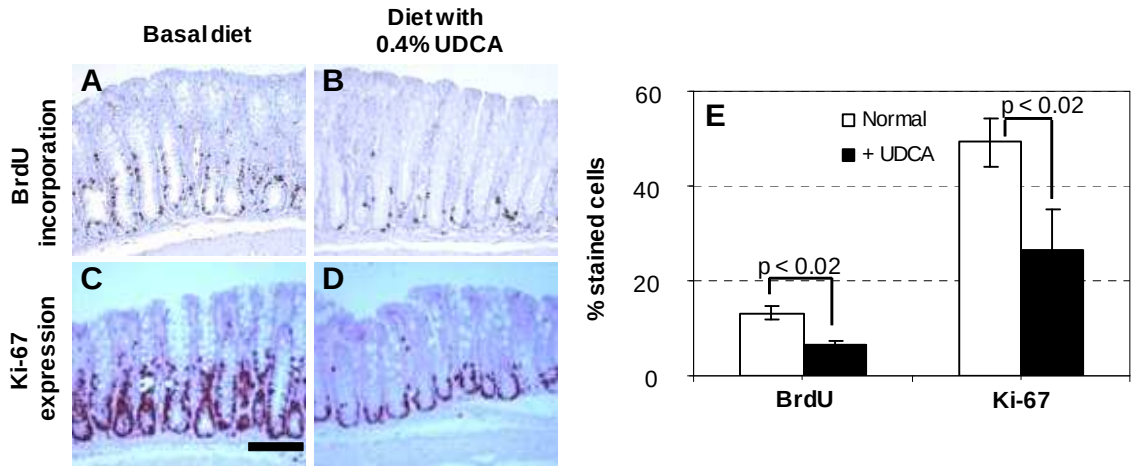

Fig. 8. Feeding UDCA (0.4%) for three weeks decreases the frequency of BrdU incorporation and Ki-67 expression in normal murine colonic epithelium.

Representative staining of: A, B.: incorporated BrdU; C, D.: Ki-67 protein; E.: More than forty crypts per mice and three (BrdU) or six (Ki-67) mice were evaluated in each group. Mean values of % of stained cells ± SD. The p-value was calculated by Student's t-test. Bar: 100 µm. Immunohistochemistry was carried out in collaboration with Prof.C.Loddenkemper at Institute of Pathology, Charité Campus Benjamin Franklin.

Treatment of mice with UDCA reduced the incorporation of BrdU from 12 % in nontreated to 6 % in UDCA treated (50 % decrease, $p<0.02$) and decreased the number of cells expressing Ki-67 from 50 % in nontreated to 29 % in UDCA treated (42% decrease, $p<0.02$). After three weeks of treatment with UDCA there was no change in the total number of epithelial cells per crypt (42 ± 6) (Fig. 6). Thus treatment of mice for 3 weeks with 0.4% UDCA decreases epithelial cell proliferation without altering the crypt length.

8.2.3 The proliferation inhibition was dose-dependent

To check if the inhibition of proliferation in mice was dose-dependent, the decrease in the frequency of Ki-67 expressing cells and of phospho-(Ser10)-HistoneH3 expressing cells was evaluated in mice treated with increasing concentrations of UDCA.

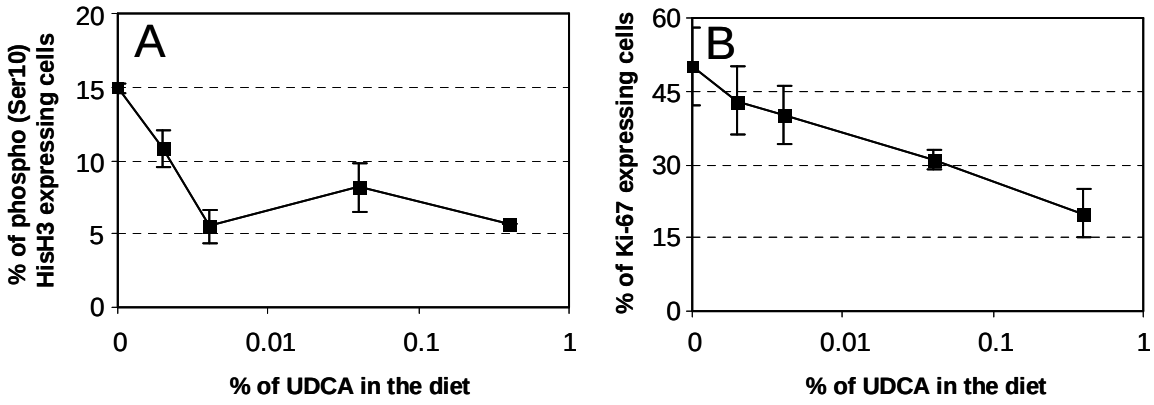

Fig. 9. Dose-dependent inhibition of proliferation of murine colonic epithelial cells by UDCA. A.: Percentage of cells expressing phosphorylated (Ser10) Histone H3; B.: Percentage of cells expressing Ki-67 protein in sections of mice treated with UDCA at different concentrations for 3 weeks. Mean $\pm$ SD. More than 50 crypts evaluated per mice.

The decrease of percentage of cells expressing Ki-67 from 15% to 6% and of cells expressing phosphorylated Histone-H3 from 27% to 10% was dose-dependent. The effect was measurable already at a very low concentration of UDCA (0.002%). There was, however, no effect on the total number of epithelial cells per crypt after treatment with 0.4% UDCA for 3 weeks (Fig. 6.).

8.2.4 UDCA influenced expression of proliferation-associated genes in murine colonic epithelial cells

To determine which genes are differentially expressed in the murine colonic epithelial cells due to UDCA treatment, the microarray data of the nontreated mice were compared with that of the UDCA (0.4%) treated mice.

8.2.4.1 Genes upregulated by UDCA treatment of mice

To find out the genes whose expression is upregulated by UDCA treatment of mice colonic epithelial cells, the signal intensities of genes in the UDCA treated group was compared with signal intensities of genes in the nontreated group. The evaluation criteria were: signal intensity > 50, fold change > 1.52, $p < 0.05$.

Table 9. Genes upregulated in normal mice after treatment with UDCA.
Genes whose expression is upregulated in mice treated with UDCA as compared to normal mice. The criteria were: signal intensity > 50, fold change >1.52 and p value < 0.05. Fold change is the ratio of signal intensity in UDCA-treated mice to the signal intensity in normal mice.

In the UDCA-treated group 137 genes were upregulated (Table 16.) and 206 genes were downregulated (Table 17.) more than 1.52 fold as compared to the normal group ($p<0.05$). Out of the 137 upregulated genes, 9 genes which might play an anti-proliferative role in the colonic epithelial cells are shown in Table 9.

8.2.4.2 Validation of microarray data by real time RT-PCR of genes upregulated by UDCA

To confirm the correctness of the array results, quantitative real time RT-PCR was performed with gene specific primers for 7 genes from Table 9, using the RNA which was used for carrying out the microarray experiment.

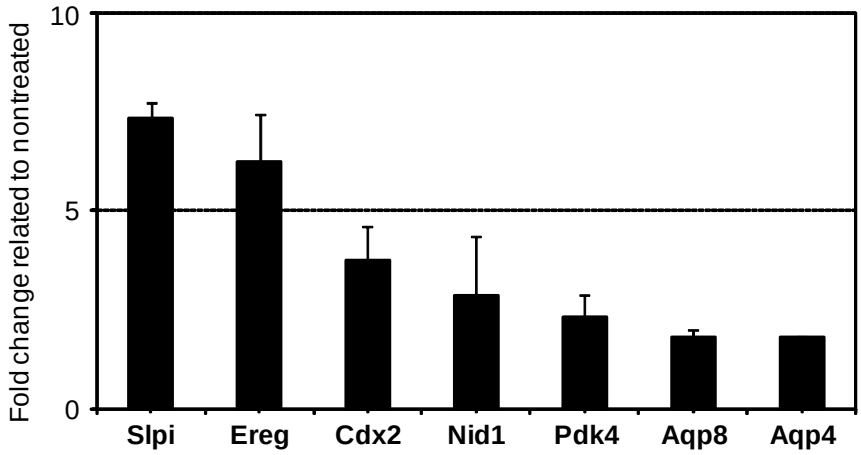

Fig. 10. Real time RT-PCR of genes upregulated by UDCA in murine colonic epithelia.
The upregulation of 7 genes selected from Table 9. was tested by real time RT-PCR. PCRs were performed twice from two different cDNA preparations from the same RNA used for the arrays. Fold change in expression relative to the expression in nontreated mice is calculated. Mean of 4 PCRs ± SD.

All the genes which were found to be upregulated in mice treated with UDCA (as found in the microarray experiment) were confirmed by real time RT-PCR to be indeed upregulated. Slpi and Ereg were the most upregulated genes and aquaporins were the least upregulated among the 9 shortlisted genes (Table 9.)

8.2.4.3 Genes downregulated by UDCA treatment in mice

To identify genes downregulated by UDCA, the signal intensities of the nontreated group were compared with those of the UDCA-treated group. The evaluation criteria were signal intensity > 50, fold change > 1.52 and $p < 0.05$.

Table 10. Genes downregulated by UDCA in normal murine colonic epithelial cells.
Genes whose expression is downregulated in mice treated with UDCA as compared to normal mice. The evaluation criteria were signal intensity > 50, fold change >1.52 and p value < 0.05. Fold change is the ratio of signal intensity in UDCA treated mice to the signal intensity in normal mice.

Affymetrix No.	Gene	Name	Fold change
1417962_s_at	Ghr	growth hormone receptor	0.68
1451739_at	Klf5	kruppel-like factor 5	0.58
1427008_at	Rnf43	ring finger protein 43	0.57
1434149_at	Tcf4	transcription factor 4	0.57
1423104_at	Irs1	insulin receptor substrate 1	0.54
1438164_x_at	Flot2	flotillin 2	0.47
1418219_at	Il15	interleukin 15	0.44
1435906_x_at	Gbp2	guanylate nucleotide binding protein 2	0.32

212 genes were downregulated more than 1.52 fold in UDCA-treated mice as compared to the normal mice ($p<0.05$) (Table 17.). Genes shown in Table 10. have been reported to be proproliferative. These genes were further explored in search of genes mediating the antiproliferative effects of UDCA.

8.2.4.4 Validation of microarray data by real time RT-PCR of genes downregulated by UDCA

To validate the microarray data, real time RT-PCR was performed with gene-specific primers for selected genes from Table 10. , using the RNA which was used for the microarray experiment.

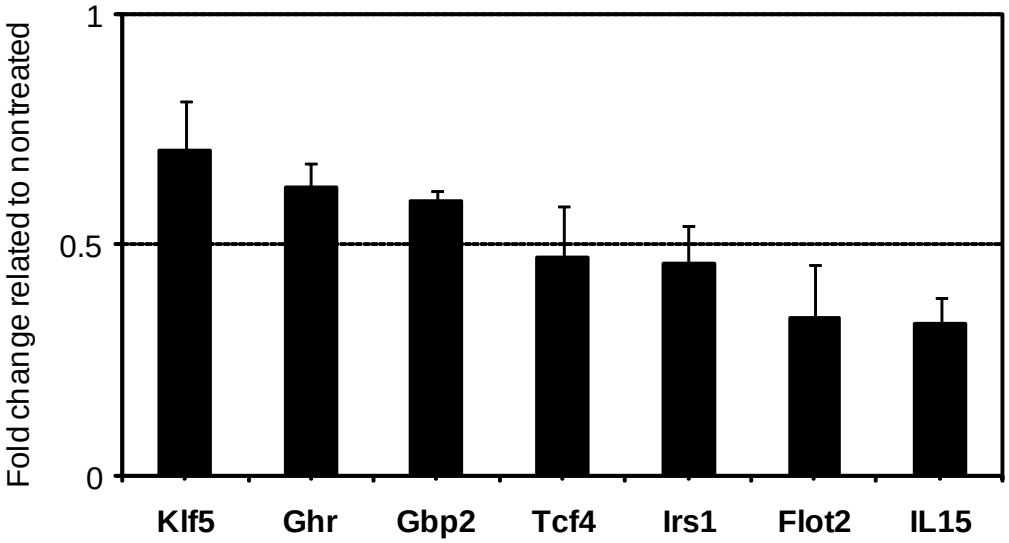

Fig. 11. Validation of microarray experiment with selected genes downregulated by UDCA in mice.
The 7 upregulated genes selected from Table 10. were tested by real time RT-PCR. PCRs were performed twice from two different cDNA preparations from the RNA used for the arrays. Fold change in expression relative to the expression in nontreated mice is calculated. Mean values of 4 PCRs $\pm$ SD.

All the changes of gene-expression observed in the microarray experiment were confirmed by real time RT-PCR. The decrease in expression of these genes was associated with a decrease in proliferation of murine colonic epithelial cells. Since these genes are proproliferative, one or more of them could be mediating the antiproliferatory effect of UDCA.

The immediate question was which of these genes are responsible for the antiproliferative effect of UDCA.

8.3 What are the effects of UDCA treatment *in vitro*?

In order to have an *in vitro* model system allowing to reconstruct the alterations occurring *in vivo* and to investigate the molecular mechanism of action of UDCA, a cell line whose proliferation was inhibited by UDCA and which shows similar genetic alterations as found in the mice, was required.

8.3.1 What are the effects of UDCA treatment on colon cancer cells *in vitro*?

Several established colon cancer cell lines were treated with UDCA and cell proliferation was investigated by MTT-assay (Fig. 12.) The effect on cell cycle was measured by analysing propidium-iodide stained cells by FACS (Fig. 13.) Changes in expression of genes previously identified *in vivo* by microarrays (Table 9. & Table 10.) were tested by real time RT-PCR.

8.3.2 Effect of UDCA on colon cancer cell proliferation

To determine the effect of UDCA on colon cancer cell proliferation, MTT test was carried out 3 days after start of treatment with UDCA (400 µM).

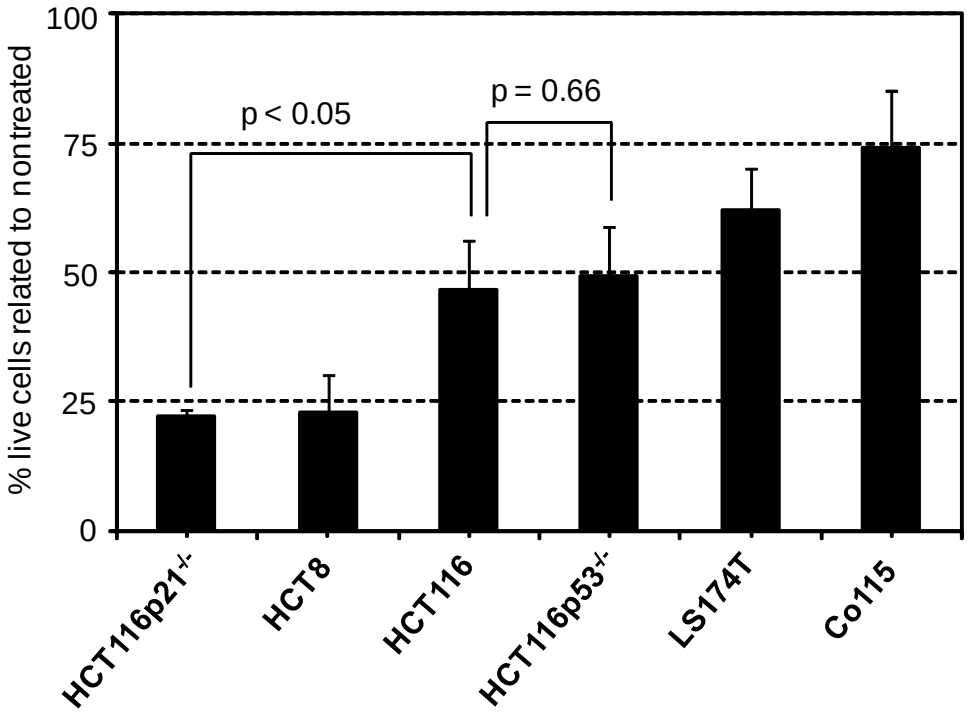

Fig. 12. Inhibition of colon cancer cell proliferation by UDCA.
MTT test of colon cancer cells treated with 400 µM UDCA for 3 d. Percentage of live cells in UDCA-treated cells related to respective nontreated controls ± SD; n>3 for each cell line. Part of the data contributed by Roser Peiro Jordan.

UDCA inhibited the proliferation of all the colon cancer cell lines investigated. The cell lines HCT8 and HCT116 were most strongly inhibited. HCT116p53$^{-/-}$ cell line had almost the same inhibition as the parental HCT116 cell line up to 50% ($p = 0.66$), ruling out a role of p53 in proliferation inhibition. HCT116p21$^{-/-}$ cell line was inhibited significantly stronger than HCT116 cell line, up to 80% ($p < 0.05$), suggesting that the absence of p21 increases the sensitivity to UDCA.

8.3.3 Effect on UDCA treatment on cell cycle progression

To check if the decrease in proliferation is due to slow down of the cell cycle, HCT116 cells were synchronized in G2/M phase by nocodazole treatment and then released in the presence or absence of UDCA (Fig. 13.) Time course of the release was followed for 45 h by FACS.

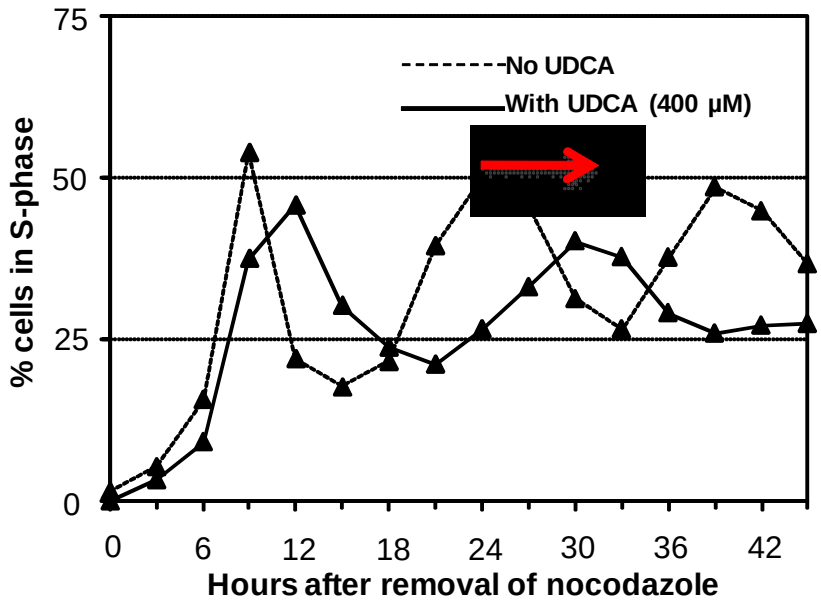

Fig. 13. Cell cycle slow-down in HCT116 cell line after UDCA treatment.
HCT116 cells were arrested in G2M phase by treatment with nocodazol (50 ng/ml, 24 h), then washed with standard medium and released in medium containing UDCA(—▲—) or medium without UDCA (–·▲·–) and harvested every 3 h for 45 h. The percentage of cells in S-phase was determined by FACS. The red arrow marks the delay of 6 h in the second S-phase peak of cells treated with UDCA. The FACS measurements were done by M.L.Hanski.

UDCA-treated HCT116 cell line shows a slower progression through the cell cycle than the nontreated. After release from the G2/M arrest, the nontreated cells enter the S-phase within 3 h and reach a maximum of 55% in 9 h. The subsequent peak of S-phase occurred 15 h later. Cells released from the G2/M arrest in the presence of 400 µM UDCA showed the first peak of S-phase at 12 h and the second peak at 30 h. The red line shows about 6 h of difference between the second S-phase peaks. The slow progression through the cell cycle will contribute to the decrease of proliferation due to UDCA.

8.3.4 Comparison of changes in gene expression caused by UDCA in mice with that in colon cancer cell lines

To investigate in colon cancer cell lines, the expression changes of the UDCA-target genes identified in mice, HCT116 and HCT8 cell lines were treated with UDCA for 3 days and RNA was isolated. The expression of some genes from Table 9. and Table 10. was checked in nontreated and UDCA treated cells by real time RT-PCR.

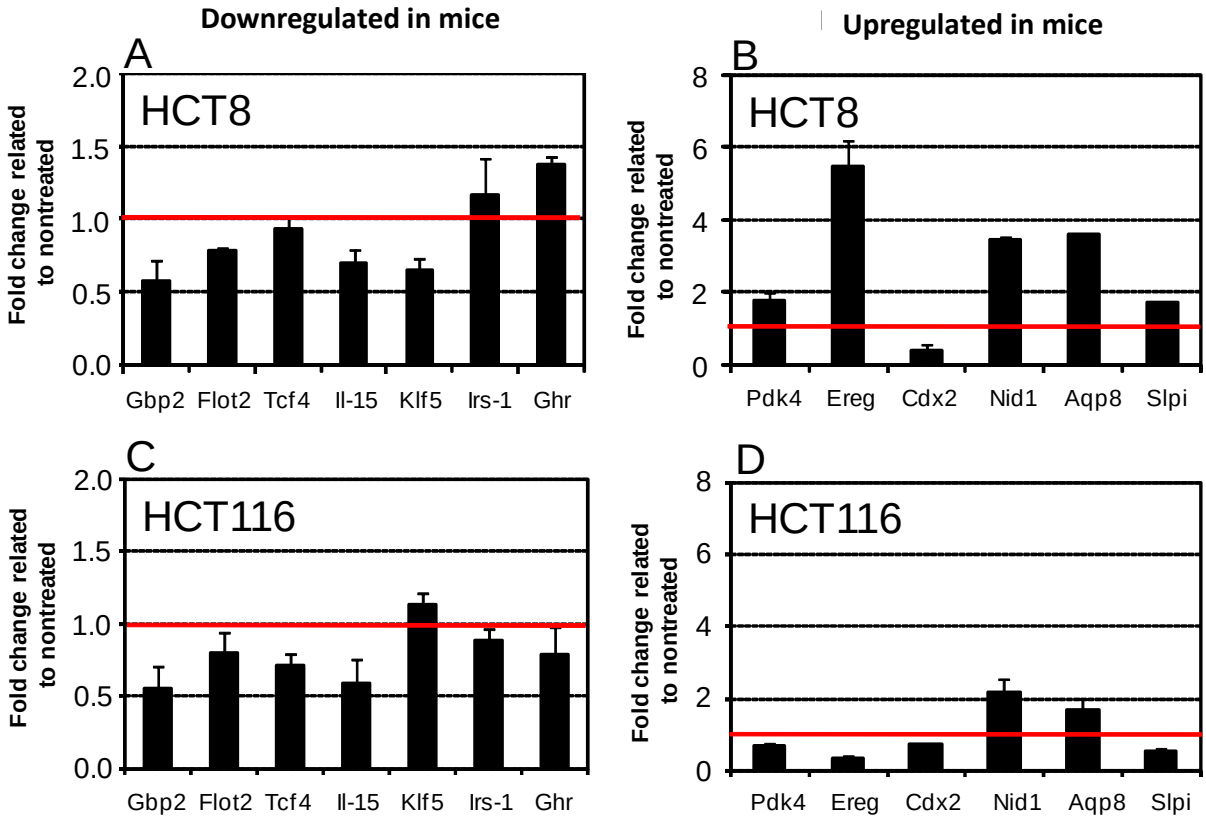

Fig. 14. UDCA-target genes identified in mice are differently affected in human colon cancer cell lines.
7 upregulated genes selected from Table 9. and 6 downregulated genes selected from Table 10. were tested by real time RT-PCR in RNA isolated from colon cancer cell lines HCT8 and HCT116. A. & B.: Up- and downregulated genes tested in HCT8 cell line; C. & D.: Up- and downregulated genes tested in HCT116 cell line. PCRs were performed twice from two different cDNA preparations. The expression level in nontreated cells is marked by the red line. Fold change in expression relative to the expression in nontreated cells is calculated. Mean values of 4 PCRs ± SD.

The UDCA-induced change of expression of most genes investigated *in vitro* in colon cancer cell lines were different from those observed in the mice. Even the two colon cancer cell lines exhibited different expression patterns of both up-and downregulated genes. Gbp2 and Tcf4 were further investigated in the HCT116 cell line as both genes were suppressed in mice as well as in HCT116 cell line after UDCA treatment.

8.3.5 Role of Gbp2 in antiproliferative effects of UDCA

Gbp2 is a member of the interferon (IFN)-induced guanylate-binding protein family of GTPases. It has been shown to be involved in Interferon-γ induced proliferation of fibroblasts (121, 122) . Gbp2 overexpressing fibroblasts also formed tumours in nude mice, whereas fibroblasts expressing mutant Gbp2 did not (121, 122). In the present data, it was the only gene which was upregulated in DSS-colitis mice and whose expression returned to normal level after treatment with UDCA. Gbp2 is also the only gene whose expression is upregulated in DSS-colitis and downregulated in DSS-colitis mice treated with UDCA. Its expression is also decreased in normal mice colonic epithelial cells and in colon cancer cells after treatment with UDCA.

8.3.5.1 Effect of UDCA on Gbp2 protein levels in vivo and in vitro

To test if Gbp2 was also suppressed at protein level, the colonic sections of normal and DSS-colitis-mice with or without UDCA treatment were stained for Gbp2 protein. Additionally, the lysates of colonic epithelial cells from normal mice were analysed by western blotting.

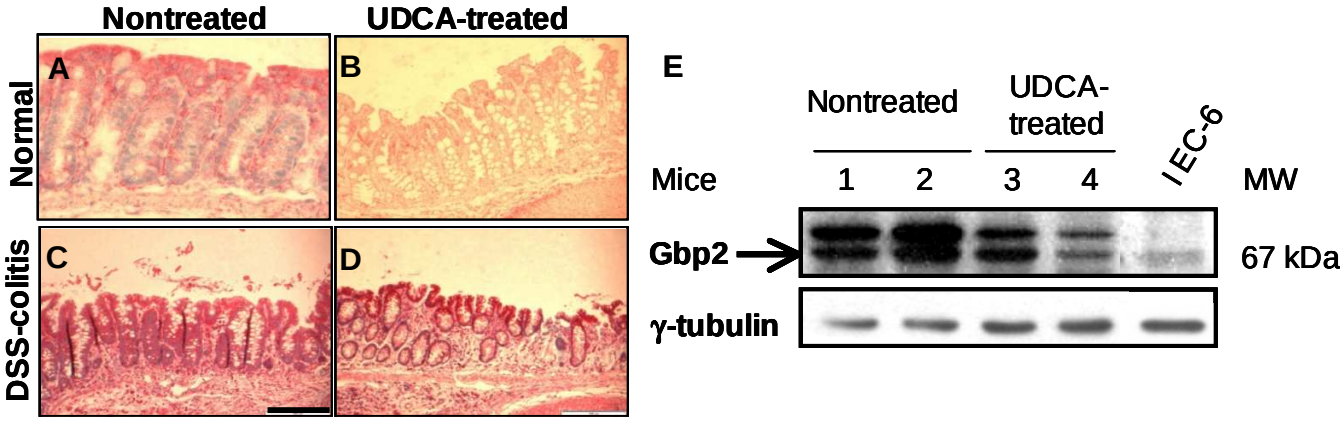

Fig. 15. UDCA-induced decrease in Gbp2 protein in murine colonic epithelial cells.
A.: to D.: Immunohistochemical staining of murine colonic sections with anti-Gbp2 antibody. Bar: 200 µm; E.: Epithelial cells isolated from the murine colonic crypts from nontreated (mice 1,2) and 0.4% UDCA-treated mice (mice 3,4) were subjected to western blotting. γ-tubulin was used as loading control. Western blot representative for 2 experiments. Immunohistochemistry was carried out in collaboration with Prof.C.Loddenkemper at Institute of Pathology, Charité Campus Benjamin Franklin

There is increased expression of Gbp2 protein in DSS-colitis mice compared to normal mice (Fig. 15 A, C). UDCA treatment decreased Gbp2 expression in normal mice (Fig. 15 A, B) and in DSS-colitis mice the expression was both decreased and additionally more concentrated on the uppermost differentiated cells of the crypt (Fig. 15 C, D). The decrease in Gbp2 protein after UDCA treatment of normal mice is also evident in the western blots (Fig. 15E). The decrease in protein amounts of Gbp2 in UDCA treated mice prompted further investigation of the gene.

8.3.5.2 Establishment of Gbp2-overexpressing clone of HCT116 cell line

To find out if decrease in Gbp2 protein levels contribute to the antiproliferative effects of UDCA, Gbp2 overexpressing clone of HCT116 cell line was generated. HCT116 cells were transfected with Gbp2-expressing plasmid (pEGFP-C2-mGbp2) and stable clones were generated by selecting the transfectants in 1 mg / ml of G418 antibiotic. The clone with the highest expression of exogenous-Gbp2 protein was named Clone 6 and the clone transfected with an empty plasmid was named Clone 43. The effect of Gbp2 expression on proliferation was measured by MTT-assay.

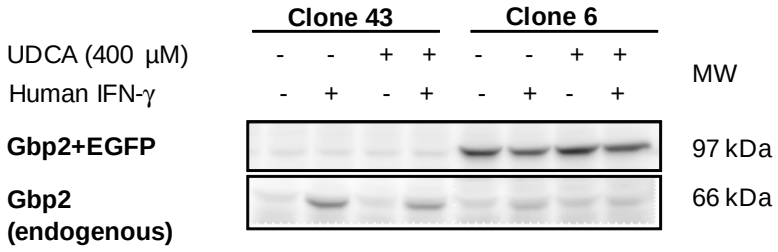

Fig. 16. Overexpression of mGbp2 in transfectant clones of HCT116 cell line.
Overexpression of exogenous Gbp2 in Clone 6. The molecular weight of Gbp2 alone is 66 k Da which together with fused EGFP gives a 97 k Da band, as detected with anti-Gbp2 antibody. Cells were treated with IFN-γ (20 ng /ml) to induce the expression of endogenous Gbp2. The clones were generated and the experiment was done by M.L.Hanski.

IFN-γ treatment induced the expression of endogenous Gbp2 in both clone 43 and clone 6. In clone 6, there was less induction of endogenous Gbp2 due to IFN-γ treatment. Treatment of clone 43 with UDCA resulted in a decrease of endogenous

Gbp2 expression. There was no effect of UDCA treatment on exogenously expressed Gbp2 in clone 6. In comparison to clone 43 the proliferation of clone 6 was 97%. IFN-γ treatment reduced proliferation in both clones by 15%. Treatment with UDCA reduced proliferation of both clone 43 and clone 6 by 35%. The conclusion was that Gbp2 overexpression does not induce basal proliferation nor influence the antiproliferative effect of UDCA.

8.3.5.3 Comparison of UDCA-effect in Gbp2-overexpressing and non-overexpressing clones of HCT116 cell line

It was hypothesized that decrease in Gbp2 protein contributes to the decrease of proliferation after UDCA treatment and hence UDCA must have less effect in Gbp2-overexpressing clones. To test this hypothesis, Clone 6 and Clone 43 were treated with 400 µM UDCA for 3 days and the inhibition of proliferation was compared.

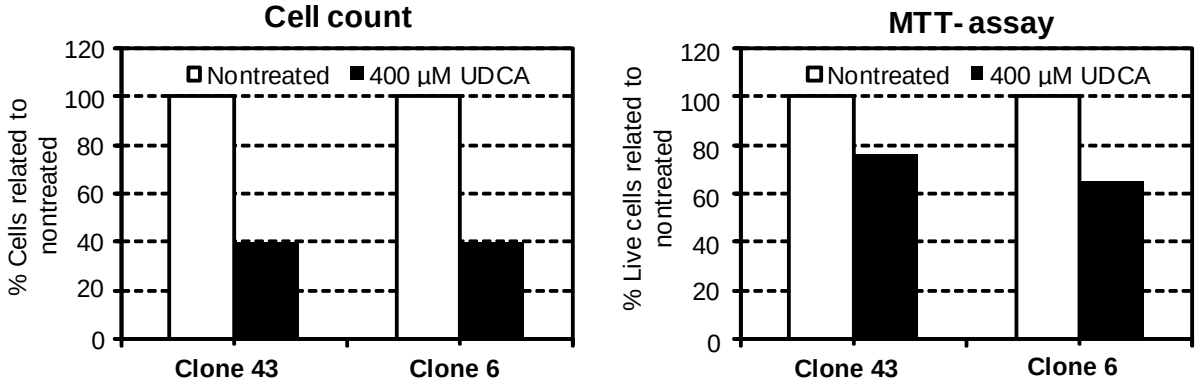

Fig. 17. Effect of UDCA on proliferation of Gbp2 overexpressing clone of HCT116 cell line.
A.: Cell count of Clone 43 and Clone 6 after 3 d of 400 µM UDCA ; B.: MTT-assay of Clone 43 and Clone 6 after 3 d of 400 µM UDCA treatment. Each experiment was done once. MTT-assay was done by M.L.Hanski.

Overexpression of mGbp2 did not influence the basal proliferation of HCT116 cell line: the number of cells was the same in Clone 43 and in Clone 6 under conditions without UDCA. Additionally, there was no difference in the proliferation inhibition caused by UDCA in Clone 43 and Clone 6. Since overexpression of Gbp2 did not influence the response to UDCA in HCT116 cell line, it was concluded that *in vitro,*

the suppression of Gbp2 by UDCA is not the cause of proliferation inhibition. In view of this result no further experiments aiming at Gbp2 suppression (siRNA or dnGbp2 expression) were carried out.

8.3.6 Investigation of Tcf4 in HCT116 cell line

T-cell factor-4 (Tcf4) is a key molecule of *wnt* / β–catenin pathway which is one of the most important pathways regulating the proliferation of colonic epithelial cells. Tcf4 is proproliferatory only when in complex with β–catenin and other Lef-family transcription factors in the nucleus. When Tcf4 is not associated with β catenin, it has been reported to be antiproliferatory (123). The transcription of Tcf4 is suppressed by UDCA treatment (Table 10.) and the question was if this suppression contributed to the antiproliferatory effect of UDCA.

8.3.6.1 Effect of UDCA treatment on Tcf4 mRNA and protein expression in colon cancer cell line

To proof the decrease in transcription of Tcf4 gene detected in arrays after UDCA treatment, HCT116 cell line was transfected with pTcf4-luci reporter plasmid treated with 400 μM UDCA for 2 days and the reporter assay was made. This reporter plasmid contains the promoter of Tcf4 upstream of the luciferase gene. β–galactosidase expression plasmid was used for normalization of transfection efficiency. In parallel, to check if the decrease in transcription also leads to decrease of Tcf4 protein expression, HCT116 cell line was treated with 400 μM UDCA for 3 days and the lysates were analysed by western blotting.

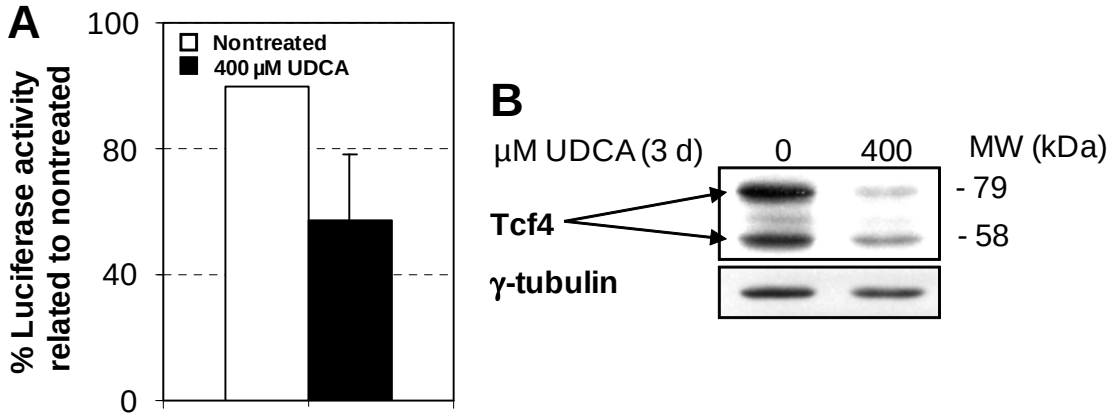

Fig. 18. Effect of UDCA treatment on Tcf4 mRNA and protein expression in HCT116 cell line. A.: The cells were transfected with pTcf4-luci and β-galactosidase expression plasmid in a 24 well plate and treated for 2 days with 400 µM UDCA. The luciferase values were normalized to β-galactosidase expression and related to the values obtained in the nontreated cells. Mean values of 3 experiments ± SD; B.: Western blot showing decrease in expression of Tcf4 in HCT116 treated with 400 µM UDCA for 3 d. γ–tubulin was used as loading control. Representative blots of more than 3 experiments.

UDCA clearly inhibited the transcription of Tcf4 in HCT116 cells as observed in the real time RT-PCR experiment (Fig. 14.). Tcf4 expression was also decreased at the level of protein as seen by western blotting. It was hypothesized that inhibition of Tcf4 by UDCA is the reason for proliferation inhibition by UDCA.

8.3.6.2 Effect of UDCA on transcriptional targets of Tcf4

To check if the decrease in Tcf4 protein expression by UDCA downregulated the transcription of Tcf4 target genes, another Tcf4 luciferase reporter assay called the TOP-Flash / FOP-Flash (Point No. 7.2.6.2) was used. The transfectants were treated with 400 µM UDCA for 2 d and the reporter assay was made.

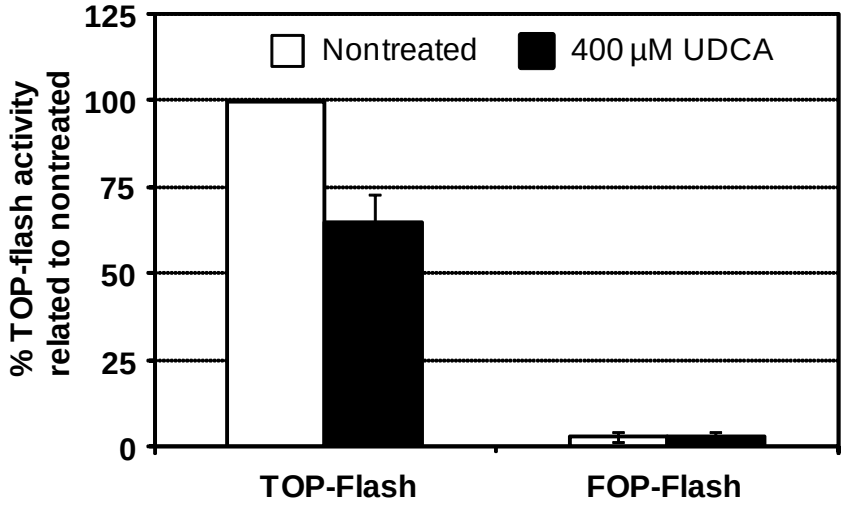

Fig. 19. TOP/FOP luciferase reporter assay in HCT116 cell line treated with UDCA.
HCT116 cell line was transfected with pTOP-Flash or pFOP-Flash reporter plasmids and treated with UDCA for 2 days. The luciferase units are normalized to β-galactosidase values and related to the values obtained in the respective nontreated cells. Mean values ± SD of 3 experiments.

UDCA treatment caused a decrease in TOP-Flash activity i.e. in the presence of UDCA there was a decrease of the transcriptional activity of Tcf4. This experiment indicates that treatment of HCT116 cells with UDCA decreases the expression of Tcf4-target genes. Thus UDCA not only suppresses the transcription of Tcf4 but has the potential to suppress the transcriptional activity of Tcf4.

8.3.6.3 Role of Tcf4 in proliferation-inhibition caused by UDCA

To test how the protein level of Tcf4 influences the antiproliferative effects of UDCA, HCT116 cells were transfected with either wild type Tcf4-expressing plasmid (pFLAG-hTcf4) or with dominant-negative Tcf4 expressing plasmid (pFLAG-hdn-Tcf4) and treated with 400 µM UDCA for 3 days and then counted. Cells transfected with pcDNA3.1-GFP plasmid were taken as control.

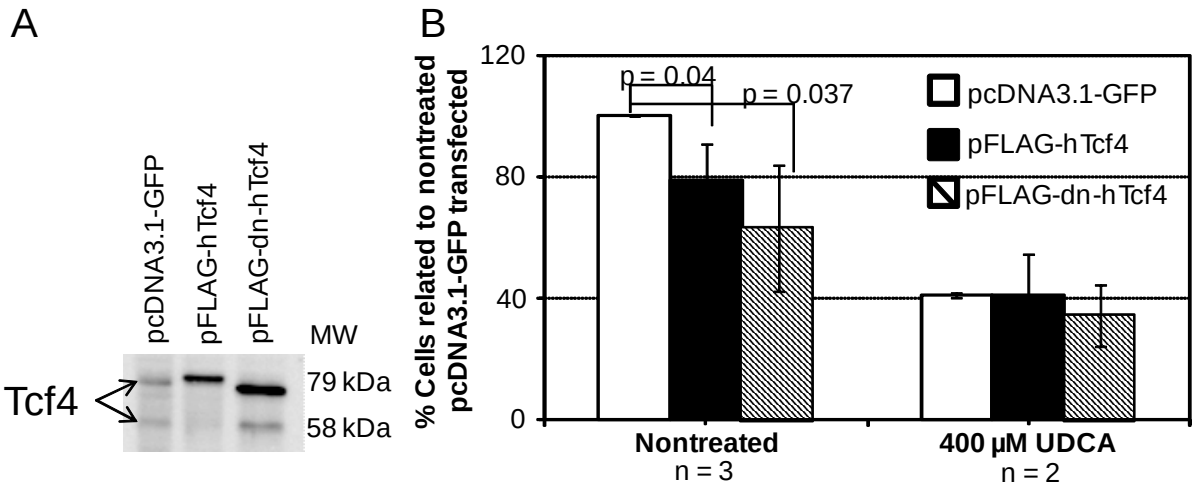

Fig. 20. Effect of Tcf4 or dN-Tcf4 overexpression on the antiproliferative action of UDCA in HCT116 cells.

A.: HCT116 cell line was transfected with plasmids expressing Tcf4 or dN-Tcf4 or with pcDNA3.1-GFP plasmid (mock-transfection) and treated with 400 µM UDCA for 3 d. The lysates were analysed by western blotting and detected using anti-Tcf4 antibody; B.: Total cell count related to the count in nontreated mock-transfectants. Mean values of 2-3 experiments.

Overexpression of either Tcf4 or dn-Tcf4 decreased the proliferation of HCT116 cell line by 20-30 %. Under the UDCA treatment conditions the Tcf4 or dN-Tcf4 overexpressing cells proliferated as the UDCA treated pcDNA3.1-GFP-transfectants (mock).

Since both overexpression of Tcf4 and suppression of endogenous Tcf4 by means of dn-Tcf4 decreased proliferation rate, a conclusive role of Tcf4 on cell proliferation could not be established. It was concluded that decrease of Tcf4 expression is unlikely to be the reason for the antiproliferatory effect of UDCA.

8.4 What are the effects of UDCA treatment on the nontransformed intestinal epithelial cells *in vitro*?

Since human colon cancer cells showed a dramatically different molecular response to UDCA than murine colonic epithelial cells *in vivo*, a nontransformed intestinal epithelial cell line of rodent origin, IEC-6, was tested as a model.

8.4.1 Effect of UDCA on proliferation of IEC-6 cells

In order to test the antiproliferative action of UDCA, IEC-6 cells were treated with UDCA at different concentrations and counted after 3 days.

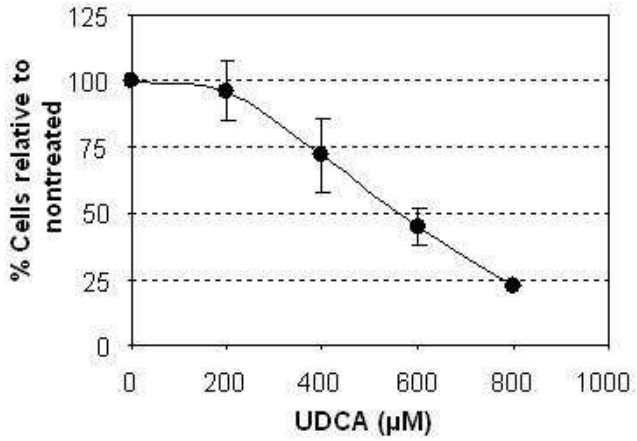

Fig. 21. Dose-dependent proliferation-inhibition of IEC-6 cells by UDCA.
IEC-6 cells were treated with UDCA for 3 d and counted. Percentage of total cell number related to nontreated was calculated. Mean values of more than 5 experiments ± SD.

UDCA treatment for 3 days caused a dose-dependent decrease in proliferation with about 50% decrease at a concentration of 600 µM.

8.4.2 Effect of UDCA on MTT to formazan conversion in IEC-6 cell line

The results of proliferation inhibition by UDCA as determined by total cell count were different to the results of the MTT-assay in IEC-6 cell line and not so in other cell lines. To answer this puzzle, the amount of formazan produced per cell was determined in IEC-6 cell line at different concentrations of UDCA.

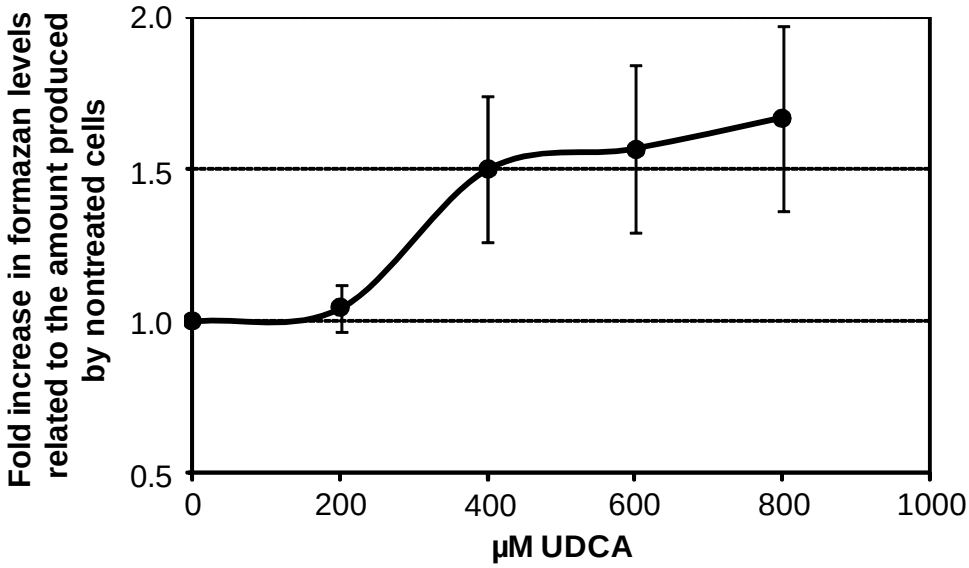

Fig. 22. UDCA treatment enhances conversion of MTT to formazan in IEC-6 cell line in a concentration dependent manner.
MTT assay of IEC-6 cells treated with different concentrations of UDCA for 3 days and then reseeded in equal numbers. The graph shows the fold increase in absorbance of UDCA-treated cells related to absorbance of the same number of nontreated cells. Mean values of 3 experiments ± SD.

UDCA treatment increased the formazan produced per cell in a dose-dependent manner (Fig. 22). This explains why the absorbance obtained in a MTT assay of IEC-6 cells treated with UDCA was not a linear function of the live cell number. The fold increase in formazan production at each UDCA concentration was calculated. It was used to normslize the values obtained in a MTT assay. The curve obtained after normalisation was comparable to the curve obtained by total cell count as readout. For simplicity total cell count was used in all further experiments concerning UDCA.

The conclusion from this experiment is that MTT assay, which is based on metabolic conversion of a substrate, need not be always a linear function of cell number. It could also be dependent on different metabolism of the cells under different treatment conditions.

8.4.3 Expression of UDCA target genes in IEC-6 cells

To check if the target genes of UDCA identified in mice are similarly regulated in IEC-6 cell line, real time RT-PCR was done with RNA isolated from IEC-6 cells cultured in the presence or absence of 600 µM UDCA for 3 days.

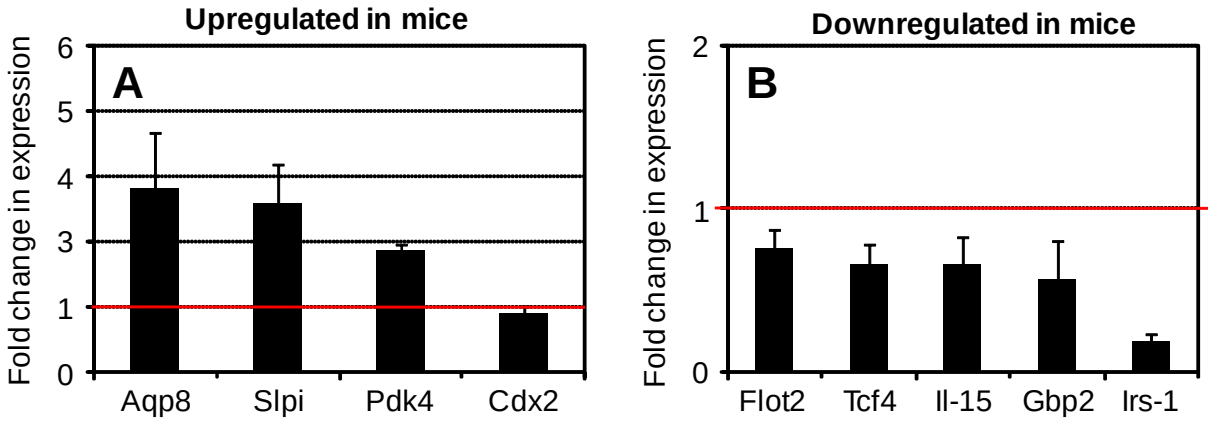

Fig. 23. Real time RT-PCR analysis of UDCA target genes in IEC-6 cells.
Genes differentially regulated in the mice were tested with RNA from IEC-6 cells treated with UDCA. A.: Upregulated genes and B.: Downregulated genes. PCRs were performed twice from two different cDNA preparations from the RNA isolated from nontreated or UDCA treated cells. Fold change in expression relative to the expression in nontreated cells was calculated. Red line indicates the expression level in the nontreated IEC-6 cells. Mean values of fold changes ± SD of 4 RT-PCR experiments.

The genes upregulated in mice were also upregulated in IEC-6, with the exception of Cdx2. The 5 downregulated genes which were downregulated in mice were also downregulated in IEC-6 cell line. Tcf4 and Gbp2 were not further investigated due to prior results. The role of Irs-1 gene was investigated in detail in IEC-6 cells as this gene was more suppressed than the other genes shortlisted.

8.4.4 Investigation of apoptosis in IEC-6 cells treated with UDCA

To test if the treatment of IEC-6 with UDCA caused any apoptosis, both the nontreated and UDCA-treated IEC-6 cells were stained with DAPI and the morphology of the nuclei was evaluated under UV-microscope.

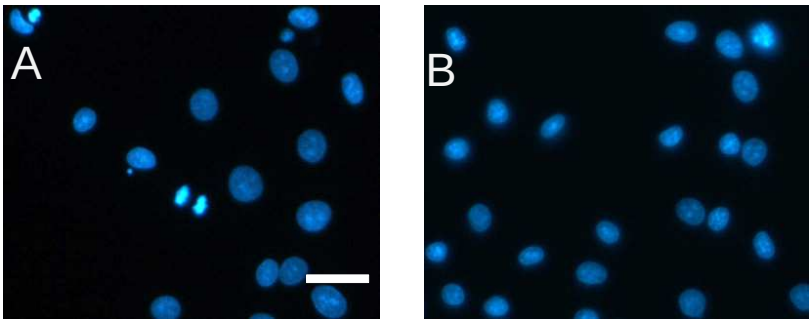

Fig. 24. Effect of UDCA treatment on nuclear morphology of IEC-6 cells.
Nontreated and UDCA-treated (600 µM) IEC-6 cells were stained with DAPI and the nuclear morphology was observed. A.: Nontreated IEC-6 cells; B.: UDCA treated (600 µM, 3d) IEC-6 cells. Photographs representative for 3 experiments. Bar: 50 µm.

There were no condensed nuclei found after UDCA treatment of IEC-6 cells. It was concluded that the decrease in proliferation was not due to apoptosis.

8.4.5 Investigation of senescence in IEC-6 cells treated with UDCA

To investigate if the decrease in proliferation caused by UDCA was due to senescence, IEC-6 cells were treated with UDCA for 3 days and then β-galactosidase (a marker of senescence) activity was detected using X-gal.

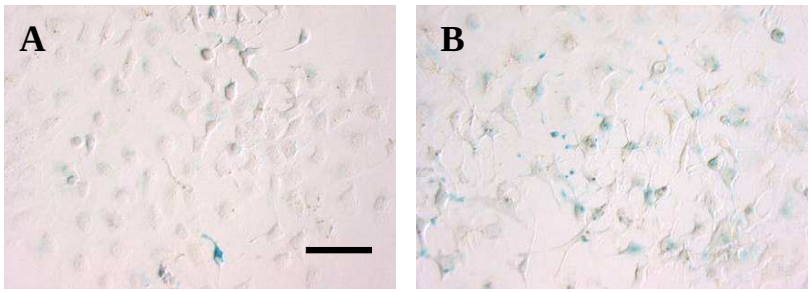

Fig. 25. Assay of β-galactosidase activity for detection of senescence in UDCA-treated IEC-6 cells.
UDCA treatment for 3 days caused minimal senescence. A.: Nontreated IEC-6 cells; B.: UDCA treated (600 µM, 3d) IEC-6 cells. β-galactosidase activity was detected by incubating cells with medium containing X-gal substrate, the hydrolysis of which yields a blue precipitate. Bar: 50 µm.

Treatment with UDCA caused minimal increase of β-galactosidase activity (Fig. 25.) which says that the senescence induced by UDCA treatment for 3 days, is neglible to explain a 50% decrease in cell number (Fig. 21.). It was concluded that

decrease in proliferation of IEC-6 cells after UDCA treatment is not due to induction of senescence.

8.4.6 UDCA treatment resulted into a change in cell cycle distribution

To check if the decrease in proliferation was associated with cell cycle changes, IEC-6 cells were treated with 600 µM UDCA for 2 days, stained with propidium iodide and then the cell cycle distribution was analysed using FACS.

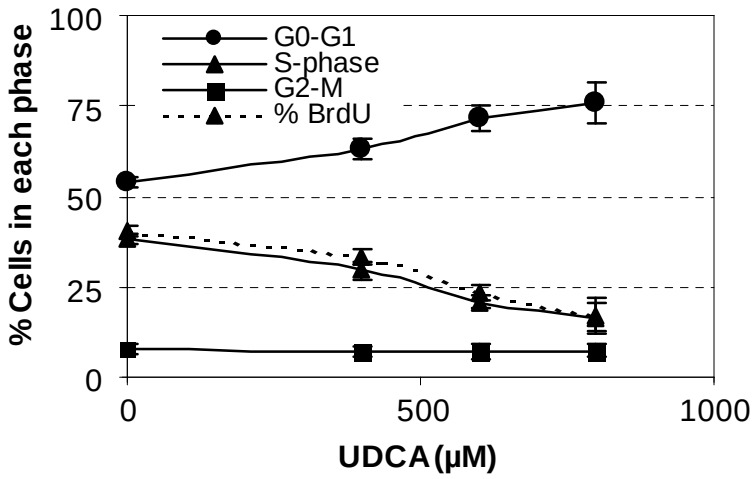

Fig. 26. Effect of UDCA on the cell cycle distribution of IEC-6 cell line.
UDCA treatment of IEC-6 cells for 2 days slows down the cell cycle, visible through the decrease of the S-phase population and of BrdU incorporation. Mean values ± SD of 3 experiments. Sub-G1 population was negligible and is not shown. FACS measurements were done by M.L.Hanski.

Two days after start of treatment (600 µM UDCA), the population in the S phase of the cell cycle decreased from 38% to 21% and the incorporation of BrdU decreased from 40% to 24% i.e. to 60% of the normal level. This indicated that there were fewer cells entering the S-phase in UDCA-treated cells than in nontreated cells. It was investigated in further experiments, which cellular process caused proliferation inhibition.

8.4.7 Effect of UDCA on Irs-1 protein expression and ERK phosphorylation

Out of the 5 genes investigated by real time RT-PCR (Fig. 23.), insulin receptor substrate-1 (Irs-1) was the most strongly suppressed gene in IEC-6 cell line after UDCA treatment. Irs-1 is an adaptor protein involved in transduction of insulin, insulin like growth factor 1 (IGF-1) and growth hormone signal, all of which are known to induce cell proliferation. It was therefore chosen for further analysis in IEC-6 cells. MAP-ERK-kinase pathway is involved in IGF-1 or growth hormone-induced proliferation (22). Therefore the effect of UDCA on ERK-kinase phosphorylation was checked.

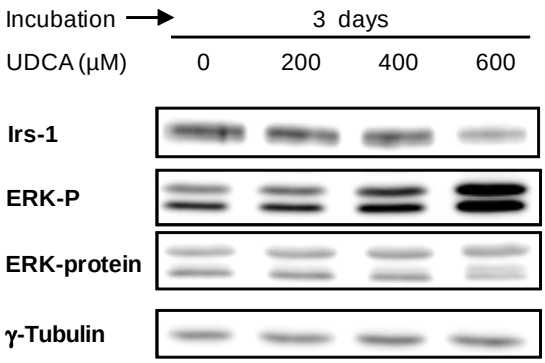

Fig. 27. Increase in phosphorylation of ERK and decrease of Irs-1 protein expression in IEC-6 cells is dependent on UDCA concentration.
Western blotting of IEC-6 cells showing a dose-dependent effect of UDCA on ERK-phosphorylation and Irs-1 protein expression. IEC-6 cells were treated with UDCA at different concentrations for 3 days, lysed in 1x-sample buffer and subjected to western blotting. γ-tubulin was used as the loading control. Experiment was repeated thrice.

UDCA treatment for 3 days dose-dependently increased phosphorylation of ERK without affecting ERK protein expression. This was demonstrable only when using sample buffer (124) which prevented immediate dephosphorylation of ERK, but not when other lysis buffers were used (data not shown). Irs-1 protein expression was dose-dependently suppressed by UDCA. Thus, high ERK-phosphorylation coincided with decrease of Irs-1 protein expression.

An increase in phosphorylation of ERK1/ERK2 and a decrease in Irs-1 protein expression were associated with inhibition of proliferation. In points 8.4.8 to 8.4.14

the systematic investigation of ERK1/ERK2 is presented and in points 8.4.15 to 8.4.17 the investigation of Irs-1 as targets of UDCA involved in the mechanism by which UDCA inhibits epithelial cell proliferation is reported.

8.4.8 Effect of UDCA on localization of ERK kinase

After establishing that UDCA treatment causes high ERK1/ERK2 phosphorylation, the cellular localization of phosphorylated ERK1/ERK2 was investigated. Since it is known that phosphorylated-ERK1/ERK2 translocates to the nucleus where it regulates the expression of target genes (29), it was hypothesized that UDCA causes nuclear accumulation of phosphorylated ERK1/ERK2. To test this hypothesis IEC-6 cells were treated with UDCA for 3 days and stained with anti-phospho-ERK1/ERK2 antibody. The distribution of ERK1/ERK2 in nontreated and UDCA-treated cells was compared.

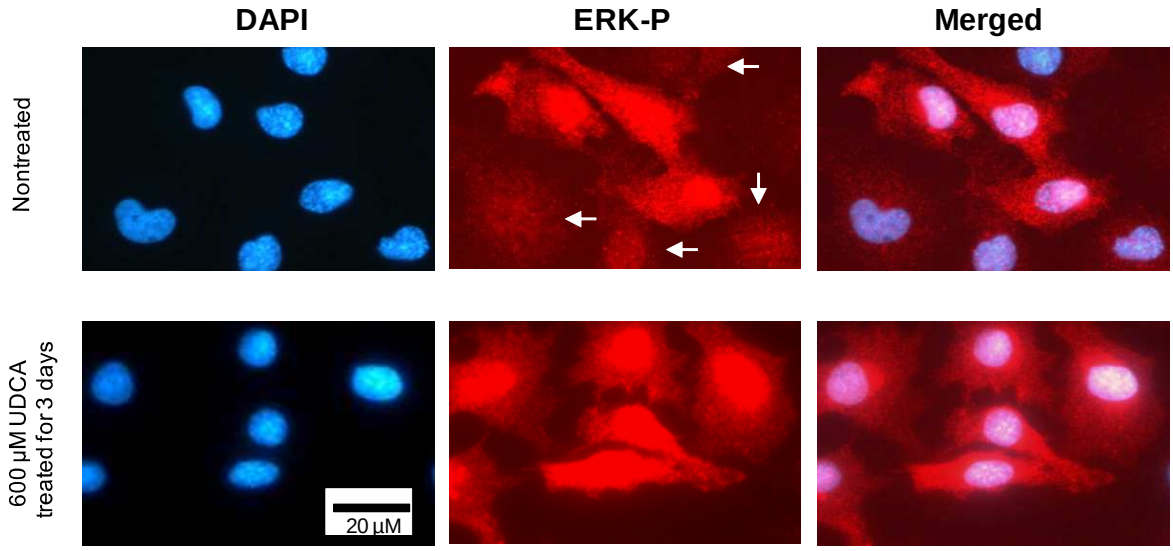

Fig. 28. Immunohistochemical staining of IEC-6 cells with anti-phospho-ERK antibody.
IEC-6 cells treated with 600 µM UDCA for 3 d were stained with anti-phospho-ERK antibody and DAPI. The white arrows show cells without high phospho-ERK grown in standard medium.

UDCA treatment for 3 days led to an increase in phosphorylation of ERK and to an increase of the percentage of cells exhibiting nuclear localization of phosphorylated ERK from 45% in the nontreated group to 87% in the treated group (Fig. 28.). Thus

the nuclear localization indirectly supported the original finding that UDCA increases the phosphorylation of ERK1/ERK2.

8.4.9 Effect of UDCA on IGF-1- and EGF-induced proliferation

To further investigate the effect of UDCA on ligand-induced proliferation, IEC-6 cells were treated with the proproliferatory ligands EGF or IGF-1 in the presence or absence of UDCA.

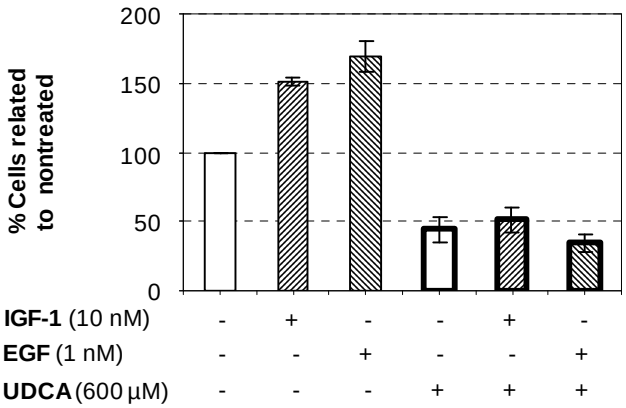

Fig. 29. Effect of UDCA on IGF-1 or EGF induced proliferation of IEC-6 cells.
IEC-6 cells were seeded in medium containing 5% of FCS and treated with 10 nM IGF-1 or 1 nM EGF for 3 days in the presence or absence of UDCA. Percentage of total cells related to nontreated was determined. Mean values ± SD of 3 experiments. Data contributed by B.Choudhary & M.L.Hanski.

Both IGF-1 and EGF induced cell proliferation. This stimulation was diminished by UDCA in a concentration dependent manner (not shown) and completely abrogated in the presence of 600 µM UDCA (Fig. 29.).

8.4.10 Effect of UDCA on duration of ERK phosphorylation

To check if UDCA alters ERK phosphorylation triggered by EGF or IGF-1 treatment, IEC-6 cells were grown in medium with 5% FCS and treated with either EGF or IGF-1. UDCA (600 µM) was added 2 h prior to addition of the ligands and it was present in the medium for the duration of the experiment.

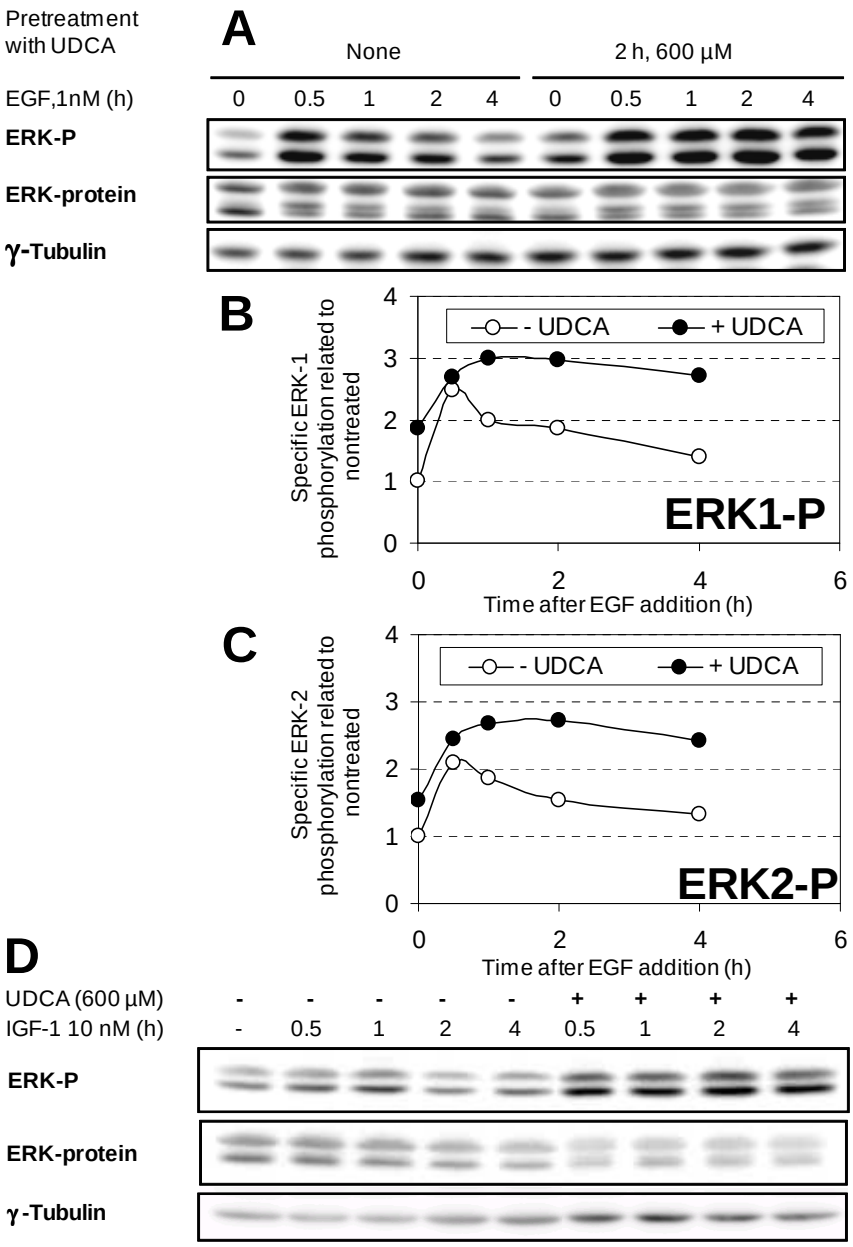

Fig. 30. Effect of EGF or IGF-1 on phosphorylation of ERK1/ERK2 in the presence or absence of UDCA.

A.: Western blot showing ERK-phosphorylation in EGF-treated IEC-6 cells in the presence or absence of UDCA; B.: Densitometric evaluation of the western blot for ERK1-phosphorylation; C.: Densitometric evaluation of the western blot for ERK2- phosphorylation; D.: Western blot showing ERK-phosphorylation in IGF-1-treated IEC-6 cells in the presence or absence of UDCA. Results representative for 3 experiments. Western blotting depicted in Fig. 29D was done by M.L.Hanski.

The addition of EGF (Fig. 30 A-C) or of IGF-1 (Fig. 30 D) resulted in a peak of ERK1/ERK2 phosphorylation at 30 min which receded to normal levels in 4 hours.

This effect coincided with proliferation increase by the ligands (Fig. 29, thin lined bars). In the presence of UDCA the phosphorylation of ERK1/ERK2 also increased within 30 min (3 fold of the normal levels) but did not recede as in the case of ligands alone. The phosphorylation was maintained at high levels for the duration of UDCA treatment. This effect coincided with proliferation inhibition (Fig. 29, thick lined bars). It was concluded that the inhibition of proliferation by UDCA was associated with a high and persistent phosphorylation of ERK1/ERK2 kinases.

8.4.11 High phosphorylation of ERK1/ERK2 coincides with cell cycle delay

To check if the persistently high phosphorylation of ERK1/ERK2 after UDCA treatment coincided with a delay of cell cycle progression, IEC-6 cells were starved by FCS removal for 24 h and then released into medium with 10% FCS either in the presence of absence of UDCA.

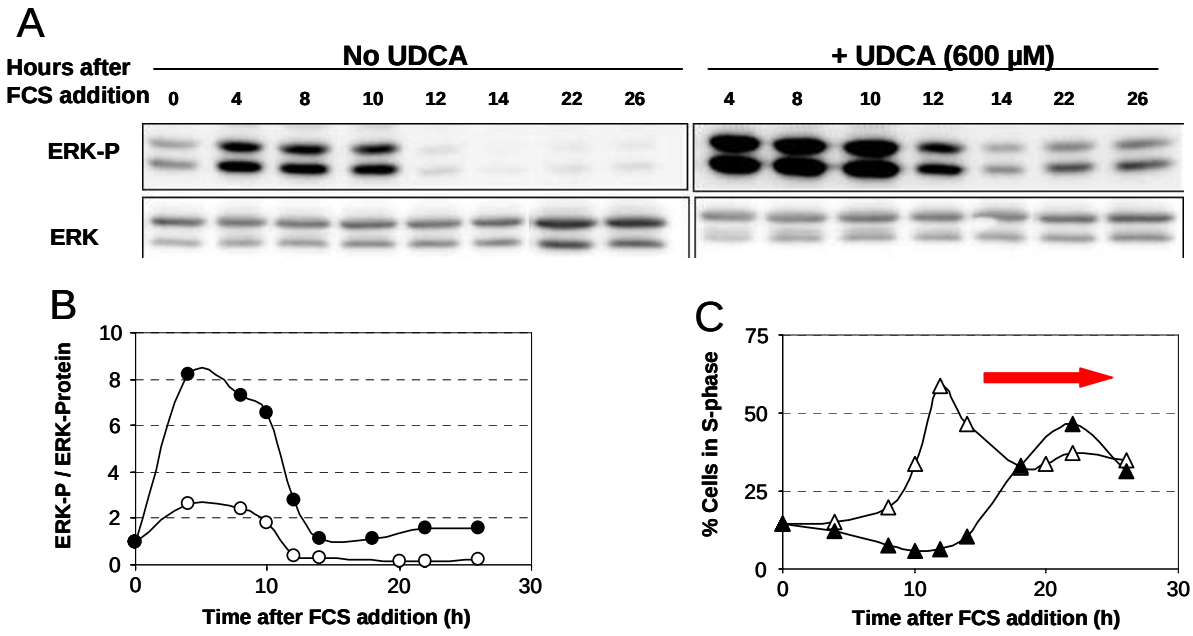

Fig. 31. Coincidence of persistent ERK phosphorylation and cell cycle slow-down after UDCA treatment in IEC-6 cells.
IEC-6 cells were starved by removal of FCS for 24 h and then released into medium with 10% FCS in the presence or absence of UDCA. A.: Western blot showing ERK phosphorylation in the presence or absence of UDCA; B.: Densitometric evaluation of western blots; C.: Change in distribution of cells in the S-phase as determined by FACS. Arrow shows a 10 h delay of the peak of S-phase population in UDCA-treated cells. Results representative for 2 experiments have been shown here. FACS measurements were done by M.L.Hanski.

Addition of FCS increased ERK1/ERK2 phosphorylation, which started to decrease after 10 h in both nontreated and in UDCA-treated cells. But as compared to the nontreated cells the ERK-phosphorylation in UDCA-treated cells was higher at every time point (Fig. 22 A, B). This high phosphorylation of ERK1/ERK2 coincided with a 10 h delay of S-phase peak (Fig. 22C).

8.4.12 Role of ERK in basal or IGF-1- or EGF-induced proliferation

Since the inhibition of the proproliferative effects of EGF or IGF-1 by UDCA was associated with a high and persistent phosphorylation of ERK1/ERK2 in IEC-6 cells (Fig. 29 & Fig. 30), the question was asked if ERK1/ERK2 are necessary for the proproliferative effects of EGF or IGF-1. To answer this question the effect of suppression of ERK1 or of ERK2 on proliferation was checked in IEC-6 cells.

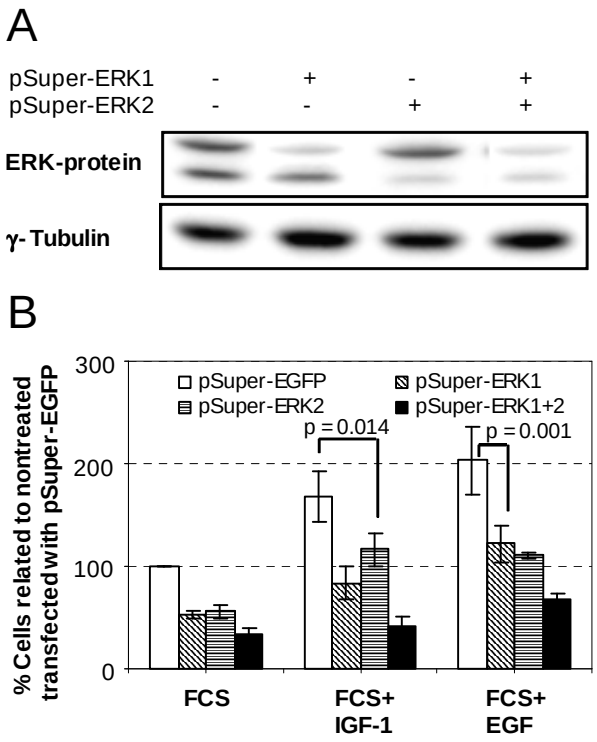

Fig. 32. Effect of suppression of ERK1 or ERK2 or both on basal, IGF-1-induced or EGF-induced proliferation.

A.: Western blot showing the suppression of ERK1/ERK2 after 2 d of transfection; representative for 3 experiments; B.: Total cell count of IEC-6 cells treated for 3 d with EGF or IGF-1 in medium with 5% FCS after ERK1 or ERK2 suppression. Mean values $\pm$ SD of cell number related to nontreated, (n=3); p-value was calculated by Student´s t-test.

Three days after transfection with pSuper-ERK1 or pSuper-ERK2 the basal proliferation was reduced to 50% and after suppression of both kinases to 30% of the nonsuppressed control. The suppression of ERK1 decreased the stimulatory effect of IGF-1 from 168 to 84%, the suppression of ERK2 decreased it from 168% to 117% and simultaneous suppression of ERK1 and ERK2 suppressed the stimulatory effect of IGF-1 to 41%. The proliferatory response to EGF was decreased by the suppression of ERK1 from 204% to 122%, by suppression of ERK2 to 111% and by the suppression of both to 67% of the nonstimulated control. These data indicated that ERK1 and ERK2 kinases contribute to the transduction of the basal proliferatory signals in 5 % FCS, as well as of the signals induced by IGF-1 and EGF.

8.4.13 Abrogation of UDCA effects by inhibition of MEK1 kinase

To assess the importance of ERK1/ERK2 phosphorylation for the response to UDCA, IEC-6 cells were treated with UDCA in the presence of a chemical inhibitor of MEK1 kinase (the kinase which phosphorylates ERK).

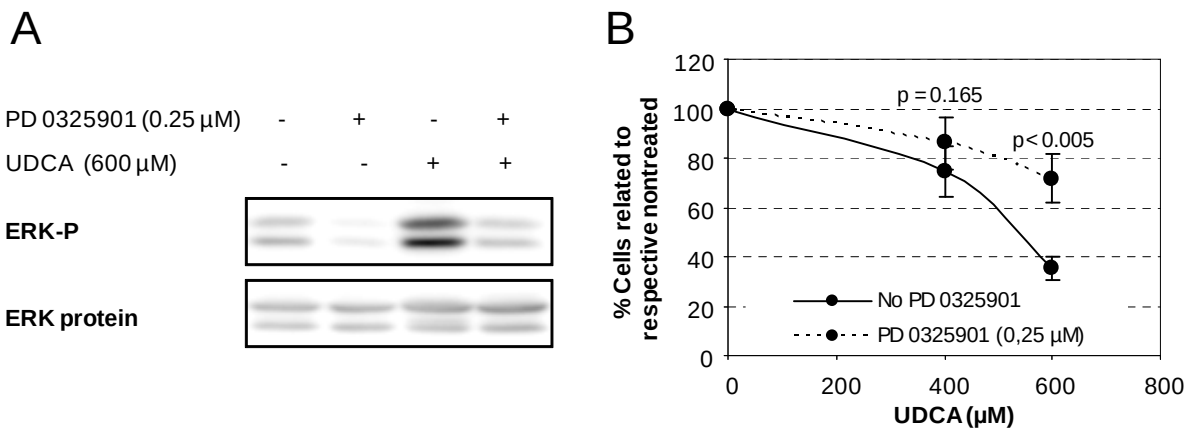

Fig. 33. Attenuation of the antiproliferative effects of UDCA by inhibition of ERK phosphorylation.

A.: Effect of UDCA treatment on ERK-phosphorylation in the presence or absence of PD0325901 (0.25 µM, 3 days) assayed by western blotting; B.: Total cell count of IEC-6 cells treated with UDCA in the presence or absence of MEK1 inhibitor PD0325901. Percentage of cells related to respective non-UDCA treated controls was calculated. Mean values of 3 experiments ± SD. p-value was determined by Student´s t-test. 1 out of 3 experiments was done by M.L.Hanski.

The inhibition of MEK1 with PD0325901 resulted in a decrease of ERK1/ERK2 phosphorylation and of the cell number to 37% three days after start of treatment. At UDCA concentration of 600 µM, IEC-6 cells treated with UDCA were inhibited after 3 days by 62 %, whereas in the presence of MEK1-inhibitor PD0325901, they were inhibited by 30 % ($p < 0.005$). Thus MEK1-inhibited IEC-6 cells were less susceptible to proliferation inhibition by UDCA (Fig. 33B).

8.4.14 Abrogation of UDCA effects by suppressing ERK protein

To further analyse the involvement of ERK kinases in mechanism of proliferation inhibition by UDCA and to avoid the potential nonspecific effects of chemical inhibitors of MEK1, ERK1 or ERK2 kinases were separately suppressed using the pSuper-ERK1 or pSuper-ERK2 plasmids and then treated with UDCA. pSuper-EGFP-transfected cells were used as a control of UDCA on proliferation and ERK-phosphorylation.

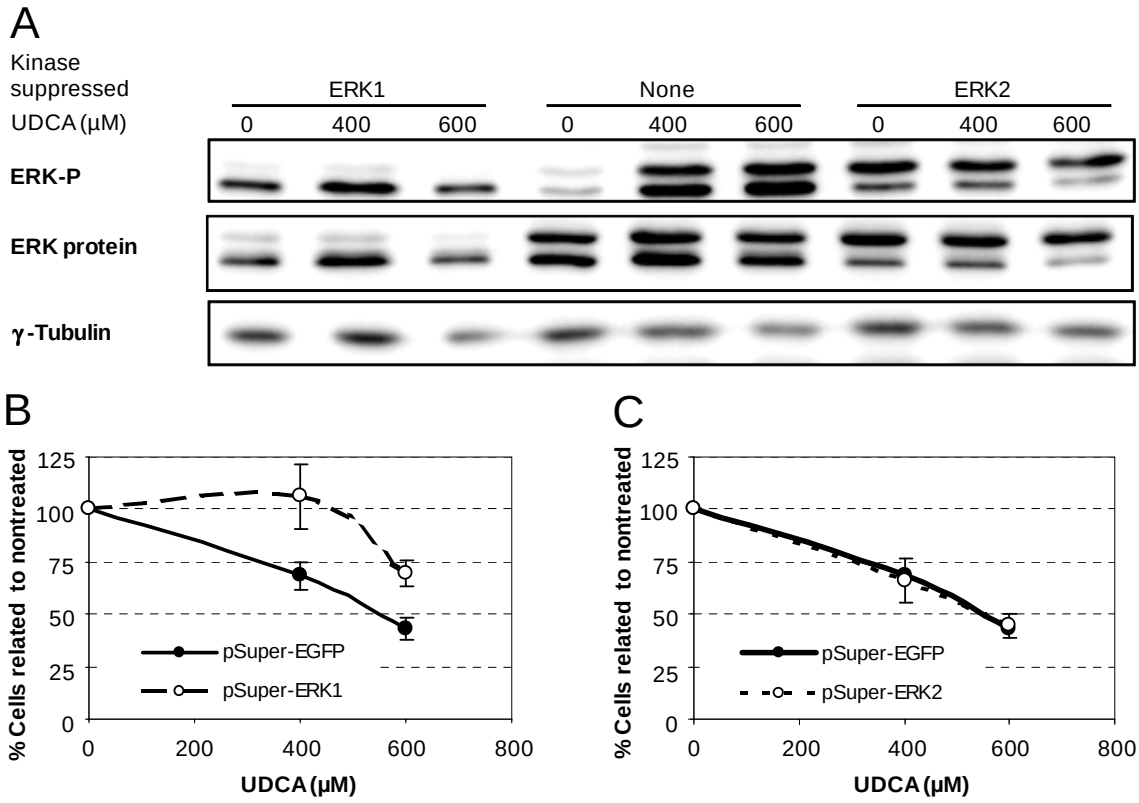

Fig. 34. Effect of suppression of ERK1 or ERK2 on proliferation-inhibition caused by UDCA. A.: The suppression of ERK1 or ERK2 is associated with the decrease of the amount of the corresponding phosphorylated proteins shown by western blotting. Representative blot of more than 3 experiments; B.: Suppression of ERK1 attenuates the inhibitory effect of UDCA; C.: Suppression of ERK2 has no influence on the proliferation inhibition by UDCA. Mean values ± SD of 3 experiments.

The ERK1-suppressed cells were completely resistant to UDCA treatment at 400 µM. At higher UDCA concentration (600 µM) ERK1-suppressed cells were inhibited by 25 % as compared to non-ERK1 suppressed cells which were inhibited by 50 % (Fig. 34B). The inhibitory effect of UDCA was similar in the ERK2-suppressed cells and in the nonsuppressed cells (both inhibited by 25 % at 400 µM and by 50 % at 600 µM UDCA) (Fig. 34C). These data suggested that the high phosphorylation of ERK1 but not of ERK2 contributes to the antiproliferatory effect of UDCA.

8.4.15 Effect of Irs-1 on basal and IGF-1- or EGF-induced proliferation

The antiproliferative effect of high ERK phosphorylation due to UDCA treatment has been clarified (8.4.7 to 8.4.14) but the effect of decrease in Irs-1 protein expression (Fig. 27) after UDCA treatment, remained to be elucidated. To establish the role of Irs-1 suppression in cell proliferation and to analyse the dependence of the signal induced by IGF-1 or EGF on Irs-1 expression, Irs-1 was suppressed using siRNA and the basal proliferatory response as well as the proliferatory response to each ligand was assessed after three days.

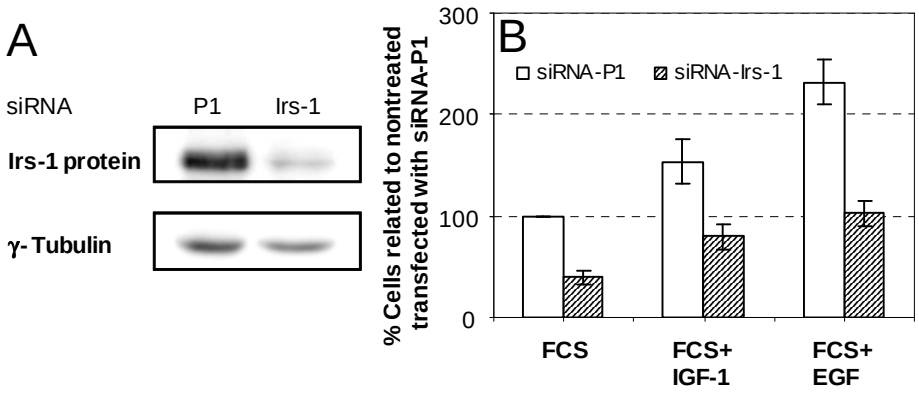

Fig. 35. Effect of Irs-1 suppression on basal, IGF-1-induced or EGF-induced proliferation in IEC-6 cells.

A.: Western blot showing suppression of Irs-1, 2 days after transfection. Representative blot of 3 experiments; B.: Total cell count of P1-transfected (white bars) or siRNA-Irs-1-transfected (hatched bars) IEC-6 cells in medium with 5% FCS alone or with either 10 nM IGF-1 or 1 nM EGF. Total cell count was related to the number of cells in 5 % FCS. Mean values ± SD of 3 experiments. 1 out of 3 experiments was done by M.L.Hanski.

The proliferatory response to IGF-1 was 152% and to EGF was 232%. After transfection with siRNA-Irs-1 the cell number was reduced to 38 % of the siRNA-P1 transfected cells (control group) after 3 days. The suppression of Irs-1 reduced the proliferatory response to IGF-1 from 152% to 79% and of EGF from 232% to 102 % of the nonstimulated control. This indicated that Irs-1 is necessary for the basal (5 % FCS) as well as IGF-1- or EGF-induced proliferation.

Involvement of Irs-1 in the proproliferatory effects of EGF is an entirely novel finding.

8.4.16 Effect of Irs-1 overexpression on cell proliferation

Among many other changes of gene expression, the decrease in cell proliferation after UDCA treatment was associated with decrease in Irs-1 protein expression (Fig. 27.). Specific suppression of Irs-1alone was sufficient to inhibit cell-proliferation (Fig. 35). To clarify, if UDCA-mediated decrease in Irs-1 protein was necessary for the decrease in proliferation, the effect of Irs-1 overexpression was checked on proliferation of nontreated and UDCA-treated cells. IEC-6 cells were transduced either with an adenovirus coding for Irs-1 expression (Adv-Irs1) or with an adenovirus coding for GFP expression (Adv-GFP) at different MOI. The cells transduced at 10 MOI were also treated with UDCA for 3 days and counted.

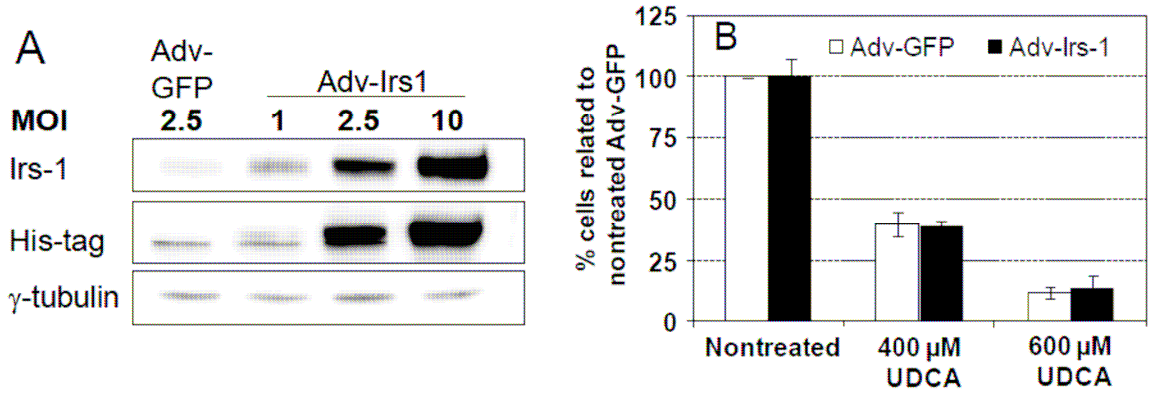

Fig. 36. Effect of Irs-1 overexpression on proliferation of IEC-6 cells in the presence or absence of UDCA.

A.: Western blot showing the overexpression of Irs-1 protein in IEC-6 cells, transfected with Adv-Irs-1 at different MOI. Cells were transfected with Adv-GFP as a control of transduction at 2.5 MOI. Representative for 3 experiments; B.: Total cell count of IEC-6 cells transduced at 2.5 MOI adenovirus and treated with UDCA for 3 d. Mean values ± SD of 3 experiments.

There was a strong overexpression of Irs-1 as assessed by western blotting (Fig. 36A). The overexpression of Irs-1 neither increased basal cell proliferation of IEC-6 cells nor decreased the antiproliferative effects of UDCA. The results of suppression of Irs-1(Fig. 35) and of overexpression of Irs-1 (Fig. 36) indicate that suppression of endogenous levels of Irs-1 causes a decrease in proliferation but overexpression of exogenous Irs-1 does not influence proliferation in IEC-6 cells.

Thus it was concluded that though it is sufficient to suppress Irs-1 to decrease proliferation, the decrease in Irs-1 protein after UDCA treatment might not be the reason for the antiproliferative effects of UDCA.

8.4.17 Regulation of Irs-1 transcription by ERK1 and ERK2

Since treatment of IEC-6 cells with UDCA caused persistently high ERK phosphorylation and a suppression of Irs-1 RNA and protein expression, it was investigated if ERK regulates Irs-1 at transcription level. To answer this question Irs-1 luciferase reporter experiments were carried out in IEC-6 cells with suppressed ERK1 or ERK2 or in the presence of MEK1 kinase inhibitors PD0325901 or U0126. Additionally, the protein expression of Irs-1 was checked by western blotting under the conditions of ERK suppression or MEK1 inhibition.

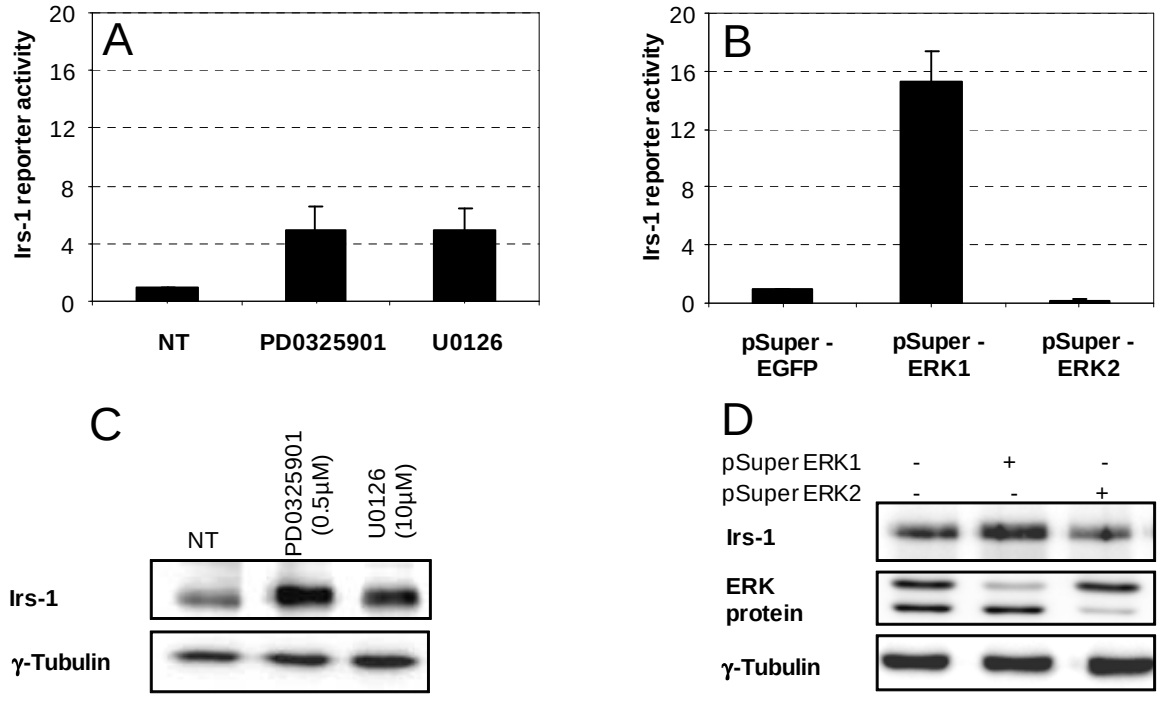

Fig. 37. Regulation of Irs-1 transcription by ERK1/ERK2.
A.: Irs-1 luciferase reporter assay in IEC-6 cells treated with PD0325901 or U0126; B.: Irs-1 luciferase reporter assay in IEC-6 cells transfected with either pSuper-EGFP or pSuper-ERK1 or pSuper-ERK2; C.: Effect of PD0325901 or U0126 on Irs-1 protein expression; D.: Effect of suppression of ERK1 or ERK2 on Irs-1 protein expression. Mean values $\pm$ SD of 3 luciferase-reporter experiments, western blots are representative for 3 experiments.

Inhibition of MEK1 kinase increased Irs-1 reporter activity (Fig. 37A) and Irs-1 protein expression (Fig. 37C). Suppression of ERK1 protein increased Irs-1 reporter activity by more than 16 fold, but suppression of ERK2 decreased Irs-1 reporter activity (Fig. 37B). There was also more Irs-1 protein in ERK1-suppressed cells but not in ERK2 suppressed cells than in non-ERK-suppressed cells (Fig. 37D). It was concluded that ERK1 suppresses the transcription of Irs-1 and ERK2 does not. Further, ERK2 might be required for Irs-1 transcription as there is a decrease of Irs-1 transcription in ERK2 suppressed cells. The effect of ERK2 suppression on Irs-1 protein expression was, however, negligible (Fig. 37D).

8.4.18 Transcriptional upregulation of p21 by high ERK-phosphorylation

It has been reported that high and persistent ERK-P leads to an upregulation of p21 protein expression and to a cell cycle slow-down (125, 126). We hypothesized that in IEC-6 cells high ERK phosphorylation leads to transcriptional upregulation of p21 leading to a decrease in proliferation rate.

8.4.19 Regulation of p21 transcription by UDCA

To find out the influence of UDCA on p21 expression the change in expression of p21 was first inspected in the microarray data. p21 mRNA was expressed 1.25 fold more in the colonic epithelial cells of UDCA treated mice than in the nontreated mice. Since the cut-off value for fold change was set as 1.52, genes altered less than 1.52 fold (like p21) did not appear in the microarray evaluation. It was decided to cross-check the effect of high ERK phosphorylation due to UDCA treatment on p21 transcription *in vitro*. IEC-6 cells were transfected with p21-luciferase reporter plasmid and treated with either 600 µM UDCA alone or 0.2 µM PD0325901 alone or UDCA+PD0325901 for 2 d. Then the reporter assay was carried out. In parallel, the cell-lysates were analysed by western blotting using anti-p21 antibody to check the effect at protein level.

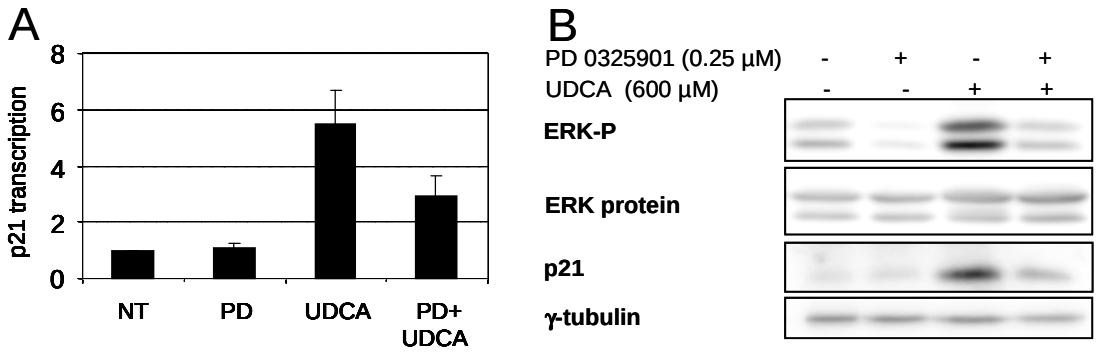

Fig. 38. UDCA increases p21 transcription. This is dependent on ERK phosphorylation.
A.: IEC-6 cells were transfected with p21 reporter plasmid and β-galactosidase expression plasmid and treated with 600 µM UDCA or 0.2 µM PD0325901 or UDCA+PD for 2 d. Then reporter assay was carried out. Luciferase values are normalized to β-galactosidase values and change is related to the values in nontreated cells. Mean values ± SD of 3 experiments; B.: IEC-6 cells treated as in the reporter experiments were analysed by western blotting. The blots are representative for 3 experiments.

UDCA increased the expression of p21 at transcriptional level more than 5 fold. The increase in p21 transcription due to UDCA treatment was abrogated in the presence of PD0325901. PD0325901 alone had no effect on p21 transcription in IEC-6 cells (Fig. 38A). There was also more p21 protein expression in UDCA-treated cells. This increase was abrogated in the presence of PD0325901 treatment (Fig. 38B). The conclusion is that high ERK phosphorylation caused by UDCA treatment induces increased transcription and protein expression of p21 in IEC-6 cells.

8.4.20 Regulation of p21 expression by UDCA *in vivo*

After finding that high ERK phosphorylation due to UDCA treatment caused a transcriptional upregulation of p21 *in vitro*, the expression of p21 protein was checked in colonic epithelium of nontreated and UDCA treated mice.

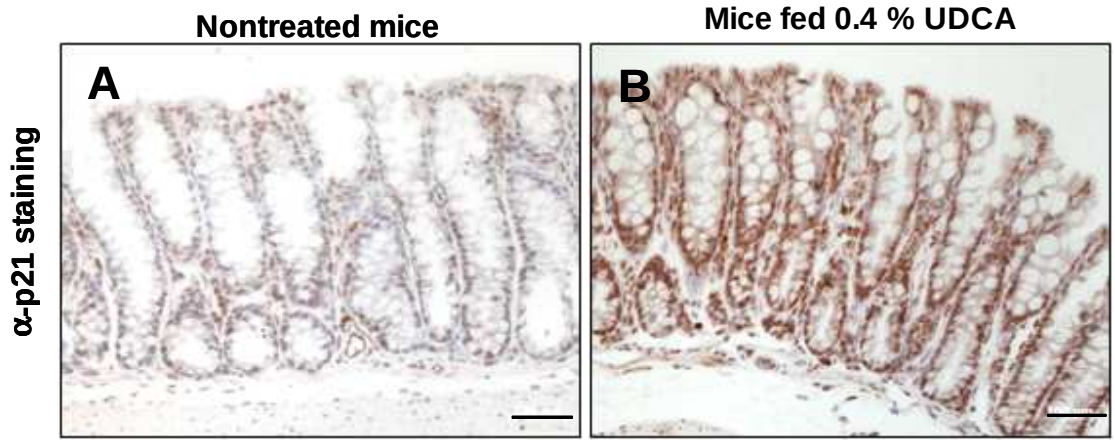

Fig. 39. Increased expression of p21 protein in colonic crypts of UDCA-treated mice.
Colonic sections of mice stained with anti-p21-antibody. A.: Colonic sections of nontreated mice. B.: Colonic sections of mice treated with UDCA (0.4 % for 3 weeks). Bar: 100 µM. Immunohistochemistry done in Institute of Pathology, Charité, Campus Benjamin Franklin.

The expression of p21 was clearly enhanced in the colonic sections of UDCA-treated mice as compared to the nontreated mice. It was concluded that treating mice with UDCA led to slight increase of p21 transcription and a strong accumulation of p21 protein.

8.4.21 Suppression of p21 decreases proliferation inhibition due to UDCA

To check if the increase in p21 protein after UDCA treatment is necessary for proliferation inhibition by UDCA, IEC-6 cells were transfected with pSuper plasmid encoding shRNA against p21 gene (pSuper-p21) and then treated with UDCA for 2 days and counted.

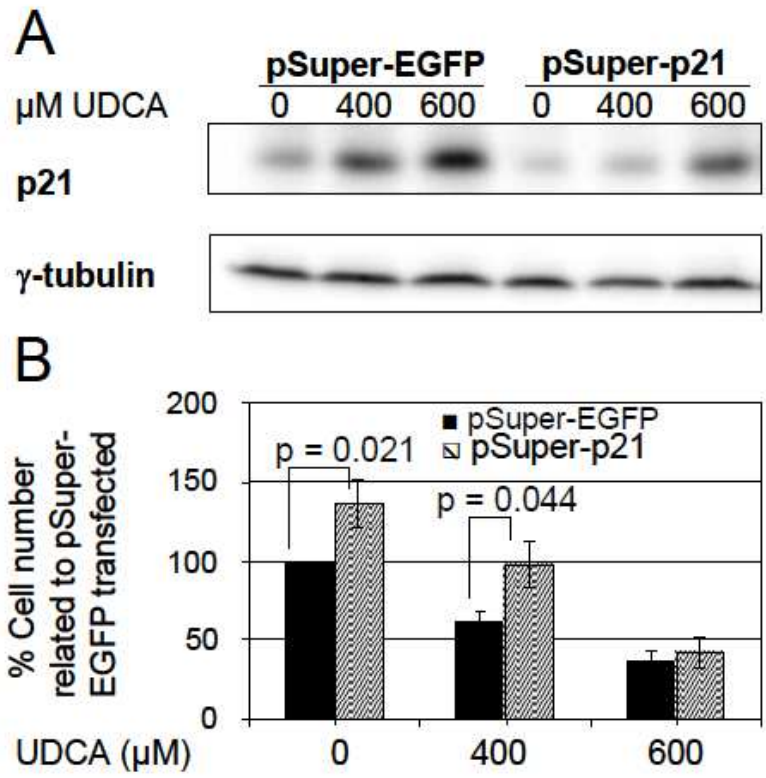

Fig. 40. p21 suppression decreases the antiproliferative effects of UDCA.
A.: The suppression of p21 in the nontreated or UDCA-treated cells was analysed by western blotting. γ-tubulin was used as a loading control. Representative for 3 experiments; B.: IEC-6 cells were transfected with pSuper-p21 or with pSuper-EGFP and treated with 400 or 600 µM UDCA for 2 d and counted. Mean values ± SD of 3 experiments.

UDCA treatment increased p21 protein expression which was suppressed by pSuper-p21. Suppression of p21 increased cell number of nontreated cells by 35%. It increased the number of UDCA-treated cells by 30%, 2d after start of UDCA treatment. In cells treated with 600 µM UDCA p21 suppression did not increase proliferation. From this experiment it was concluded that increase of p21 contributes to proliferation inhibition after UDCA treatment.

At UDCA concentration of 600 µM, other factors than p21 may inhibit cell proliferation. Alternatively, the increase of p21 expression due to treatment with 600 µM UDCA was not reduced enough by pSuper-p21 plasmid transfection to allow the abrogation of the antiproliferatory effect.

9 Discussion

9.1 Inflammation increases epithelial cell proliferation

In mice, DSS-colitis caused an increase in the total number of epithelial cells per crypt and also the number of Ki-67-expressing epithelial cells per crypt (Fig. 6). It has been previously shown that DSS-colitis influences the proliferation of colonic epithelial cells (127, 128). Boismenu et al. have reported that short-term exposure to DSS decreases epithelial cell proliferation (127). Mizoguchi et al. have systematically evaluated colonic epithelial cell proliferation in a mice model of DSS-colitis. They report that epithelial cell proliferation decreases in the initial (day 0 to 5) days of DSS-colitis but increases in the later (day 6 to 12) days (128). In the present work since the mice were sacrificed after 6 months of DSS-colitis, the increase in proliferation is in agreement with the data of Mizoguchi et al. This supported the notion that DSS-colitis contributes to colon carcinogenesis due to high rate of epithelial cell proliferation and that the reduction of proliferation rate prevents carcinogenesis.

9.2 UDCA reduces epithelial cell hyperproliferation in mice with DSS-colitis

In view of the hypothesis mentioned above the effect of UDCA on colonic epithelial cell proliferation was checked. Treatment of DSS-colitis mice with UDCA decreased the number of epithelial cells per crypt. The number of Ki-67 expressing cells per crypt was also significantly lower in mice with DSS-colitis treated with UDCA as compared to DSS-colitis mice not treated with UDCA (Fig. 6.). It has been reported that in a mice model of carcinogenesis induced with azoxymethane + DSS, UDCA treatment decreased the % of PCNA (a marker of proliferation) expressing cells per crypt and reduced tumour prevalence (81). These two observations (Fig. 6 and (81)) suggest that the chemopreventive property of UDCA in colitis conditions could be due to its ability to suppress epithelial cell proliferation. Our observation is also the first evidence of antiproliferatory action of UDCA in a mice model of DSS-colitis.

Since it proved to be difficult to interpret the mechanism of proliferation-inhibition by UDCA in a DSS-colitis model, it was decided to first determine the mechanism of action of UDCA on colonic epithelial cell proliferation in normal mice.

9.3 Inflammation-associated alterations of gene expression

The genes whose expression is changed in mice with DSS-colitis were identified by microarray (Table 4. & Table 5.). The proproliferative genes Creb3l3, Gbp2, Ereg and Igfbp4 were upregulated and Chek1, an antiproliferative gene was suppressed in the DSS-colitis mice compared to normal mice. It has been recently shown that inflammation-associated increase of expression of Gbp2, Ereg and Igfbp4 is also observed in patients with ulcerative colitis (129). We also observe increased expression of Gbp2, Ereg and Igfbp4 genes in DSS-colitis mice which is in agreement with Fang et al.(129). It was therefore interesting to check the effect of UDCA treatment on the expression of these genes.

9.4 UDCA suppresses inflammation-associated alterations of gene expression

Since UDCA inhibited epithelial cell proliferation in DSS-colitis mice, a hypothesis was put forward that the proproliferative-genes which are induced in DSS-colitis mice (discussed in 9.3) and brought to normal level by UDCA treatment could be the potential target genes of UDCA participating in carcinogenesis. Indeed, in mice with DSS-colitis, several proproliferative genes were upregulated whose expression was brought back to normal level by UDCA treatment (Table 8.). One of such genes is Gbp2 which has been shown to be involved in interferon-γ-induced proliferation of fibroblasts (121). Gbp2 overexpressing fibroblasts also formed tumours in nude mice, whereas fibroblasts expressing mutant-Gbp2 did not (121). It is also the only gene in Table 8. which is upregulated in ulcerative colitis patients (129).

It was therefore hypothesized that Gbp2 is a gene whose suppression by UDCA causes decrease in proliferation rate. Since the overexpression of Gbp2 in HCT116

cell line neither influenced basal cell proliferation nor UDCA effects (Fig. 16 and Fig. 17), this hypothesis was discarded.

9.5 UDCA inhibits epithelial cell proliferation in normal mice

Mice fed with UDCA at different concentrations for three weeks showed a dose-dependent decrease in colonic epithelial cell proliferation rate (Figure 9 and 10). So far, the effect of UDCA on epithelial cell proliferation has been investigated in either AOM rat model where crypt cell hyperproliferation was decreased after UDCA treatment (79) or in a mice model of AOM+DSS-colitis where a decrease in the % of PCNA expressing epithelial cells within the adenocarcinoma was reported (81). The present work is the first report on the antiproliferative effect of UDCA in normal intestinal epithelial cells *in vivo* and *in vitro*.

9.6 UDCA suppresses proproliferative genes in normal mice

Treatment of normal mice with UDCA caused the suppression of several proproliferative genes like Tcf4, Ghr, Gbp2, Il-15, Flot2, Irs-1 and Klf5 in the colonic epithelial cells (Table 10.). Prior to this work the investigation of molecular targets of UDCA has been carried out rodent models of inflammation-associated colon cancer. Additionally, Castro et al. have investigated UDCA target genes in primary rat hepatocytes (100). Chen et al. have reported the downregulation of the genes of protein biosynthetic pathway in patients with primary biliary cirrhosis (73). The present work is the first investigation of genes targeted by UDCA in normal mice colonic epithelia. Since UDCA is used as a drug in patients with hepatic-disorders more reports are available for genes altered by UDCA in hepatocytes. The present work will widen the understanding of the mechanism of action of UDCA in the intestine.

9.7 UDCA inhibits proliferation of human colon cancer cells *in vitro*

UDCA inhibited the proliferation of colon cancer cells *in vitro* (Fig. 12). The antiproliferative effect of UDCA on colon cancer cells has been reporter previously (82, 85, 86, 91, 92, 130). It was hypothesized that although the decrease in proliferation of these cell lines was a common observation, the mechanisms involved could be greatly different due to different mutations in colon cancer cells. To test this hypothesis it was checked if the changes in gene expression caused by UDCA treatment in the colon cancer cells are similar to that in the murine epithelium.

9.8 Changes in gene expression caused by UDCA in colon cancer cells are different from those found in mice

The genes which were differentially expressed in mice treated with UDCA as compared with normal mice have been identified (point 9.11.). Change in expression of some of those genes like Ghr, Gbp2, Tcf4, IL-15 and Irs-1 were checked by real time RT-PCR in colon cancer cell lines HCT116 and HCT8 (Fig. 14). There was little correspondence between the transcriptional changes (due to UDCA treatment) in the mice and in the cell lines (Fig. 10 and Fig. 11 vs. Fig. 14). Several authors have used these cell models for the investigation of the molecular targets of UDCA. UDCA treatment increased the expression of cytokeratin-18 and E-cadherin (79), decreased the expression of C/EBPβ and Cox2 in HCA-7 colon cancer cell line (82) and caused caveolin-1 dependent degradation of EGFR in HT-29 cells (88). None of the models used reflect the situation *in vivo* and none of the molecules investigated explains the mechanism of action of UDCA in regulating proliferation in normal intestinal epithelial cells.

9.9 Decrease in Tcf4 expression caused by UDCA treatment does not contribute to proliferation inhibition in colon cancer cells

Although the changes in gene expression caused by UDCA treatment were different between mice and colon cancer cell lines, the decrease in expression of Tcf4 was a

common observation. It was therefore investigated in HCT116 cell line if the decrease in proliferation after UDCA treatment is caused by decreased Tcf4 expression. UDCA inhibited the transcription of Tcf4 in mice (Fig. 11) and inhibited its transcription and protein expression in colon cancer cells (Fig. 14). UDCA treatment of colon cancer cells also decreased the transcriptional of Tcf4 (The TOP/FOP assay-Fig. 19), which signifies the potential of UDCA to suppress the transcription of Tcf4 target genes. It has been previously shown that Tcf4 is essential for crypt epithelial cell proliferation (17) and that dn-Tcf4 inhibited proliferation in LS174T and DLD1 cell lines (17) and in *Wnt*-activated-AGS tumor cell line (131). In the present work, however, both the overexpression of exogenous Tcf4 as well as suppression of endogenous Tcf4 activity with dominant negative Tcf4, led to a decrease of cell proliferation in HCT116 cell line (Fig. 20). Therefore, the role of Tcf4 as an UDCA target gene, whose suppression would cause proliferation inhibition, could not be established. Since LS174T or DLD1 and HCT116 behaved differently with respect to the role of Tcf4 on proliferation we concluded that colon cancer cell lines are not a good model to study the molecular effects of UDCA.

9.10 UDCA inhibits the proliferation in nontransformed rodent epithelial cells in *vitro*

UDCA inhibited the proliferation of normal intestinal epithelial cells also *in vitro*. 50% inhibition of proliferation was achieved in IEC-6 cell line *in vitro* with UDCA at a concentration of 500 µM (Fig. 21). IEC-6 is a nontransformed rodent intestinal epithelial cell line (132) which could serve as a model to verify the changes observed in mice.

9.11 UDCA treatment suppresses the expression of proproliferative genes in nontransformed rodent epithelial cell line IEC-6

The proproliferative genes which were suppressed by UDCA treatment in mice were also suppressed in IEC-6 cell line (Fig. 23). The nontransformed cells hitherto used *in vitro* to study the mechanism of action of UDCA were either primary rat hepatocytes

(95-97, 99) or fibroblasts (133). This is the first study where a nontransformed intestinal epithelial cell line has been used to study the mechanism of antiproliferative action of UDCA. This model allows studying the genetic changes observed in the mice without the interference of unknown mutations found in colon cancer cells.

9.12 Decrease in cell proliferation was due to cell cycle slow-down and not due to apoptosis or senescence

The decrease of proliferation rate after treatment of IEC-6 cells with 600 µM UDCA was due to the slow-down of the cell cycle which was associated with a delay of the G1→S transition (Fig. 31) and to an increase in the percentage of cells in the G1-phase (Fig. 26). Also in HCT116 colon cancer cell line, UDCA treatment resulted in a slow-down of cell cycle (Fig. 13).

In IEC-6 cells, UDCA did not cause apoptosis, as seen by DAPI staining (Fig. 24.). It has been reported that UDCA abrogates the apoptosis caused by DCA in colon cancer cell line HCT116 (92) and abrogates the TGF-β–induced apoptosis in hepatocytes (96, 134). Our data show that the decrease in proliferation rate caused by UDCA treatment is not due to cell death or apoptosis.

Martinez et al. have reported that passage of HCT116 colon cancer cell line for 3 generations in medium containing 500 µM UDCA caused senescence and little apoptosis (85). On the other hand, 3 d treatment with 400 µM UDCA caused a 50 % decrease in cell number with negligible senescence in HCT116 cell line (doctoral work of Roser Peiro Jordan). In IEC-6 cell line, senescence, as seen by β-galactosidase staining (Fig. 25.) was too low to explain a 50% decrease in cell number after 3 days of incubation with 600 µM UDCA. Hence senescence or apoptosis cannot be the reason for decrease in proliferation.

9.13 MTT assay is not the correct readout for cell proliferation in case of IEC-6 cells treated with UDCA

MTT-assay is a widely accepted method for the estimation of viable cell number. UDCA treatment increased the total amount of formazan produced per cell in IEC-6 cell line (Fig. 22). Therefore the absorbance at 550 nm was not proportional to the number of live cells in the well but to a product of cell number and the amount of formazan produced, which was dependent on UDCA concentration. Use of MTT-assay for assaying proliferation after treatment with different drugs must be dealt with caution.

9.14 High and persistent phosphorylation of ERK due to UDCA treatment decreased FCS- or EGF- or IGF-1-induced proliferation

EGF or IGF-1 induced cell proliferation and a short-lived peak of ERK phosphorylation which subsided to normal level within 4 hours. Treatment with UDCA abrogated the proproliferative effects of EGF and IGF-1 and induced a high phosphorylation of ERK which persisted for the duration of the treatment (Fig. 29 and Fig. 30). Inhibition of UDCA-induced high phosphorylation of ERK by specific inhibitors PD0325901 or U0126 abrogated the proliferation-inhibition by UDCA (Fig. 33).

Growth factors such as EGF, IGF-1 or insulin, stimulate the proliferation of epithelial cells in the intestine and induce MAPK-ERK pathway. The short-lasting ERK activation brought about by growth factors is proproliferative whereas the long-lasting / persistent ERK phosphorylation is antiproliferatory (35, 38, 104, 135, 136). In prostate cancer cells constitutive activation of MAPK/ERK led to proliferation inhibition via upregulation of BRCA2 (34). In Hep3B hepatoma cells, treatment with an inhibitor of cdc25A phosphatase (Cpd5) led to a sustained phosphorylation of ERK and to decrease in proliferation. The novel finding of this work that UDCA causes sustained phosphorylation of ERK, which decreases proliferation, is in agreement with the results of others. Thus, the present work in combination with previous reports

indicates that the suppression of the signaling pathway (through suppression of ERK protein or inhibition of its phosphorylation) as well as its jamming (through a persistent phosphorylation of ERK) slows down proliferation. The steady-state phosphorylation of ERK is affected by the phosphorylation/ dephosphorylation processes. Whether UDCA activates the phosphorylation or inhibits the dephosphorylation of ERK is not known at present.

UDCA also caused a change in the subcellular distribution of phosphorylated ERK in IEC-6 cells. There was a high and nuclear accumulation of phosphorylated ERK in IEC-6 upon treatment with 600 µM UDCA (Fig. 28). It has been reported that the phosphorylation-state of ERK determines its subcellular localisation; phosphorylated ERK is nuclear whereas cytoplasmic ERK was found to be dephorphorylated (29, 137). It has not been investigated whether the UDCA-induced nuclear localisation of phosphorylated ERK contributes to proliferative inhibition.

9.15 Suppression of ERK1 but not of ERK2 abrogated the proliferation-inhibition caused by UDCA treatment

After ascertaining that high and persistent ERK phosphorylation causes proliferation inhibition in response to UDCA, the individual role of either ERK1 or ERK2 on cell proliferation and on the response to UDCA was checked. Inhibition of either ERK1 or of ERK2 led to 40 to 50 % decrease of proliferation of IEC-6 cells (Fig. 32). The role of ERK1 or ERK2 in cell proliferation has been reported previously. ERK1 activity compensates the loss of ERK2 in fibroblasts (31). In hepatocytes, suppression of ERK2 and not of ERK1 inhibited DNA synthesis *in vitro* and *in vivo* (32). In contrast, we find that the inhibition of either ERK1 alone or ERK2 alone inhibited proliferation of IEC-6 cells. This leads to the conclusion that in intestinal epithelial cells neither of these two kinases is redundant.

In case of UDCA treatment, cells in which ERK1 was suppressed but not cells in which ERK2 was suppressed were resistant to UDCA treatment at a concentration of 400 µM. They were also less susceptible at a concentration of 600 µM (Fig. 34). Based on this result it was concluded that ERK1 is necessary for the antiproliferative

action of UDCA. The identification of ERK1 as a target of UDCA and the specific involvement of ERK1 and not of ERK2 in determining the antiproliferative effect of UDCA is a novel finding.

Development of chemical inhibitors specific for one of these two kinases without inhibiting the other could help in the further understanding of the differential regulation brought about by ERK1 and ERK2.

9.16 UDCA transcriptionally suppresses Irs-1 which is required for basal- or EGF- or IGF-1-driven proliferation

UDCA treatment for 3 d decreased Irs-1 mRNA (Fig. 23) and protein expression (Fig. 27) in IEC-6 cell line. When Irs-1 was specifically suppressed by means of siRNA, an inhibition of basal as well as of IGF-1- or EGF-induced cell growth was observed (Fig. 35). This indicated that the UDCA-induced suppression of Irs-1 contributed to the antiproliferatory effect. Surprisingly, overexpression of Irs-1 had no effect on proliferation (Fig. 36). The importance of Irs-1 for basal proliferation in breast (111) and colon carcinoma (113) cells as well as for IGF-1-induced proliferation of breast carcinoma cells (111) was reported previously. By contrast, the observation that Irs-1 is a mediator of the EGF proliferative signal is novel. The involvement of Irs-1 in both IGF-1 and EGF signaling pathways demonstrated here may explain the recently reported cross-talk between EGF and IGF-1 signaling (138) with Irs-1 as a common signaling molecule.

9.17 ERK regulates Irs-1 transcription

The protein expression of Irs-1 increased in IEC-6 cells treated with MEK1 kinase inhibitor PD0325901 or U0126 (Fig. 37C). This effect was also observed at transcriptional level (Fig. 37A), thereby associating high phosphorylation of ERK with low expression of Irs-1 mRNA/protein.

Furthermore Irs-1 protein increasd in ERK1 suppressed cells but not in ERK2 suppressed cells (Fig. 37D). The regulation of Irs-1 by UDCA at transcriptional level

was already detected by means of the arrays (Table 10.) and by RT-PCR (Fig. 23), but the specific role of ERK1 was evident from Irs-1-luciferase reporter experiments with specific ERK1 or ERK2 suppression. Irs-1 transcription increased after suppression of ERK1 but decreased after suppression of ERK2 (Fig. 37B).

It has been reported before that ERK regulates Irs-1 protein expression by phosphorylating the serine residues in Irs-1 protein and causing its degradation (139). The transcriptional regulation of Irs-1 by ERK1 and ERK2 differentially i.e. ERK1 suppressing and ERK2 enhancing the transcription of Irs-1 is a novel finding in this work.

9.18 UDCA treatment increases p21 expression which is ERK1 dependent

To investigate the link between high ERK phosphorylation and slow down of cell cycle, the expression of genes regulating the G1/S-phase of the cell cycle was checked in the array data. Expression of p21 mRNA was upregulated 1.3 fold in UDCA-treated mice as compared to that in the normal mice. Colonic epithelial cells of UDCA-treated mice showed higher expression of p21 mRNA and protein than those of the normal mice (Fig. 39). Treatment of IEC-6 cells with UDCA resulted in higher p21 mRNA and protein expression which was dependent on high phosphorylation of ERK. Suppression of p21 increased proliferation in the presence of UDCA (Fig. 40). Increase of p21 in IEC-6 cells after UDCA treatment was dependent on ERK1 and not on ERK2 (Fig. 38); a regulation similar to that of Irs-1 in UDCA-treated cells.

p21 expression induced by high and persistent ERK-phosphorylation has been reported (126). Inactivation of calmodulin caused sustained activation of ERK2 in NIH3T3 fibroblasts which led to increased expression of p21 and proliferation inhibition (140). In primary rat hepatocytes, high and persistent phosphorylation of ERK correlated with high p21 expression and inhibition of DNA synthesis (141). The specific involvement of ERK1 and not of ERK2 in increasing p21 expression by UDCA, is a novel finding. Secondly, this is also the first proof for the involvement of p21 in antiproliferative effect of UDCA.

10 Conclusions

1. UDCA inhibits the proliferation of normal intestinal epithelial cells by causing high and persistent ERK phosphorylation wherein an ERK1-dependent transcriptional suppression of Irs-1 and upregulation of p21 contributes to the decrease of cell proliferation.

2. The chemopreventive property of UDCA in colitis-associated colon cancer is attributed to decreased proliferation of epithelial cells due to suppression of several proproliferative genes.

11 Perspectives

The present work shows that the persistent ERK-P phosphorylation can neutralise the proliferative signals of EGF and of IGF-1 in colonic epithelial cells. How far this inhibition is responsible for the prevention of colitis-associated carcinogenesis by UDCA, is not clear at present. Numerous observations suggest that both pathways play a significant role in colitis-associated colon carcinogenesis. Both receptors EGFR and IGF-1R are overexpressed in the colonic mucosa of patients with ulcerative colitis (142, 143) and both pathways are associated with colon carcinogenesis. In particular ERK activation, common to both signaling pathways, is increased in the mucosa of IBD patients as well as during AOM/DSS carcinogenesis (144). Selective blocking of the signaling with antibodies (144) or specific MEK1 inhibitors (145) or simultaneous inhibition of both pathways (146) was recently shown to inhibit tumour cell proliferation. It is therefore likely that the observed blockage of IGF-1 and EGF pathways by UDCA treatment is essential for the chemopreventive effects of UDCA on colitis-associated carcinogenesis observed in the animal model. Whether in patients the UDCA concentration in the tissue indeed reaches the level necessary to obtain similar effects, requires further study. The ability of UDCA to inhibit essential signaling pathways may also explain the recent observations indicating that UDCA potentiates the cytotoxic effect of oxaliplatin (101) or SN-38 (147). Inhibition of the EGF pathway in combination with chemotherapy or radiotherapy has been shown to enhance the effect of both cytotoxic agents as well as of ionizing irradiation (148) and represents a promising option for colon carcinoma treatment. In view of the negligible side-effects of UDCA, this potential application warrants further investigation.

12 References

1. Quirke P, Risio M, Lambert R, von Karsa L, Vieth M. Quality assurance in pathology in colorectal cancer screening and diagnosis-European recommendations. Virchows Arch. 2010.

2. Fearon ER, Vogelstein B. A genetic model for colorectal tumorigenesis. Cell 1990;61(5):759-67.

3. Vogelstein B, Fearon ER, Hamilton SR*, et al.* Genetic alterations during colorectal-tumor development. N Engl J Med 1988;319(9):525-32.

4. Jones S, Chen WD, Parmigiani G*, et al.* Comparative lesion sequencing provides insights into tumor evolution. Proc Natl Acad Sci U S A 2008;105(11):4283-8.

5. Kinzler KW, Nilbert MC, Su LK*, et al.* Identification of FAP locus genes from chromosome 5q21. Science 1991;253(5020):661-5.

6. Nishisho I, Nakamura Y, Miyoshi Y*, et al.* Mutations of chromosome 5q21 genes in FAP and colorectal cancer patients. Science 1991;253(5020):665-9.

7. Vogelstein B, Kinzler KW. Cancer genes and the pathways they control. Nat Med 2004;10(8):789-99.

8. Schneikert J, Behrens J. The canonical Wnt signalling pathway and its APC partner in colon cancer development. Gut 2007;56(3):417-25.

9. He TC, Sparks AB, Rago C*, et al.* Identification of c-MYC as a target of the APC pathway. Science 1998;281(5382):1509-12.

10. Tetsu O, McCormick F. Beta-catenin regulates expression of cyclin D1 in colon carcinoma cells. Nature 1999;398(6726):422-6.

11. Araki Y, Okamura S, Hussain SP*, et al.* Regulation of cyclooxygenase-2 expression by the Wnt and ras pathways. Cancer Res 2003;63(3):728-34.

12. Du Q, Park KS, Guo Z*, et al.* Regulation of human nitric oxide synthase 2 expression by Wnt beta-catenin signaling. Cancer Res 2006;66(14):7024-31.

13. Zhang X, Gaspard JP, Chung DC. Regulation of vascular endothelial growth factor by the Wnt and K-ras pathways in colonic neoplasia. Cancer Res 2001;61(16):6050-4.

14. Wu B, Crampton SP, Hughes CC. Wnt signaling induces matrix metalloproteinase expression and regulates T cell transmigration. Immunity 2007;26(2):227-39.

15. McDonald SA, Preston SL, Lovell MJ, Wright NA, Jankowski JA. Mechanisms of disease: from stem cells to colorectal cancer. Nat Clin Pract Gastroenterol Hepatol 2006;3(5):267-74.

16. Potten CS, Loeffler M. Stem cells: attributes, cycles, spirals, pitfalls and uncertainties. Lessons for and from the crypt. Development 1990;110(4):1001-20.

17. van de Wetering M, Sancho E, Verweij C*, et al.* The beta-catenin/TCF-4 complex imposes a crypt progenitor phenotype on colorectal cancer cells. Cell 2002;111(2):241-50.

18. Roger L, Jullien L, Gire V, Roux P. Gain of oncogenic function of p53 mutants regulates E-cadherin expression uncoupled from cell invasion in colon cancer cells. J Cell Sci;123(Pt 8):1295-305.

19. Ruijs MW, Verhoef S, Rookus MA*, et al.* TP53 germline mutation testing in 180 families suspected of Li-Fraumeni syndrome: mutation detection rate and relative frequency of cancers in different familial phenotypes. J Med Genet;47(6):421-8.

20. Varley JM. Germline TP53 mutations and Li-Fraumeni syndrome. Hum Mutat 2003;21(3):313-20.

21. Takayama T, Miyanishi K, Hayashi T, Sato Y, Niitsu Y. Colorectal cancer: genetics of development and metastasis. J Gastroenterol 2006;41(3):185-92.

22. Pearson G, Robinson F, Beers Gibson T*, et al.* Mitogen-activated protein (MAP) kinase pathways: regulation and physiological functions. Endocr Rev 2001;22(2):153-83.

23. Cohen G, Mustafi R, Chumsangsri A*, et al.* Epidermal growth factor receptor signaling is up-regulated in human colonic aberrant crypt foci. Cancer Res 2006;66(11):5656-64.

24. Dougherty U, Cerasi D, Taylor I*, et al.* Epidermal growth factor receptor is required for colonic tumor promotion by dietary fat in the azoxymethane/dextran sulfate sodium model: roles of transforming growth factor-{alpha} and PTGS2. Clin Cancer Res 2009;15(22):6780-9.

25. Fichera A, Little N, Jagadeeswaran S*, et al.* Epidermal growth factor receptor signaling is required for microadenoma formation in the mouse azoxymethane model of colonic carcinogenesis. Cancer Res 2007;67(2):827-35.

26. Pouyssegur J, Volmat V, Lenormand P. Fidelity and spatio-temporal control in MAP kinase (ERKs) signalling. Biochem Pharmacol 2002;64(5-6):755-63.

27. Meloche S. Cell cycle reentry of mammalian fibroblasts is accompanied by the sustained activation of p44mapk and p42mapk isoforms in the G1 phase and their inactivation at the G1/S transition. J Cell Physiol 1995;163(3):577-88.

28. Chen RH, Sarnecki C, Blenis J. Nuclear localization and regulation of erk- and rsk-encoded protein kinases. Mol Cell Biol 1992;12(3):915-27.

29. Shankaran H, Ippolito DL, Chrisler WB*, et al.* Rapid and sustained nuclear-cytoplasmic ERK oscillations induced by epidermal growth factor. Mol Syst Biol 2009;5:332.

30. Dumesic PA, Scholl FA, Barragan DI, Khavari PA. Erk1/2 MAP kinases are required for epidermal G2/M progression. J Cell Biol 2009;185(3):409-22.

31. Lefloch R, Pouyssegur J, Lenormand P. Single and combined silencing of ERK1 and ERK2 reveals their positive contribution to growth signaling depending on their expression levels. Mol Cell Biol 2008;28(1):511-27.

32. Bessard A, Fremin C, Ezan F, Fautrel A, Gailhouste L, Baffet G. RNAi-mediated ERK2 knockdown inhibits growth of tumor cells in vitro and in vivo. Oncogene 2008;27(40):5315-25.

33. Roovers K, Assoian RK. Integrating the MAP kinase signal into the G1 phase cell cycle machinery. Bioessays 2000;22(9):818-26.

34. Moro L, Arbini AA, Marra E, Greco M. Constitutive activation of MAPK/ERK inhibits prostate cancer cell proliferation through upregulation of BRCA2. Int J Oncol 2007;30(1):217-24.

35. Hong SK, Yoon S, Moelling C, Arthan D, Park JI. Noncatalytic function of ERK1/2 can promote Raf/MEK/ERK-mediated growth arrest signaling. J Biol Chem 2009;284(48):33006-18.

36. Collins NL, Reginato MJ, Paulus JK, Sgroi DC, Labaer J, Brugge JS. G1/S cell cycle arrest provides anoikis resistance through Erk-mediated Bim suppression. Mol Cell Biol 2005;25(12):5282-91.

37. Wang Z, Zhang B, Wang M, Carr BI. Persistent ERK phosphorylation negatively regulates cAMP response element-binding protein (CREB) activity via recruitment of CREB-binding protein to pp90RSK. J Biol Chem 2003;278(13):11138-44.

38. Goulet AC, Chigbrow M, Frisk P, Nelson MA. Selenomethionine induces sustained ERK phosphorylation leading to cell-cycle arrest in human colon cancer cells. Carcinogenesis 2005;26(1):109-17.

39. Gryfe R. Inherited colorectal cancer syndromes. Clin Colon Rectal Surg 2009;22(4):198-208.

40. Lynch HT, Krush AJ. Cancer family "G" revisited: 1895-1970. Cancer 1971;27(6):1505-11.

41. de la Chapelle A. Genetic predisposition to colorectal cancer. Nat Rev Cancer 2004;4(10):769-80.

42. Lynch HT, Shaw TG, Lynch JF. Inherited predisposition to cancer: a historical overview. Am J Med Genet C Semin Med Genet 2004;129C(1):5-22.

43. Bhagirath T, Condie A, Dunlop MG, Wyllie AH, Prosser J. Exclusion of constitutional p53 mutations as a cause of genetic susceptibility to colorectal cancer. Br J Cancer 1993;68(4):712-4.

44. Itzkowitz SH, Yio X. Inflammation and cancer IV. Colorectal cancer in inflammatory bowel disease: the role of inflammation. Am J Physiol Gastrointest Liver Physiol 2004;287(1):G7-17.

45. Vagefi PA, Longo WE. Colorectal cancer in patients with inflammatory bowel disease. Clin Colorectal Cancer 2005;4(5):313-9.

46. Aggarwal BB, Shishodia S, Sandur SK, Pandey MK, Sethi G. Inflammation and cancer: how hot is the link? Biochem Pharmacol 2006;72(11):1605-21.

47. Greten FR, Eckmann L, Greten TF*, et al.* IKKbeta links inflammation and tumorigenesis in a mouse model of colitis-associated cancer. Cell 2004;118(3):285-96.

48. Jones SA, Richards PJ, Scheller J, Rose-John S. IL-6 transsignaling: the in vivo consequences. J Interferon Cytokine Res 2005;25(5):241-53.

49. Grivennikov S, Karin E, Terzic J*, et al.* IL-6 and Stat3 are required for survival of intestinal epithelial cells and development of colitis-associated cancer. Cancer Cell 2009;15(2):103-13.

50. Turini ME, DuBois RN. Cyclooxygenase-2: a therapeutic target. Annu Rev Med 2002;53:35-57.

51. Giardiello FM, Hamilton SR, Krush AJ*, et al.* Treatment of colonic and rectal adenomas with sulindac in familial adenomatous polyposis. N Engl J Med 1993;328(18):1313-6.

52. Huls G, Koornstra JJ, Kleibeuker JH. Non-steroidal anti-inflammatory drugs and molecular carcinogenesis of colorectal carcinomas. Lancet 2003;362(9379):230-2.

53. Kune GA, Kune S, Watson LF. Colorectal cancer risk, chronic illnesses, operations, and medications: case control results from the Melbourne Colorectal Cancer Study. Cancer Res 1988;48(15):4399-404.

54. Kune GA. Colorectal cancer chemoprevention: aspirin, other NSAID and COX-2 inhibitors. Aust N Z J Surg 2000;70(6):452-5.

55. Waddell WR, Loughry RW. Sulindac for polyposis of the colon. J Surg Oncol 1983;24(1):83-7.

56. Barnes CJ, Lee M. Chemoprevention of spontaneous intestinal adenomas in the adenomatous polyposis coli Min mouse model with aspirin. Gastroenterology 1998;114(5):873-7.

57. Jacoby RF, Seibert K, Cole CE, Kelloff G, Lubet RA. The cyclooxygenase-2 inhibitor celecoxib is a potent preventive and therapeutic agent in the min mouse model of adenomatous polyposis. Cancer Res 2000;60(18):5040-4.

58. Oshima M, Murai N, Kargman S*, et al.* Chemoprevention of intestinal polyposis in the Apcdelta716 mouse by rofecoxib, a specific cyclooxygenase-2 inhibitor. Cancer Res 2001;61(4):1733-40.

59. Lala PK, Chakraborty C. Role of nitric oxide in carcinogenesis and tumour progression. Lancet Oncol 2001;2(3):149-56.

60. Tamir S, Burney S, Tannenbaum SR. DNA damage by nitric oxide. Chem Res Toxicol 1996;9(5):821-7.

61. Tamir S, Tannenbaum SR. The role of nitric oxide (NO.) in the carcinogenic process. Biochim Biophys Acta 1996;1288(2):F31-6.

62. Zhuang JC, Wright TL, deRojas-Walker T, Tannenbaum SR, Wogan GN. Nitric oxide-induced mutations in the HPRT gene of human lymphoblastoid TK6 cells and in Salmonella typhimurium. Environ Mol Mutagen 2000;35(1):39-47.

63. Kim YJ, Lee JS, Hong KS, Chung JW, Kim JH, Hahm KB. Novel application of proton pump inhibitor for the prevention of colitis-induced colorectal carcinogenesis beyond acid suppression. Cancer Prev Res (Phila);3(8):963-74.

64. Velayos FS, Loftus EV, Jr., Jess T*, et al.* Predictive and protective factors associated with colorectal cancer in ulcerative colitis: A case-control study. Gastroenterology 2006;130(7):1941-9.

65. Moody GA, Jayanthi V, Probert CS, Mac Kay H, Mayberry JF. Long-term therapy with sulphasalazine protects against colorectal cancer in ulcerative colitis: a retrospective study of colorectal cancer risk and compliance with treatment in Leicestershire. Eur J Gastroenterol Hepatol 1996;8(12):1179-83.

66. Rubin DT, LoSavio A, Yadron N, Huo D, Hanauer SB. Aminosalicylate therapy in the prevention of dysplasia and colorectal cancer in ulcerative colitis. Clin Gastroenterol Hepatol 2006;4(11):1346-50.

67. Lyakhovich A, Gasche C. Systematic review: molecular chemoprevention of colorectal malignancy by mesalazine. Aliment Pharmacol Ther 2010;31(2):202-9.

68. Debruyne PR, Bruyneel EA, Li X, Zimber A, Gespach C, Mareel MM. The role of bile acids in carcinogenesis. Mutat Res 2001;480-481:359-69.

69. Asciutti S, Castellani D, Nardi E*, et al.* A new amino acid derivative of ursodeoxycholate, (N-L-Glutamyl)-UDCA (UDCA-Glu), to selectively release UDCA in the colon. Anticancer Res 2009;29(12):4971-9.

70. Balan V, LaRusso NF. Hepatobiliary disease in inflammatory bowel disease. Gastroenterol Clin North Am 1995;24(3):647-69.

71. Pardi DS, Loftus EV, Jr., Kremers WK, Keach J, Lindor KD. Ursodeoxycholic acid as a chemopreventive agent in patients with ulcerative colitis and primary sclerosing cholangitis. Gastroenterology 2003;124(4):889-93.

72. Tung BY, Emond MJ, Haggitt RC*, et al.* Ursodiol use is associated with lower prevalence of colonic neoplasia in patients with ulcerative colitis and primary sclerosing cholangitis. Ann Intern Med 2001;134(2):89-95.

73. Chen L, Borozan I, Milkiewicz P*, et al.* Gene expression profiling of early primary biliary cirrhosis: possible insights into the mechanism of action of ursodeoxycholic acid. Liver Int 2008;28(7):997-1010.

74. Arenas F, Hervias I, Uriz M, Joplin R, Prieto J, Medina JF. Combination of ursodeoxycholic acid and glucocorticoids upregulates the AE2 alternate promoter in human liver cells. J Clin Invest 2008;118(2):695-709.

75. Serfaty L, De Leusse A, Rosmorduc O*, et al.* Ursodeoxycholic acid therapy and the risk of colorectal adenoma in patients with primary biliary cirrhosis: an observational study. Hepatology 2003;38(1):203-9.

76. Ochsenkuhn T, Marsteller I, Hay U*, et al.* Does ursodeoxycholic acid change the proliferation of the colorectal mucosa?. A randomized, placebo-controlled study. Digestion 2003;68(4):209-16.

77. Alberts DS, Martinez ME, Hess LM*, et al.* Phase III trial of ursodeoxycholic acid to prevent colorectal adenoma recurrence. J Natl Cancer Inst 2005;97(11):846-53.

78. Khare S, Cerda S, Wali RK*, et al.* Ursodeoxycholic acid inhibits Ras mutations, wild-type Ras activation, and cyclooxygenase-2 expression in colon cancer. Cancer Res 2003;63(13):3517-23.

79. Wali RK, Khare S, Tretiakova M*, et al.* Ursodeoxycholic acid and F(6)-D(3) inhibit aberrant crypt proliferation in the rat azoxymethane model of colon cancer: roles of cyclin D1 and E-cadherin. Cancer Epidemiol Biomarkers Prev 2002;11(12):1653-62.

80. Earnest DL, Holubec H, Wali RK*, et al.* Chemoprevention of azoxymethane-induced colonic carcinogenesis by supplemental dietary ursodeoxycholic acid. Cancer Res 1994;54(19):5071-4.

81. Kohno H, Suzuki R, Yasui Y, Miyamoto S, Wakabayashi K, Tanaka T. Ursodeoxycholic acid versus sulfasalazine in colitis-related colon carcinogenesis in mice. Clin Cancer Res 2007;13(8):2519-25.

82. Khare S, Mustafi R, Cerda S*, et al.* Ursodeoxycholic acid suppresses Cox-2 expression in colon cancer: roles of Ras, p38, and CCAAT/enhancer-binding protein. Nutr Cancer 2008;60(3):389-400.

83. Loddenkemper C, Keller S, Hanski ML*, et al.* Prevention of colitis-associated carcinogenesis in a mouse model by diet supplementation with ursodeoxycholic acid. Int J Cancer 2006;118(11):2750-7.

84. Jacoby RF, Cole CE, Hawk ET, Lubet RA. Ursodeoxycholate/Sulindac combination treatment effectively prevents intestinal adenomas in a mouse model of polyposis. Gastroenterology 2004;127(3):838-44.

85. Akare S, Jean-Louis S, Chen W, Wood DJ, Powell AA, Martinez JD. Ursodeoxycholic acid modulates histone acetylation and induces differentiation and senescence. Int J Cancer 2006;119(12):2958-69.

86. Powell AA, LaRue JM, Batta AK, Martinez JD. Bile acid hydrophobicity is correlated with induction of apoptosis and/or growth arrest in HCT116 cells. Biochem J 2001;356(Pt 2):481-6.

87. Shiraki K, Ito T, Sugimoto K*, et al.* Different effects of bile acids, ursodeoxycholic acid and deoxycholic acid, on cell growth and cell death in human colonic adenocarcinoma cells. Int J Mol Med 2005;16(4):729-33.

88. Feldman R, Martinez JD. Growth suppression by ursodeoxycholic acid involves caveolin-1 enhanced degradation of EGFR. Biochim Biophys Acta 2009;1793(8):1387-94.

89. Qiao D, Stratagouleas ED, Martinez JD. Activation and role of mitogen-activated protein kinases in deoxycholic acid-induced apoptosis. Carcinogenesis 2001;22(1):35-41.

90. Shah SA, Volkov Y, Arfin Q, Abdel-Latif MM, Kelleher D. Ursodeoxycholic acid inhibits interleukin 1 beta [corrected] and deoxycholic acid-induced activation of NF-kappaB and AP-1 in human colon cancer cells. Int J Cancer 2006;118(3):532-9.

91. Im E, Martinez JD. Ursodeoxycholic acid (UDCA) can inhibit deoxycholic acid (DCA)-induced apoptosis via modulation of EGFR/Raf-1/ERK signaling in human colon cancer cells. J Nutr 2004;134(2):483-6.

92. Im E, Akare S, Powell A, Martinez JD. Ursodeoxycholic acid can suppress deoxycholic acid-induced apoptosis by stimulating Akt/PKB-dependent survival signaling. Nutr Cancer 2005;51(1):110-6.

93. Byrne AM, Foran E, Sharma R*, et al.* Bile acids modulate the Golgi membrane fission process via a protein kinase C - eta and protein kinase D-dependent pathway in colonic epithelial cells. Carcinogenesis 2010;31(4):737-44.

94. Shah SA, Looby E, Volkov Y, Long A, Kelleher D. Ursodeoxycholic acid inhibits translocation of protein kinase C in human colonic cancer cell lines. Eur J Cancer 2005;41(14):2160-9.

95. Sola S, Amaral JD, Castro RE*, et al.* Nuclear translocation of UDCA by the glucocorticoid receptor is required to reduce TGF-beta1-induced apoptosis in rat hepatocytes. Hepatology 2005;42(4):925-34.

96. Sola S, Castro RE, Kren BT, Steer CJ, Rodrigues CM. Modulation of nuclear steroid receptors by ursodeoxycholic acid inhibits TGF-beta1-induced E2F-1/p53-mediated apoptosis of rat hepatocytes. Biochemistry 2004;43(26):8429-38.

97. Sola S, Ma X, Castro RE, Kren BT, Steer CJ, Rodrigues CM. Ursodeoxycholic acid modulates E2F-1 and p53 expression through a caspase-independent mechanism in transforming growth factor beta1-induced apoptosis of rat hepatocytes. J Biol Chem 2003;278(49):48831-8.

98. Amaral JD, Castro RE, Sola S, Steer CJ, Rodrigues CM. p53 is a key molecular target of ursodeoxycholic acid in regulating apoptosis. J Biol Chem 2007;282(47):34250-9.

99. Castro RE, Amaral JD, Sola S, Kren BT, Steer CJ, Rodrigues CM. Differential regulation of cyclin D1 and cell death by bile acids in primary rat hepatocytes. Am J Physiol Gastrointest Liver Physiol 2007;293(1):G327-34.

100. Castro RE, Sola S, Ma X*, et al.* A distinct microarray gene expression profile in primary rat hepatocytes incubated with ursodeoxycholic acid. J Hepatol 2005;42(6):897-906.

101. Lim SC, Choi JE, Kang HS, Han SI. Ursodeoxycholic acid switches oxaliplatin-induced necrosis to apoptosis by inhibiting reactive oxygen species production and activating p53-caspase 8 pathway in HepG2 hepatocellular carcinoma. Int J Cancer;126(7):1582-95.

102. Arisawa S, Ishida K, Kameyama N*, et al.* Ursodeoxycholic acid induces glutathione synthesis through activation of PI3K/Akt pathway in HepG2 cells. Biochem Pharmacol 2009;77(5):858-66.

103. Weitzel C, Stark D, Kullmann F, Scholmerich J, Holstege A, Falk W. Ursodeoxycholic acid induced activation of the glucocorticoid receptor in primary rat hepatocytes. Eur J Gastroenterol Hepatol 2005;17(2):169-77.

104. Menges CW, McCance DJ. Constitutive activation of the Raf-MAPK pathway causes negative feedback inhibition of Ras-PI3K-AKT and cellular arrest through the EphA2 receptor. Oncogene 2008;27(20):2934-40.

105. Wee S, Jagani Z, Xiang KX*, et al.* PI3K pathway activation mediates resistance to MEK inhibitors in KRAS mutant cancers. Cancer Res 2009;69(10):4286-93.

106. Liang L, Zhou T, Jiang J, Pierce JH, Gustafson TA, Frank SJ. Insulin receptor substrate-1 enhances growth hormone-induced proliferation. Endocrinology 1999;140(5):1972-83.

107. Wu A, Chen J, Baserga R. Nuclear insulin receptor substrate-1 activates promoters of cell cycle progression genes. Oncogene 2008;27(3):397-403.

108. Chang Q, Li Y, White MF, Fletcher JA, Xiao S. Constitutive activation of insulin receptor substrate 1 is a frequent event in human tumors: therapeutic implications. Cancer Res 2002;62(21):6035-8.

109. Surmacz E, Burgaud JL. Overexpression of insulin receptor substrate 1 (IRS-1) in the human breast cancer cell line MCF-7 induces loss of estrogen requirements for growth and transformation. Clin Cancer Res 1995;1(11):1429-36.

110. del Rincon SV, Rousseau C, Samanta R, Miller WH, Jr. Retinoic acid-induced growth arrest of MCF-7 cells involves the selective regulation of the IRS-1/PI 3-kinase/AKT pathway. Oncogene 2003;22(22):3353-60.

111. Byron SA, Horwitz KB, Richer JK, Lange CA, Zhang X, Yee D. Insulin receptor substrates mediate distinct biological responses to insulin-like growth factor receptor activation in breast cancer cells. Br J Cancer 2006;95(9):1220-8.

112. La Rocca G, Badin M, Shi B*, et al.* Mechanism of growth inhibition by MicroRNA 145: the role of the IGF-I receptor signaling pathway. J Cell Physiol 2009;220(2):485-91.

113. Shi B, Sepp-Lorenzino L, Prisco M, Linsley P, deAngelis T, Baserga R. Micro RNA 145 targets the insulin receptor substrate-1 and inhibits the growth of colon cancer cells. J Biol Chem 2007;282(45):32582-90.

114. Dearth RK, Cui X, Kim HJ*, et al.* Mammary tumorigenesis and metastasis caused by overexpression of insulin receptor substrate 1 (IRS-1) or IRS-2. Mol Cell Biol 2006;26(24):9302-14.

115. Udelhoven M, Leeser U, Freude S*, et al.* Identification of a region in the human IRS2 promoter essential for stress induced transcription depending on SP1, NFI binding and ERK activation in HepG2 cells. J Mol Endocrinol 2010;44(2):99-113.

116. Zeng YX, Somasundaram K, el-Deiry WS. AP2 inhibits cancer cell growth and activates p21WAF1/CIP1 expression. Nat Genet 1997;15(1):78-82.

117. Hirose Y, Berger MS, Pieper RO. p53 effects both the duration of G2/M arrest and the fate of temozolomide-treated human glioblastoma cells. Cancer Res 2001;61(5):1957-63.

118. Sato S, Fujita N, Tsuruo T. Modulation of Akt kinase activity by binding to Hsp90. Proc Natl Acad Sci U S A 2000;97(20):10832-7.

119. Benzeno S, Narla G, Allina J*, et al.* Cyclin-dependent kinase inhibition by the KLF6 tumor suppressor protein through interaction with cyclin D1. Cancer Res 2004;64(11):3885-91.

120. Sangodkar J, Shi J, DiFeo A*, et al.* Functional role of the KLF6 tumour suppressor gene in gastric cancer. Eur J Cancer 2009;45(4):666-76.

121. Gorbacheva VY, Lindner D, Sen GC, Vestal DJ. The interferon (IFN)-induced GTPase, mGBP-2. Role in IFN-gamma-induced murine fibroblast proliferation. J Biol Chem 2002;277(8):6080-7.

122. Messmer-Blust AF, Balasubramanian S, Gorbacheva VY, Jeyaratnam JA, Vestal DJ. The interferon-gamma-induced murine guanylate-binding protein-2 inhibits rac activation during cell spreading on fibronectin and after platelet-derived growth factor treatment: role for phosphatidylinositol 3-kinase. Mol Biol Cell 2010;21(14):2514-28.

123. Cavallo RA, Cox RT, Moline MM*, et al.* Drosophila Tcf and Groucho interact to repress Wingless signalling activity. Nature 1998;395(6702):604-8.

124. Laemmli UK. Cleavage of structural proteins during the assembly of the head of bacteriophage T4. Nature 1970;227(5259):680-5.

125. Ciccarelli C, Marampon F, Scoglio A*, et al.* p21WAF1 expression induced by MEK/ERK pathway activation or inhibition correlates with growth arrest, myogenic differentiation and onco-phenotype reversal in rhabdomyosarcoma cells. Mol Cancer 2005;4:41-59.

126. Kim WJ, Lee SJ, Choi YD, Moon SK. Decursin inhibits growth of human bladder and colon cancer cells via apoptosis, G1-phase cell cycle arrest and extracellular signal-regulated kinase activation. Int J Mol Med;25(4):635-41.

127. Boismenu R, Chen Y, Chou K, El-Sheikh A, Buelow R. Orally administered RDP58 reduces the severity of dextran sodium sulphate induced colitis. Ann Rheum Dis 2002;61 Suppl 2:ii19-24.

128. Mizoguchi E, Xavier RJ, Reinecker HC*, et al.* Colonic epithelial functional phenotype varies with type and phase of experimental colitis. Gastroenterology 2003;125(1):148-61.

129. Fang K, Bruce M, Pattillo CB*, et al.* Temporal Genome Wide Expression Profiling of DSS Colitis Reveals Novel Inflammatory and Angiogenesis Genes Similar to Ulcerative Colitis. Physiol Genomics.

130. Powell AA, Akare S, Qi W*, et al.* Resistance to ursodeoxycholic acid-induced growth arrest can also result in resistance to deoxycholic acid-induced apoptosis and increased tumorgenicity. BMC Cancer 2006;6:219-227.

131. Asciutti S, Akiri G, Grumolato L, Vijayakumar S, Aaronson SA. Diverse mechanisms of Wnt activation and effects of pathway inhibition on proliferation of human gastric carcinoma cells. Oncogene.

132. Quaroni A, Wands J, Trelstad RL, Isselbacher KJ. Epithelioid cell cultures from rat small intestine. Characterization by morphologic and immunologic criteria. J Cell Biol 1979;80(2):248-65.

133. Hiramatsu K, Matsumoto Y, Miyazaki M, Tsubouchi H, Yamamoto I, Gohda E. Inhibition of hepatocyte growth factor production in human fibroblasts by ursodeoxycholic acid. Biol Pharm Bull 2005;28(4):619-24.

134. Liang TJ, Yuan JH, Tan YR*, et al.* Effect of ursodeoxycholic acid on TGF beta1/Smad signaling pathway in rat hepatic stellate cells. Chin Med J (Engl) 2009;122(10):1209-13.

135. Murphy LO, Smith S, Chen RH, Fingar DC, Blenis J. Molecular interpretation of ERK signal duration by immediate early gene products. Nat Cell Biol 2002;4(8):556-64.

136. Meloche S, Pouyssegur J. The ERK1/2 mitogen-activated protein kinase pathway as a master regulator of the G1- to S-phase transition. Oncogene 2007;26(22):3227-39.

137. Mebratu Y, Tesfaigzi Y. How ERK1/2 activation controls cell proliferation and cell death: Is subcellular localization the answer? Cell Cycle 2009;8(8):1168-75.

138. Haluska P, Carboni JM, TenEyck C*, et al.* HER receptor signaling confers resistance to the insulin-like growth factor-I receptor inhibitor, BMS-536924. Mol Cancer Ther 2008;7(9):2589-98.

139. De Fea K, Roth RA. Modulation of insulin receptor substrate-1 tyrosine phosphorylation and function by mitogen-activated protein kinase. J Biol Chem 1997;272(50):31400-6.

140. Bosch M, Gil J, Bachs O, Agell N. Calmodulin inhibitor W13 induces sustained activation of ERK2 and expression of p21(cip1). J Biol Chem 1998;273(34):22145-50.

141. Tombes RM, Auer KL, Mikkelsen R*, et al.* The mitogen-activated protein (MAP) kinase cascade can either stimulate or inhibit DNA synthesis in primary cultures of rat hepatocytes depending upon whether its activation is acute/phasic or chronic. Biochem J 1998;330 (Pt 3):1451-60.

142. Sipos F, Galamb O, Herszenyi L*, et al.* Elevated insulin-like growth factor 1 receptor, hepatocyte growth factor receptor and telomerase protein expression in mild ulcerative colitis. Scand J Gastroenterol 2008;43(3):289-98.

143. Malecka-Panas E, Kordek R, Biernat W, Tureaud J, Liberski PP, Majumdar AP. Differential activation of total and EGF receptor (EGF-R) tyrosine kinase (tyr-k) in the rectal mucosa in patients with adenomatous polyps, ulcerative colitis and colon cancer. Hepatogastroenterology 1997;44(14):435-40.

144. Fichera A, Little N, Dougherty U*, et al.* A vitamin D analogue inhibits colonic carcinogenesis in the AOM/DSS model. J Surg Res 2007;142(2):239-45.

145. Marampon F, Bossi G, Ciccarelli C*, et al.* MEK/ERK inhibitor U0126 affects in vitro and in vivo growth of embryonal rhabdomyosarcoma. Mol Cancer Ther 2009;8(3):543-51.

146. Kaulfuss S, Burfeind P, Gaedcke J, Scharf JG. Dual silencing of insulin-like growth factor-I receptor and epidermal growth factor receptor in colorectal cancer cells is associated with decreased proliferation and enhanced apoptosis. Mol Cancer Ther 2009;8(4):821-33.

147. Ikegami T, Matsuzaki Y, Al Rashid M, Ceryak S, Zhang Y, Bouscarel B. Enhancement of DNA topoisomerase I inhibitor-induced apoptosis by ursodeoxycholic acid. Mol Cancer Ther 2006;5(1):68-79.

148. Ciardiello F, Tortora G. A novel approach in the treatment of cancer: targeting the epidermal growth factor receptor. Clin Cancer Res 2001;7(10):2958-70.

Note : The reference-information is incomplete for certain rescent publications which have appeared ahead of print on Pubmed.

13 Supplementary tables: Affymetrix Microarray evaluation

Table 11. List of all genes upregulated due to DSS-colitis compared to normal.

Affymetrix id	Gene Name	Full Name	Fold Change
1425519_a_at	Cd74	CD74 antigen (invariant polypeptide of major histocompatibility complex, class II antigen-associated)	38,98
1418536_at	H2-Q5	Q7 alpha chain precursor (QA-2 antigen) /// similar to MHC class Ib antigen	16,66
1450648_s_at	H2-Ab1	histocompatibility 2, class II antigen A, beta 1	12,51
1423858_a_at	Hmgcs2	3-hydroxy-3-methylglutaryl-Coenzyme A synthase 2	9,28
1434881_s_at	Kctd12	potassium channel tetramerisation domain containing 12	8,61
1427482_a_at	Car8	carbonic anhydrase 8	7,31
1419043_a_at	Iigp1	interferon inducible GTPase 1	6,79
1424509_at	Cd177	CD177 antigen	6,66
1429381_x_at	Igh /// Igh-2 /// Igh-VJ558 /// LOC677563	immunoglobulin heavy chain (J558 family) /// immunoglobulin heavy chain complex /// immunoglobulin heavy chain 2 (serum IgA) /// similar to Ig heavy chain V region VH558 A1/A4 precursor	6,58
1448573_a_at	Ceacam10	CEA-related cell adhesion molecule 10	6,54
1427746_x_at	LOC100044874	similar to H-2K(d) antigen	6,05
1424948_x_at	H2-D1 /// H2-K1 /// LOC100044874	histocompatibility 2, D region locus 1 /// histocompatibility 2, K1, K region /// similar to H-2K(d) antigen	5,80
1419132_at	Tlr2	toll-like receptor 2	5,67
1428485_at	Car12	carbonic anyhydrase 12	5,60
1417936_at	Ccl9	chemokine (C-C motif) ligand 9	5,25
1417160_s_at	Expi	extracellular proteinase inhibitor	4,79
1416380_at	Mov10	Moloney leukemia virus 10	4,73
1448377_at	Slpi	secretory leukocyte peptidase inhibitor	4,53
1429994_s_at	Cyp2c65	cytochrome P450, family 2, subfamily c, polypeptide 65	4,46
1419700_a_at	Prom1	prominin 1	4,39
1416016_at	Tap1	transporter 1, ATP-binding cassette, sub-family B (MDR/TAP)	4,01
1422678_at	Dgat2	diacylglycerol O-acyltransferase 2	3,97
1422962_a_at	Psmb8	proteasome (prosome, macropain) subunit, beta type 8 (large multifunctional peptidase 7)	3,86
1450387_s_at	Ak3l1 /// LOC100047616	adenylate kinase 3 alpha-like 1 /// similar to adenylate kinase 4	3,85
1451969_s_at	Parp3	poly (ADP-ribose) polymerase family, member 3	3,77
1422772_at	C1galt1	core 1 synthase, glycoprotein-N-acetylgalactosamine 3-beta-galactosyltransferase, 1	3,72
1428319_at	Pdlim7	PDZ and LIM domain 7	3,63
1423140_at	Lipa	lysosomal acid lipase A	3,60
1450271_at	Ptk6	PTK6 protein tyrosine kinase 6	3,57
1422974_at	Nt5e	5' nucleotidase, ecto	3,49
1448233_at	Prnp	prion protein	3,48
1426225_at	LOC100047573 /// Rbp4	retinol binding protein 4, plasma /// similar to retinol binding protein	3,47
1424830_at	Ccnk	cyclin K	3,46

Table 11. List of all genes upregulated due to DSS-colitis compared to normal.

Affymetrix id	Gene Name	Full Name	Fold Change
1426550_at	Sidt1	SID1 transmembrane family, member 1	3,32
1422619_at	Ppap2a	phosphatidic acid phosphatase 2a	3,28
1420610_at	Prkacb	protein kinase, cAMP dependent, catalytic, beta	3,27
1450537_at	Mid2	midline 2	3,25
1416576_at	Socs3	suppressor of cytokine signaling 3	3,25
1450355_a_at	Capg	capping protein (actin filament), gelsolin-like	3,22
1428443_a_at	Rap1gap	Rap1 GTPase-activating protein	3,21
1425952_a_at	Gcg	glucagon	3,20
1450528_at	B3galt5	UDP-Gal:betaGlcNAc beta 1,3-galactosyltransferase, polypeptide 5	3,14
1435906_x_at	Gbp2	guanylate nucleotide binding protein 2	3,05
1427137_at	Ces5	carboxylesterase 5	3,04
1416673_at	Bace2	beta-site APP-cleaving enzyme 2	3,01
1420505_a_at	Stxbp1	syntaxin binding protein 1	3,01
1424688_at	Creb3l3	cAMP responsive element binding protein 3-like 3	3,01
1452357_at	Gp1bb /// LOC100044138 /// Sept5	glycoprotein Ib, beta polypeptide /// septin 5 /// similar to CDCrel-1A I	2,99
1449896_at	Mlph	melanophilin	2,98
1435716_x_at	Snrpn /// Snurf	small nuclear ribonucleoprotein N /// SNRPN upstream reading frame	2,90
1432453_a_at	Ms4a10	membrane-spanning 4-domains, subfamily A, member 10	2,90
1459903_at	Sema7a	sema domain, immunoglobulin domain (Ig), and GPI membrane anchor, (semaphorin) 7A	2,89
1417333_at	Rasa4	RAS p21 protein activator 4	2,88
1451970_at	Daglb	diacylglycerol lipase, beta	2,87
1423865_at	Slc44a1	solute carrier family 44, member 1	2,84
1426098_a_at	Cast	calpastatin	2,83
1427398_at	Muc4	mucin 4	2,82
1425598_a_at	LOC676654 /// Lyn	Yamaguchi sarcoma viral (v-yes-1) oncogene homolog /// similar to Yamaguchi sarcoma viral (v-yes-1) oncogene homolog	2,77
1435857_s_at	Aplp1	amyloid beta (A4) precursor-like protein 1	2,70
1425273_s_at	Emp2	epithelial membrane protein 2	2,68
1424901_at	Gcnt3	glucosaminyl (N-acetyl) transferase 3, mucin type	2,65
1426324_at	H2-D1	histocompatibility 2, D region locus 1	2,64
1426114_at	Hnrpab	heterogeneous nuclear ribonucleoprotein A/B	2,64
1427711_a_at	Ceacam1	CEA-related cell adhesion molecule 1	2,63
1418099_at	Tnfrsf1b	tumor necrosis factor receptor superfamily, member 1b	2,62
1422635_at	Ache	acetylcholinesterase	2,59
1419570_at	Slc28a3	solute carrier family 28 (sodium-coupled nucleoside transporter), member 3	2,59

Table 11. List of all genes upregulated due to DSS-colitis compared to normal.

Affymetrix id	Gene Name	Full Name	Fold Change
1451438_s_at	Clec2h	C-type lectin domain family 2, member h	2,55
1448998_at	Lpo	lactoperoxidase	2,55
1421156_a_at	Dsc2	desmocollin 2	2,54
1422876_at	Capn9	calpain 9 (nCL-4) /// similar to calpain 9 (nCL-4)	2,50
1420760_s_at	Ndrg1	N-myc downstream regulated gene 1	2,49
1418925_at	Celsr1	cadherin, EGF LAG seven-pass G-type receptor 1 (flamingo homolog, Drosophila)	2,48
1421646_a_at	Pias3	protein inhibitor of activated STAT 3	2,43
1436766_at	Luc7l2	LUC7-like 2 (S. cerevisiae)	2,43
1454268_a_at	Cyba	cytochrome b-245, alpha polypeptide	2,42
1422705_at	Tmepai	transmembrane, prostate androgen induced RNA	2,40
1424612_at	Npal2	NIPA-like domain containing 2	2,39
1448883_at	Lgmn	legumain	2,39
1451794_at	Tmcc3	transmembrane and coiled coil domains 3	2,37
1422597_at	Mmp15	matrix metallopeptidase 15	2,37
1419103_a_at	Abhd6	abhydrolase domain containing 6	2,37
1460380_at	Dsg2	desmoglein 2	2,36
1455593_at	Apob	apolipoprotein B	2,36
1421848_at	Slc22a5	solute carrier family 22 (organic cation transporter), member 5	2,34
1454704_at	Scarb2	scavenger receptor class B, member 2	2,34
1460042_at	Slc23a3	solute carrier family 23 (nucleobase transporters), member 3	2,33
1436077_a_at	Fcho1	FCH domain only 1	2,33
1450518_at	Hnf4g	hepatocyte nuclear factor 4, gamma	2,31
1420971_at	Ubr1	ubiquitin protein ligase E3 component n-recognin 1	2,31
1427348_at	Zc3h12a	zinc finger CCCH type containing 12A	2,31
1451318_a_at	LOC676654 /// Lyn	Yamaguchi sarcoma viral (v-yes-1) oncogene homolog /// similar to Yamaguchi sarcoma viral (v-yes-1) oncogene homolog	2,29
1421594_a_at	Sytl2	synaptotagmin-like 2	2,28
1449165_at	Capn5	calpain 5	2,27
1450534_x_at	H2-K1	histocompatibility 2, K1, K region	2,26
1418243_at	Fcna	ficolin A	2,25
1449553_at	Nkain1	Na+/K+ transporting ATPase interacting 1	2,24
1437689_x_at	Clu /// LOC100046120	clusterin /// similar to clusterin	2,24
1423597_at	Atp8a1	ATPase, aminophospholipid transporter (APLT), class I, type 8A, member 1	2,23
1431213_a_at	LOC100041156 /// LOC100041932	hypothetical protein LOC100041156 /// hypothetical protein LOC100041932	2,23
1425862_a_at	Pik3c2a	phosphatidylinositol 3-kinase, C2 domain containing, alpha polypeptide	2,22

Table 11. List of all genes upregulated due to DSS-colitis compared to normal.

Affymetrix id	Gene Name	Full Name	Fold Change
1425355_at	Acsf2 /// EG433604	acyl-CoA synthetase family member 2 /// predicted gene, EG433604	2,22
1418020_s_at	Cpd	carboxypeptidase D /// similar to carboxypeptidase D	2,21
1427164_at	Il13ra1	interleukin 13 receptor, alpha 1	2,21
1425739_at	Pld1	phospholipase D1	2,20
1449150_at	Krba1	KRAB-A domain containing 1	2,19
1422706_at	Tmepai	transmembrane, prostate androgen induced RNA	2,19
1455066_s_at	Mia3	melanoma inhibitory activity 3	2,18
1421813_a_at	Psap	prosaposin	2,18
1451619_at	Golph3l	golgi phosphoprotein 3-like	2,18
1426628_at	Tmem34	transmembrane protein 34	2,17
1426523_a_at	Gnpda2	glucosamine-6-phosphate deaminase 2	2,15
1426227_s_at	Vps37c	vacuolar protein sorting 37C (yeast)	2,15
1423186_at	Tiam2	T-cell lymphoma invasion and metastasis 2	2,14
1425188_s_at	Sel1l	sel-1 suppressor of lin-12-like (C. elegans)	2,13
1425783_at	Tc2n	tandem C2 domains, nuclear	2,13
1417669_at	Abhd12	abhydrolase domain containing 12	2,12
1419030_at	Ero1l	ERO1-like (S. cerevisiae)	2,11
1423637_at	Galnt4	UDP-N-acetyl-alpha-D-galactosamine:polypeptide N-acetylgalactosaminyltransferase 4	2,10
1436954_at	Wipf1	WAS/WASL interacting protein family, member 1	2,10
1427251_at	Atp2a2	ATPase, Ca++ transporting, cardiac muscle, slow twitch 2	2,09
1419585_at	Rp2h	retinitis pigmentosa 2 homolog (human)	2,05
1452145_at	H6pd	hexose-6-phosphate dehydrogenase (glucose 1-dehydrogenase)	2,04
1460331_at	Tm9sf2	transmembrane 9 superfamily member 2	2,04
1421908_a_at	Tcf12	transcription factor 12	2,03
1424618_at	Hpd	4-hydroxyphenylpyruvic acid dioxygenase	2,03
1417336_a_at	Sytl4	synaptotagmin-like 4	2,01
1426524_at	Gnpda2	glucosamine-6-phosphate deaminase 2	1,99
1425333_at	Rab43	RAB43, member RAS oncogene family	1,97
1438705_at	Cbfa2t3	core-binding factor, runt domain, alpha subunit 2, translocated to, 3 (human)	1,97
1416975_at	Stam2	signal transducing adaptor molecule (SH3 domain and ITAM motif) 2	1,97
1423194_at	Arhgap5	Rho GTPase activating protein 5	1,97
1450376_at	Mxi1	Max interacting protein 1	1,96
1422574_at	Mxd4	Max dimerization protein 4	1,95
1419467_at	Clec14a	C-type lectin domain family 14, member a	1,95
1460409_at	Cpt1a	carnitine palmitoyltransferase 1a, liver	1,95
1417481_at	Ramp1	receptor (calcitonin) activity modifying protein 1	1,92
1423134_at	Rilpl2	Rab interacting lysosomal protein-like 2	1,89
1425929_a_at	Rnf14	ring finger protein 14	1,88
1425284_a_at	Rab27a	RAB27A, member RAS oncogene family	1,86
1460377_a_at	Tmem8	transmembrane protein 8 (five membrane-spanning domains)	1,86
1424354_at	Tmem140	transmembrane protein 140	1,84
1438712_at	Dennd2d	DENN/MADD domain containing 2D	1,76

Table 12. List of all genes downregulated due to DSS-colitis compared to normal.

Affymetrix id	Gene Name	Full Name	Fold Change
1418207_at	Fxyd4	FXYD domain-containing ion transport regulator 4	0,07
1416713_at	Tppp3	tubulin polymerization-promoting protein family member 3	0,11
1418171_at	Tceal8	transcription elongation factor A (SII)-like 8 /// similar to transcription elongation factor A (SII)-like 8	0,13
1418095_at	Smpx	small muscle protein, X-linked	0,16
1448236_at	Rdx	radixin	0,18
1435277_x_at	Nme1	expressed in non-metastatic cells 1, protein	0,19
1421811_at	LOC640441 /// Thbs1	thrombospondin 1 /// similar to thrombospondin 1	0,19
1416039_x_at	Cyr61	cysteine rich protein 61	0,20
1452730_at	Rps4y2	ribosomal protein S4, Y-linked 2	0,21
1419397_at	Pola1	polymerase (DNA directed), alpha 1	0,22
1428014_at	Hist1h4h	histone cluster 1, H4h	0,23
1436704_x_at	Mthfd1	methylenetetrahydrofolate dehydrogenase (NADP+ dependent), methenyltetrahydrofolate cyclohydrolase, formyltetrahydrofolate synthase	0,23
1417938_at	Rad51ap1	RAD51 associated protein 1	0,24
1416299_at	Shcbp1	Shc SH2-domain binding protein 1	0,24
1416505_at	Nr4a1	nuclear receptor subfamily 4, group A, member 1	0,24
1434440_at	Gnai1	guanine nucleotide binding protein (G protein), alpha inhibiting 1	0,25
1415964_at	Scd1	stearoyl-Coenzyme A desaturase 1	0,25
1418377_a_at	Siva1	SIVA1, apoptosis-inducing factor	0,25
1449061_a_at	Prim1	DNA primase, p49 subunit	0,26
1417823_at	Gcat	glycine C-acetyltransferase (2-amino-3-ketobutyrate-coenzyme A ligase)	0,26
1422430_at	Fignl1	fidgetin-like 1	0,26
1415810_at	Uhrf1	ubiquitin-like, containing PHD and RING finger domains, 1	0,27
1417541_at	Hells	helicase, lymphoid specific	0,27
1417951_at	Eno3	enolase 3, beta muscle	0,27
1434496_at	Plk3	polo-like kinase 3	0,27
1451246_s_at	Aurkb	aurora kinase B	0,27
1455540_at	Cps1	carbamoyl-phosphate synthetase 1	0,28
1435194_at	Hspa4	heat shock protein 4	0,28
1419513_a_at	Ect2	ect2 oncogene	0,28
1416802_a_at	Cdca5	cell division cycle associated 5	0,28
1429171_a_at	Ncapg	on-SMC condensin I complex, subunit G	0,28
1449568_at	Klb	klotho beta	0,28
1423520_at	Lmnb1	lamin B1	0,29
1424854_at	Hist1h4i	histone cluster 1, H4i	0,29
1451128_s_at	Kif22	kinesin family member 22	0,29
1419913_at	Strap	Serine/threonine kinase receptor associated protein	0,29

Table 12. List of all genes downregulated due to DSS-colitis compared to normal.

Affymetrix id	Gene Name	Full Name	Fold Change
1418709_at	Cox7a1	cytochrome c oxidase, subunit VIIa 1	0,29
1424278_a_at	Birc5	baculoviral IAP repeat-containing 5	0,30
1430811_a_at	Nuf2	NUF2, NDC80 kinetochore complex component, homolog (S. cerevisiae)	0,30
1417724_at	Thoc4	THO complex 4	0,30
1418949_at	Gdf15	growth differentiation factor 15	0,30
1417926_at	Ncapg2	non-SMC condensin II complex, subunit G2	0,30
1424046_at	Bub1	budding uninhibited by benzimidazoles 1 homolog (S. cerevisiae)	0,31
1418687_at	Arc	activity regulated cytoskeletal-associated protein	0,31
1448226_at	Rrm2	ribonucleotide reductase M2	0,31
1438852_x_at	Mcm6	minichromosome maintenance deficient 6 (MIS5 homolog, S. pombe) (S. cerevisiae)	0,31
1438009_at	Hist1h2ao /// RP23-480B19.10	histone cluster 1, H2ao /// similar to histone 2a	0,31
1417889_at	Apobec2	apolipoprotein B editing complex 2	0,31
1426612_at	Tipin	timeless interacting protein	0,31
1437992_x_at	Gja1	gap junction protein, alpha 1	0,31
1424629_at	Brca1	breast cancer 1	0,31
1424351_at	Wfdc2	WAP four-disulfide core domain 2	0,31
1416757_at	Zwilch	Zwilch, kinetochore associated, homolog (Drosophila)	0,31
1425815_a_at	Hmmr	hyaluronan mediated motility receptor (RHAMM)	0,32
1439005_x_at	Ywhaz	tyrosine 3-monooxygenase/tryptophan 5-monooxygenase activation protein, zeta polypeptide	0,32
1451608_a_at	Tspan33	tetraspanin 33	0,32
1439377_x_at	Cdc20	cell division cycle 20 homolog (S. cerevisiae)	0,32
1417586_at	Timeless	timeless homolog (Drosophila)	0,32
1420028_s_at	LOC100045677 /// Mcm3	minichromosome maintenance deficient 3 (S. cerevisiae) /// similar to DNA replication licensing factor MCM3 (DNA polymerase alpha holoenzyme-associated protein P1) (P1-MCM3)	0,33
1449171_at	Ttk	Ttk protein kinase	0,33
1433893_s_at	Spag5	sperm associated antigen 5	0,33
1451989_a_at	Mapre2	microtubule-associated protein, RP/EB family, member 2	0,33
1448568_a_at	Slc20a1	solute carrier family 20, member 1	0,33
1416558_at	Melk	maternal embryonic leucine zipper kinase	0,33
1448113_at	LOC100039888 /// LOC623112 /// Stmn1	stathmin 1 /// similar to Stathmin 1/oncoprotein 18 /// similar to Pr22	0,34
1422993_s_at	Refbp2 /// Thoc4	THO complex 4 /// RNA and export factor binding protein 2	0,34
1452954_at	Ube2c	ubiquitin-conjugating enzyme E2C	0,34
1416214_at	Mcm4	minichromosome maintenance deficient 4 homolog (S. cerevisiae)	0,34
1427751_a_at	Krt36	keratin 36	0,34

Table 12. List of all genes downregulated due to DSS-colitis compared to normal.

Affymetrix id	Gene Name	Full Name	Fold Change
1436707_x_at	Ncaph	non-SMC condensin I complex, subunit H	0,35
1448229_s_at	Ccnd2	cyclin D2	0,35
1417910_at	Ccna2	cyclin A2	0,35
1450407_a_at	Anp32a	acidic (leucine-rich) nuclear phosphoprotein 32 family, member A	0,35
1434748_at	Ckap2	cytoskeleton associated protein 2	0,36
1434695_at	Dtl	denticleless homolog (Drosophila)	0,36
1429270_a_at	Syce2	synaptonemal complex central element protein 2	0,36
1426817_at	Mki67	antigen identified by monoclonal antibody Ki 67	0,36
1415772_at	Ncl	nucleolin	0,36
1422462_at	Ube2t	ubiquitin-conjugating enzyme E2T (putative)	0,36
1434278_at	Mtm1	X-linked myotubular myopathy gene 1	0,36
1455012_s_at	Trim37	tripartite motif protein 37	0,37
1436981_a_at	Yw haz	tyrosine 3-monooxygenase/tryptophan 5-monooxygenase activation protein, zeta polypeptide	0,37
1416321_s_at	Prelp	proline arginine-rich end leucine-rich repeat	0,37
1422552_at	Rprm	reprimo, TP53 dependent G2 arrest mediator candidate	0,37
1427161_at	Cenpf	centromere protein F	0,37
1449708_s_at	Chek1	checkpoint kinase 1 homolog (S. pombe)	0,37
1423619_at	Rasd1	RAS, dexamethasone-induced 1	0,37
1418186_at	Gstt1	glutathione S-transferase, theta 1	0,38
1418764_a_at	Bpnt1	bisphosphate 3'-nucleotidase 1	0,38
1424321_at	Rfc4	replication factor C (activator 1) 4	0,38
1456573_x_at	Nnt	nicotinamide nucleotide transhydrogenase	0,39
1419522_at	Zmynd19	zinc finger, MYND domain containing 19	0,39
1449207_a_at	Kif20a	kinesin family member 20A	0,39
1418206_at	Sdf2l1	stromal cell-derived factor 2-like 1	0,39
1426473_at	Dnajc9	DnaJ (Hsp40) homolog, subfamily C, member 9	0,39
1415849_s_at	Stmn1	stathmin 1	0,39
1415935_at	Smoc2	SPARC related modular calcium binding 2	0,39
1431362_a_at	Smoc2	SPARC related modular calcium binding 2	0,39
1416497_at	Pdia4	protein disulfide isomerase associated 4	0,40
1429295_s_at	Trip13	thyroid hormone receptor interactor 13	0,40
1448510_at	Efna1	ephrin A1	0,41
1450044_at	Fzd7	frizzled homolog 7 (Drosophila)	0,41

Table 12. List of all genes downregulated due to DSS-colitis compared to normal.

Affymetrix id	Gene Name	Full Name	Fold Change
1452305_s_at	Cenpn	centromere protein N	0,41
1424936_a_at	Dnahc8	dynein, axonemal, heavy chain 8	0,41
1460403_at	Psip1	PC4 and SFRS1 interacting protein 1	0,41
1428104_at	Tpx2	TPX2, microtubule-associated protein homolog (Xenopus laevis)	0,42
1420295_x_at	Clcn5	chloride channel 5	0,42
1439463_x_at	Hmg1l1	high mobility group box 1	0,42
1418184_at	Cenpm	centromere protein M	0,42
1418305_s_at	Nola1	nucleolar protein family A, member 1 (H/ACA small nucleolar RNPs)	0,42
1423463_a_at	D2Ertd750e	DNA segment, Chr 2, ERATO Doi 750, expressed	0,42
1419591_at	Gsdmc1	gasdermin C1	0,43
1438320_s_at	Mcm7	minichromosome maintenance deficient 7 (S. cerevisiae)	0,43
1456055_x_at	Pold1	polymerase (DNA directed), delta 1, catalytic subunit	0,43
1451185_at	Sf3b5	splicing factor 3b, subunit 5	0,43
1453162_at	Utp11l	UTP11-like, U3 small nucleolar ribonucleoprotein, (yeast)	0,43
1434820_s_at	Pkig	protein kinase inhibitor, gamma	0,43
1419270_a_at	Dut	deoxyuridine triphosphatase	0,43
1437711_x_at	LOC676173 /// Odc1	ornithine decarboxylase, structural 1 /// similar to Ornithine decarboxylase (ODC) /// similar to Odc1 protein /// predicted gene, EG666231 /// predicted gene, EG668343	0,43
1450337_a_at	Nek8	NIMA (never in mitosis gene a)-related expressed kinase 8	0,43
1436994_a_at	Hist1h1c	histone cluster 1, H1c	0,43
1419759_at	Abcb1a	ATP-binding cassette, sub-family B (MDR/TAP), member 1A	0,43
1417705_at	LOC100046081 /// Otub1	OTU domain, ubiquitin aldehyde binding 1 /// similar to OTU domain, ubiquitin aldehyde binding 1	0,44
1422579_at	Hspe1	heat shock protein 1 (chaperonin 10)	0,44
1424143_a_at	Cdt1	chromatin licensing and DNA replication factor 1	0,44
1426533_at	Nol5a	nucleolar protein 5A	0,44
1417696_at	Soat1	sterol O-acyltransferase 1	0,45
1425415_a_at	Slc1a1	solute carrier family 1 (neuronal/epithelial high affinity glutamate transporter, system Xag), member 1	0,45
1450563_at	Mgst3	microsomal glutathione S-transferase 3	0,45
1436750_a_at	Oxct1	3-oxoacid CoA transferase 1	0,45
1449194_at	Mrps25	mitochondrial ribosomal protein S25	0,45
1418715_at	Pank1	pantothenate kinase 1	0,45
1422884_at	Snrpd3	small nuclear ribonucleoprotein D3	0,45
1437687_x_at	Fkbp9	FK506 binding protein 9	0,46

Table 12. List of all genes downregulated due to DSS-colitis compared to normal.

Affymetrix id	Gene Name	Full Name	Fold Change
1416042_s_at	LOC100043974 /// Nasp	nuclear autoantigenic sperm protein (histone-binding) /// similar to nuclear autoantigenic sperm protein; NASP	0,46
1417352_s_at	Snrpa1	small nuclear ribonucleoprotein polypeptide A'	0,47
1448190_at	Mrpl33	mitochondrial ribosomal protein L33	0,47
1452659_at	Dek	DEK oncogene (DNA binding)	0,47
1447924_at	Nucks1	nuclear casein kinase and cyclin-dependent kinase substrate 1	0,47
1437520_a_at	Nup85	nucleoporin 85	0,47
1419499_at	Gpam	glycerol-3-phosphate acyltransferase, mitochondrial	0,47
1424048_a_at	Cyb5r1	cytochrome b5 reductase 1	0,47
1423211_at	Nola3	nucleolar protein family A, member 3	0,47
1455901_at	Chpt1	choline phosphotransferase 1	0,47
1438977_x_at	LOC100045999 /// Ran	RAN, member RAS oncogene family /// similar to RAN, member RAS oncogene family	0,48
1426741_a_at	Fastkd2	FAST kinase domains 2	0,48
1419472_s_at	Nudc /// Nudc-ps1	nuclear distribution gene C homolog (Aspergillus) /// nuclear distribution gene C homolog (Aspergillus), pseudogene 1 /// similar to MNUDC protein	0,48
1431947_at	Ldlr	low density lipoprotein receptor	0,48
1417506_at	Gmnn	geminin	0,49
1451366_at	Cops6	COP9 (constitutive photomorphogenic) homolog, subunit 6 (Arabidopsis thaliana)	0,49
1451776_s_at	Hopx	HOP homeobox	0,49
1456244_x_at	Glrx3	glutaredoxin 3	0,49
1449633_s_at	Nt5c3l	5'-nucleotidase, cytosolic III-like	0,49
1417580_s_at	Selenbp1	selenium binding protein 1 /// hypothetical protein LOC100044204	0,49
1437313_x_at	Hmgb2	high mobility group box 2	0,49
1416452_at	Oat	ornithine aminotransferase	0,49
1424991_s_at	Tyms /// Tyms-ps	thymidylate synthase /// thymidylate synthase, pseudogene	0,50
1417144_at	Tubg1	tubulin, gamma 1	0,50
1437608_x_at	Ywhaq	tyrosine 3-monooxygenase/tryptophan 5-monooxygenase activation protein, theta polypeptide	0,51
1417511_at	Lyar	Ly1 antibody reactive clone	0,51
1439453_x_at	Rnaseh2c	ribonuclease H2, subunit C	0,51
1420726_x_at	Tmlhe	trimethyllysine hydroxylase, epsilon	0,52
1452621_at	Pcbd2	pterin 4 alpha carbinolamine dehydratase/dimerization cofactor of hepatocyte nuclear factor 1 alpha (TCF1) 2	0,53
1415941_s_at	Zfand2a	zinc finger, AN1-type domain 2A	0,53
1448665_at	Dmd	dystrophin, muscular dystrophy	0,53
1431085_a_at	Pcmt1	protein-L-isoaspartate (D-aspartate) O-methyltransferase 1	0,54
1456590_x_at	Akr1b3	aldo-keto reductase family 1, member B3 (aldose reductase)	0,54
1438092_x_at	H2afz	H2A histone family, member Z	0,56
1448357_at	Snrpg	small nuclear ribonucleoprotein polypeptide G	0,56

Table 13. List of all genes upregulated in DSS-Colitis mice treated with UDCA compared to DSS-colitis mice alone.

Affymetrix id	Gene symbol	Full name	Fold change
1427642_at	Trpm6	transient receptor potential cation channel, subfamily M, member 6	3,34
1420917_at	Prpf40a	PRP40 pre-mRNA processing factor 40 homolog A (yeast)	2,38
1418188_a_at	Malat1	metastasis associated lung adenocarcinoma transcript 1 (non-coding RNA)	2,37
1460699_at	Rps27	ribosomal protein S27	2,16
1448377_at	Slpi	secretory leukocyte peptidase inhibitor	2,13
1425993_a_at	Hsph1	heat shock 105kDa/110kDa protein 1	2,08
1419582_at	Cyp2c55	cytochrome P450, family 2, subfamily c, polypeptide 55	2,07
1421355_at	Tgm3	transglutaminase 3, E polypeptide	1,98
1460290_at	Lpin2	lipin 2	1,92
1450035_a_at	Prpf40a	PRP40 pre-mRNA processing factor 40 homolog A (yeast)	1,91
1427473_at	Gstm3	glutathione S-transferase, mu 3	1,89
1423520_at	Lmnb1	lamin B1	1,87
1434748_at	Ckap2	cytoskeleton associated protein 2	1,86
1452360_a_at	Jarid1a	jumonji, AT rich interactive domain 1A (Rbp2 like)	1,86
1416123_at	Ccnd2	cyclin D2	1,86
1420966_at	Slc25a15	solute carrier family 25 (mitochondrial carrier ornithine transporter), member 15	1,84
1427276_at	Smc4	structural maintenance of chromosomes 4	1,81
1427708_a_at	Nf2	neurofibromatosis 2	1,80
1425716_s_at	Bak1	BCL2-antagonist/killer 1	1,80
1417910_at	Ccna2	cyclin A2	1,78
1426645_at	Hsp90aa1	heat shock protein 90, alpha (cytosolic), class A member 1	1,78
1423600_a_at	Tcof1	Treacher Collins Franceschetti syndrome 1, homolog	1,78
1418069_at	Apoc2	apolipoprotein C-II	1,77
1416505_at	Nr4a1	nuclear receptor subfamily 4, group A, member 1	1,77
1418824_at	Arf6	ADP-ribosylation factor 6	1,77
1424351_at	Wfdc2	WAP four-disulfide core domain 2	1,77
1416563_at	Ctps	cytidine 5'-triphosphate synthase	1,77
1420935_a_at	Srrm1	serine/arginine repetitive matrix 1	1,76
1422910_s_at	Smc6	structural maintenance of chromosomes 6	1,76
1452315_at	Kif11	kinesin family member 11	1,75
1421488_at	Rabgap1l	RAB GTPase activating protein 1-like	1,75
1421041_s_at	Gsta1/2	glutathione S-transferase, alpha 1 (Ya)	1,74
1419209_at	Cxcl1	chemokine (C-X-C motif) ligand 1	1,73
1448949_at	Car4	carbonic anhydrase 4	1,73
1430829_s_at	Fto	fat mass and obesity associated	1,72
1420517_at	Chmp4c	chromatin modifying protein 4C	1,72
1452088_at	Zbed3	zinc finger, BED domain containing 3	1,72
1417450_a_at	Tacc3	transforming, acidic coiled-coil containing protein 3	1,72
1433893_s_at	Spag5	sperm associated antigen 5	1,72
1416157_at	Vcl	vinculin	1,72
1448813_at	Aadac	arylacetamide deacetylase (esterase)	1,71
1424658_at	Taok1	TAO kinase 1	1,70
1422167_at	Sema5a	sema domain	1,70
1417938_at	Rad51ap1	RAD51 associated protein 1	1,70
1427912_at	Cbr3	carbonyl reductase 3	1,70
1448890_at	Klf2	Kruppel-like factor 2 (lung)	1,70
1448794_s_at	Dnajc2	DnaJ (Hsp40) homolog, subfamily C, member 2	1,69
1460353_at	Tmem48	transmembrane protein 48	1,69
1420931_at	Mapk8	mitogen-activated protein kinase 8	1,69
1417971_at	Nrm	nurim (nuclear envelope membrane protein)	1,69
1428563_at	Ddx10	DEAD (Asp-Glu-Ala-Asp) box polypeptide 10	1,68
1423184_at	Itsn2	intersectin 2	1,68
1419397_at	Pola1	polymerase (DNA directed), alpha 1	1,68
1438133_a_at	Cyr61	cysteine rich protein 61	1,67
1416661_at	Eif3a	eukaryotic translation initiation factor 3, subunit A	1,67
1451884_a_at	Lsm2	LSM2 homolog, U6 small nuclear RNA associated (S. cerevisiae)	1,67

Table 13. List of all genes upregulated in DSS-Colitis mice treated with UDCA compared to DSS-colitis mice alone.

Affymetrix id	Gene symbol	Full name	Fold change
1424308_at	Slc24a3	solute carrier family 24 (sodium/potassium/calcium exchanger), member 3	1,67
1449042_at	Ctcf	CCCTC-binding factor	1,66
1425019_at	Ubxn2a	UBX domain protein 2A	1,66
1423920_at	Ncaph	non-SMC condensin I complex, subunit H	1,66
1451246_s_at	Aurkb	aurora kinase B	1,66
1427742_a_at	Klf6	Kruppel-like factor 6	1,65
1450100_a_at	Tcerg1	transcription elongation regulator 1 (CA150)	1,65
1418764_a_at	Bpnt1	bisphosphate 3'-nucleotidase 1	1,65
1418601_at	Aldh1a7	aldehyde dehydrogenase family 1, subfamily A7	1,65
1449168_a_at	Akap2 /// Palm2	A kinase (PRKA) anchor protein 2 /// paralemmin 2	1,65
1415811_at	Uhrf1	ubiquitin-like, containing PHD and RING finger domains, 1	1,65
1422430_at	Fignl1	fidgetin-like 1	1,64
1416299_at	Shcbp1	Shc SH2-domain binding protein 1	1,64
1449486_at	Ces1	carboxylesterase 1	1,64
1436746_at	Wnk1	WNK lysine deficient protein kinase 1	1,64
1431981_at	Hif1a	hypoxia inducible factor 1, alpha subunit	1,64
1452534_a_at	Hmgb2	high mobility group box 2	1,63
1423436_at	Gsta3	glutathione S-transferase, alpha 3	1,62
1451771_at	Tpcn1	tw o pore channel 1	1,62
1418949_at	Gdf15	grow th differentiation factor 15	1,62
1417951_at	Eno3	enolase 3, beta muscle	1,62
1425711_a_at	Akt1	thymoma viral proto-oncogene 1 /// similar to serine/threonine protein kinase	1,62
1439075_at	Polr3f	polymerase (RNA) III (DNA directed) polypeptide F	1,61
1426326_at	Zfp91	zinc finger protein 91	1,61
1433899_x_at	Tsc22d1	TSC22 domain family, member 1	1,61
1422943_a_at	Hspb1	heat shock protein 1	1,61
1453498_x_at	Steap3	STEAP family member 3	1,61
1415878_at	Rrm1	ribonucleotide reductase M1	1,61
1451128_s_at	Kif22	kinesin family member 22	1,60
1421008_at	Rsad2	radical S-adenosyl methionine domain containing 2	1,60
1452885_at	Sfrs2ip	splicing factor, arginine/serine-rich 2, interacting protein	1,60
1438686_at	Eif4g1	eukaryotic translation initiation factor 4, gamma 1	1,60
1420479_a_at	Nap1l1	nucleosome assembly protein 1-like 1	1,59
1436343_at	Chd4	chromodomain helicase DNA binding protein 4	1,59
1460729_at	Rock1	Rho-associated coiled-coil containing protein kinase 1	1,59
1422460_at	Mad2l1	MAD2 (mitotic arrest deficient, homolog)-like 1 (yeast)	1,59
1417871_at	Hsd17b7	hydroxysteroid (17-beta) dehydrogenase 7	1,59
1416258_at	Tk1	thymidine kinase 1	1,59
1454011_a_at	Rpa2	replication protein A2	1,59
1450157_a_at	Hmmr	hyaluronan mediated motility receptor (RHAMM)	1,59
1452521_a_at	Plaur	plasminogen activator, urokinase receptor	1,59
1419943_s_at	Ccnb1	cyclin B1	1,59
1450506_a_at	Aen	apoptosis enhancing nuclease	1,58
1419734_at	Actb	actin, beta	1,58
1448627_s_at	Pbk	PDZ binding kinase	1,58
1423092_at	Incenp	inner centromere protein	1,58
1437611_x_at	Kif2c	kinesin family member 2C	1,58
1448191_at	Plk1	polo-like kinase 1 (Drosophila)	1,57
1415945_at	Mcm5	minichromosome maintenance deficient 5, cell division cycle 46 (S. cerevisiae)	1,57

Table 13. List of all genes upregulated in DSS-Colitis mice treated with UDCA compared to DSS-colitis mice alone.

Affymetrix id	Gene symbol	Full name	Fold change
1434751_at	Ids	iduronate 2-sulfatase	1,57
1424325_at	Esco1	establishment of cohesion 1 homolog 1 (S. cerevisiae)	1,57
1423522_at	Npm3	similar to Nucleoplasmin-3	1,57
1425415_a_at	Slc1a1	solute carrier family 1 (neuronal/epithelial high affinity glutamate transporter, system Xag), member 1	1,57
1436393_a_at	Trim37	tripartite motif-containing 37	1,57
1449207_a_at	Kif20a	kinesin family member 20A	1,56
1423877_at	Chaf1b	chromatin assembly factor 1, subunit B (p60)	1,56
1418431_at	Kif5b	kinesin family member 5B	1,56
1438183_x_at	Sord	sorbitol dehydrogenase	1,56
1422709_a_at	Wdr46	WD repeat domain 46	1,56
1418264_at	Cenpk	centromere protein K	1,56
1421208_at	Ikbkg	inhibitor of kappaB kinase gamma	1,56
1436505_at	Ppig	peptidyl-prolyl isomerase G (cyclophilin G)	1,56
1422528_a_at	Zfp36l1	zinc finger protein 36, C3H type-like 1	1,56
1423674_at	Usp1	ubiquitin specific peptdiase 1	1,55
1454904_at	Mtm1	X-linked myotubular myopathy gene 1	1,55
1448851_a_at	Dnajc5	DnaJ (Hsp40) homolog, subfamily C, member 5	1,55
1417299_at	Nek2	NIMA (never in mitosis gene a)-related expressed kinase 2	1,55
1419615_at	Trpv6	transient receptor potential cation channel, subfamily V, member 6	1,55
1449171_at	Ttk	Ttk protein kinase	1,55
1451103_at	D14Ertd500e	DNA segment, Chr 14, ERATO Doi 500, expressed	1,55
1426485_at	Ubxn4	UBX domain protein 4	1,55
1416664_at	Cdc20	cell division cycle 20 homolog (S. cerevisiae)	1,55
1415773_at	Ncl	nucleolin	1,55
1416076_at	Ccnb1	cyclin B1 /// cyclin B1	1,55
1448236_at	Rdx	radixin	1,54
1424955_at	Ccdc5	coiled-coil domain containing 5	1,54
1417828_at	Aqp8	aquaporin 8	1,54
1424629_at	Brca1	breast cancer 1	1,54
1450377_at	Thbs1	similar to thrombospondin 1	1,54
1460302_at	Thbs1	thrombospondin 1	1,54
1423480_at	Nol11	nucleolar protein 11	1,54
1450747_at	Keap1	kelch-like ECH-associated protein 1	1,54
1424278_a_at	Birc5	baculoviral IAP repeat-containing 5	1,54
1449391_at	Zfp37	zinc finger protein 37	1,54
1450986_at	Nol5	nucleolar protein 5	1,54
1455618_x_at	Tspan33	tetraspanin 33	1,53
1416309_at	Nusap1	nucleolar and spindle associated protein 1	1,53
1424266_s_at	AU018778	expressed sequence AU018778	1,53
1448314_at	Cdc2a	cell division cycle 2 homolog A (S. pombe)	1,53
1427099_at	Maz	MYC-associated zinc finger protein (purine-binding transcription factor)	1,53
1426085_a_at	Pxn	paxillin	1,53
1460179_at	Dnaja1	DnaJ (Hsp40) homolog, subfamily A, member 1	1,53
1450838_x_at	100043481 / Rpl37	ribosomal protein L37	1,53
1422513_at	Ccnf	cyclin F	1,52
1422462_at	Ube2t	ubiquitin-conjugating enzyme E2T (putative)	1,52
1426184_a_at	Pdcd6ip	programmed cell death 6 interacting protein	1,52
1451768_a_at	Slc20a2	solute carrier family 20, member 2	1,52

Table 14. List of all genes downregulated in DSS-Colitis mice treated with UDCA compared to DSS-colitis mice alone.

Affymetrix id	Gene symbol	Full name	Fold change
1455462_at	Adcy2	adenylate cyclase 2	0,57
1421830_at	Ak3l1	adenylate kinase 3-like 1	0,49
1424959_at	Anxa13	annexin A13	0,40
1460359_at	Armcx3	armadillo repeat containing, X-linked 3	0,59
1418655_at	B4galnt1	beta-1,4-N-acetyl-galactosaminyl transferase 1	0,57
1424218_a_at	Creb3l4	cAMP responsive element binding protein 3-like 4	0,60
1427482_a_at	Car8	carbonic anhydrase 8	0,45
1416777_at	Ceacam12	carcinoembryonic antigen-related cell adhesion molecule 12	0,58
1448898_at	Ccl9	chemokine (C-C motif) ligand 9	0,57
1449984_at	Cxcl2	chemokine (C-X-C motif) ligand 2	0,45
1421210_at	Ciita	class II transactivator	0,60
1416051_at	C2	complement component 2 (within H-2S)	0,53
1451206_s_at	Cytip	cytohesin 1 interacting protein	0,59
1418174_at	Dbp	D site albumin promoter binding protein	0,34
1417991_at	Dio1	deiodinase, iodothyronine, type I	0,58
1418773_at	Fads3	fatty acid desaturase 3	0,60
1438982_s_at	Flywch2	FLYWCH family member 2	0,59
1435906_x_at	Gbp2	guanylate binding protein 2	0,56
1419235_s_at	Helb	helicase (DNA) B	0,59
1435939_s_at	Hepacam2	HEPACAM family member 2	0,58
1435290_x_at	H2-Aa	histocompatibility 2, class II antigen A, alpha	0,57
1452431_s_at	H2-Aa	histocompatibility 2, class II antigen A, alpha	0,50
1425477_x_at	H2-Ab1 /// Rmcs2	metastatic cancers 2 /// response to metastatic cancers 5	0,46
1417025_at	H2-Eb1	histocompatibility 2, class II antigen E beta	0,48
1422527_at	H2-DMa	histocompatibility 2, class II, locus DMa	0,52
1450170_x_at	H2-D1	histocompatibility 2, D region locus 1	0,48
1418536_at	H2-Q7	histocompatibility 2, Q region locus 7	0,46
1421653_a_at	Igh /// Igh-2	immunoglobulin heavy chain complex	0,55
1420437_at	Indo	indoleamine-pyrrole 2,3 dioxygenase	0,53
1417292_at	Ifi47	interferon gamma inducible protein 47	0,54
1419043_a_at	Igp1	interferon inducible GTPase 1	0,55
1419286_s_at	Ift81	intraflagellar transport 81 homolog (Chlamydomonas)	0,58
1429212_a_at	Lrrc51	leucine rich repeat containing 51	0,55
1451989_a_at	Mapre2	microtubule-associated protein, RP/EB family, member 2	0,57
1417275_at	Mal	myelin and lymphocyte protein, T-cell differentiation protein	0,39
1449071_at	Myl7	myosin, light polypeptide 7, regulatory	0,43

Table 14. List of all genes downregulated in DSS-Colitis mice treated with UDCA compared to DSS-colitis mice alone

Affymetrix id	Gene symbol	Full name	Fold change
1428319_at	Pdlim7	PDZ and LIM domain 7	0,59
1427918_a_at	Rhoq	ras homolog gene family, member Q	0,57
1416297_s_at	Reg3b	regenerating islet-derived 3 beta	0,42
1448872_at	Reg3g	regenerating islet-derived 3 gamma	0,36
1418368_at	Retnlb	resistin like beta	0,33
1419394_s_at	S100a8	S100 calcium binding protein A8 (calgranulin A)	0,60
1437995_x_at	Sep-7	septin 7	0,54
1417426_at	Srgn	serglycin	0,45
1451190_a_at	Sbk1	SH3-binding kinase 1	0,59
1420334_at	Slc12a8	member 8	0,59
1431379_a_at	Slc13a1	member 1	0,51
1460197_a_at	Steap4	STEAP family member 4	0,54
1416783_at	Tac1	tachykinin 1	0,56
1449009_at	Tgtp	T-cell specific GTPase	0,50
1455900_x_at	Tgm2	transglutaminase 2, C polypeptide	0,50
1449564_at	Tpsg1	tryptase gamma 1	0,59
1427990_at	Usp45	ubiquitin specific petidase 45	0,58
1452054_at	Ube2w	ubiquitin-conjugating enzyme E2W (putative)	0,57
1455912_x_at	Unc45a	Unc-45 homolog A (C. elegans)	0,58
1448562_at	Upp1	uridine phosphorylase 1	0,59

Table 15. List of genes upregulated in DSS-colitis mice related to normal but not in DSS-colitis + UDCA mice related to normal.

Affymetrix id	Gene Name	Full Name
1417669_at	Abhd12	abhydrolase domain containing 12
1419103_a_at	Abhd6	abhydrolase domain containing 6
1422635_at	Ache	acetylcholinesterase
1425355_at	Acsf2 ///	acyl-CoA synthetase family member 2 /// predicted gene, EG433604
1450387_s_at	Ak3l1 ///	adenylate kinase 3 alpha-like 1 /// similar to adenylate kinase 4
1416134_at	Aplp1	amyloid beta (A4) precursor-like protein 1
1427251_at	Atp2a2	ATPase, Ca++ transporting, cardiac muscle, slow twitch 2
1423597_at	Atp8a1	ATPase, aminophospholipid transporter (APLT), class I, type 8A, member 1
1424930_s_at	AW544981	expressed sequence AW544981
1416673_at	Bace2	beta-site APP-cleaving enzyme 2
1452351_at	C030027K23Rik ///	RIKEN cDNA C030027K23 gene /// poly (ADP-ribose) polymerase family, member 4
1449165_at	Capn5	calpain 5
1422876_at	Capn9 ///	calpain 9 (nCL-4) /// similar to calpain 9 (nCL-4)
1438705_at	Cbfa2t3	core-binding factor, runt domain, alpha subunit 2, translocated to, 3 (human)
1417936_at	Ccl9	chemokine (C-C motif) ligand 9
1424830_at	Ccnk	cyclin K
1451438_s_at	Clec2h	C-type lectin domain family 2, member h
1437689_x_at	Clu	clusterin
1424688_at	Creb3l3	cAMP responsive element binding protein 3-like 3
1454268_a_at	Cyba	cytochrome b-245, alpha polypeptide
1451970_at	Daglb	diacylglycerol lipase, beta
1438712_at	Dennd2d	DENN/MADD domain containing 2D
1419030_at	Ero1l	ERO1-like (S. cerevisiae)
1436077_a_at	Fcho1	FCH domain only 1
1418243_at	Fcna	ficolin A
1423637_at	Galnt4	UDP-N-acetyl-alpha-D-galactosamine:polypeptide N-
1418240_at	Gbp2	guanylate nucleotide binding protein 2
1425952_a_at	Gcg	glucagon
1424901_at	Gcnt3	glucosaminyl (N-acetyl) transferase 3, mucin type
1426523_a_at	Gnpda2	glucosamine-6-phosphate deaminase 2
1450648_s_at	H2-Ab1	histocompatibility 2, class II antigen A, beta 1
1451683_x_at	H2-D1	histocompatibility 2, D region locus 1
1450534_x_at	H2-K1	histocompatibility 2, K1, K region
1452145_at	H6pd	hexose-6-phosphate dehydrogenase (glucose 1-dehydrogenase)
1450518_at	Hnf4g	hepatocyte nuclear factor 4, gamma
1424618_at	Hpd	4-hydroxyphenylpyruvic acid dioxygenase
1429381_x_at	Igh /// Igh-2 /// Igh-	immunoglobulin heavy chain (J558 family) /// immunoglobulin heavy chain complex ///
1419042_at	Iigp1	interferon inducible GTPase 1
1427164_at	Il13ra1	interleukin 13 receptor, alpha 1

Table 15. List of genes upregulated in DSS-colitis mice related to normal but not in DSS-colitis + UDCA mice related to normal

Affymetrix id	Gene Name	Full Name
1449150_at	Krba1	KRAB-A domain containing 1
1448883_at	Lgmn	legumain
1426225_at	LOC100047573 ///	retinol binding protein 4, plasma /// similar to retinol binding protein
1451318_a_at	LOC676654 ///	Yamaguchi sarcoma viral (v-yes-1) oncogene homolog /// similar to Yamaguchi
1436766_at	Luc7l2	LUC7-like 2 (S. cerevisiae)
1455066_s_at	Mia3	melanoma inhibitory activity 3
1427398_at	Muc4	mucin 4
1422574_at	Mxd4	Max dimerization protein 4
1450376_at	Mxi1	Max interacting protein 1
1449553_at	Nkain1	Na+/K+ transporting ATPase interacting 1
1428319_at	Pdlim7	PDZ and LIM domain 7
1422619_at	Ppap2a	phosphatidic acid phosphatase 2a
1422962_a_at	Psmb8	proteasome (prosome, macropain) subunit, beta type 8 (large multifunctional
1425284_a_at	Rab27a	RAB27A, member RAS oncogene family
1425333_at	Rab43	RAB43, member RAS oncogene family
1417481_at	Ramp1	receptor (calcitonin) activity modifying protein 1
1428443_a_at	Rap1gap	Rap1 GTPase-activating protein
1417333_at	Rasa4	RAS p21 protein activator 4
1423134_at	Rilpl2	Rab interacting lysosomal protein-like 2
1425929_a_at	Rnf14	ring finger protein 14
1460235_at	Scarb2	scavenger receptor class B, member 2
1459903_at	Sema7a	sema domain, immunoglobulin domain (Ig), and GPI membrane anchor, (semaphorin)
1426550_at	Sidt1	SID1 transmembrane family, member 1
1421848_at	Slc22a5	solute carrier family 22 (organic cation transporter), member 5
1460042_at	Slc23a3	solute carrier family 23 (nucleobase transporters), member 3
1435716_x_at	Snrpn /// Snurf	small nuclear ribonucleoprotein N /// SNRPN upstream reading frame
1416576_at	Socs3	suppressor of cytokine signaling 3
1416975_at	Stam2	signal transducing adaptor molecule (SH3 domain and ITAM motif) 2
1420505_a_at	Stxbp1	syntaxin binding protein 1
1421594_a_at	Sytl2	synaptotagmin-like 2
1417336_a_at	Sytl4	synaptotagmin-like 4
1416016_at	Tap1	transporter 1, ATP-binding cassette, sub-family B (MDR/TAP)
1451838_a_at	Tc2n	tandem C2 domains, nuclear
1423186_at	Tiam2	T-cell lymphoma invasion and metastasis 2
1451794_at	Tmcc3	transmembrane and coiled coil domains 3
1424354_at	Tmem140	transmembrane protein 140
1426628_at	Tmem34	transmembrane protein 34
1460377_a_at	Tmem8	transmembrane protein 8 (five membrane-spanning domains)
1422706_at	Tmepai	transmembrane, prostate androgen induced RNA
1426227_s_at	Vps37c	vacuolar protein sorting 37C (yeast)
1427348_at	Zc3h12a	zinc finger CCCH type containing 12A

Table 16. List of all genes upregulated after UDCA treatment related to nontreated in normal mice

Affymetrix id	Gene name	Full name	Fold change
1416570_s_at	Gfm1	G elongation factor, mitochondrial 1	1,51
1420622_a_at	Hspa8	heat shock protein 8	1,52
1450919_at	Mpp1	membrane protein, palmitoylated	1,56
1451178_at	Mrpl53	mitochondrial ribosomal protein L53	1,56
1424223_at	1700020C11Rik	RIKEN cDNA 1700020C11 gene	1,57
1426645_at	Hsp90aa1	heat shock protein 90kDa alpha (cytosolic), class A member 1	1,57
1429568_x_at	Ube2f	ubiquitin-conjugating enzyme E2F (putative)	1,57
1432426_a_at	Ube2f	ubiquitin-conjugating enzyme E2F (putative)	1,57
1437497_a_at	Hsp90aa1	heat shock protein 90kDa alpha (cytosolic), class A member 1	1,57
1449002_at	Phlda3	pleckstrin homology-like domain, family A, member 3	1,57
1451194_at	Aldob	aldolase 2, B isoform	1,57
1417233_at	Chchd4	coiled-coil-helix-coiled-coil-helix domain containing 4	1,62
1418547_at	Tfpi2	tissue factor pathway inhibitor 2	1,62
1418601_at	Aldh1a7	aldehyde dehydrogenase family 1, subfamily A7	1,62
1424266_s_at	AU018778	expressed sequence AU018778	1,62
1425120_x_at	1810023F06Rik	RIKEN cDNA 1810023F06 gene	1,62
1428112_at	Armet	arginine-rich, mutated in early stage tumors	1,62
1450275_x_at	Ube2f	ubiquitin-conjugating enzyme E2F (putative)	1,62
1454109_a_at	Jmjd6	jumonji domain containing 6	1,62
1416559_at	1500003O22Rik	RIKEN cDNA 1500003O22 gene	1,68
1422579_at	Hspe1	heat shock protein 1 (chaperonin 10)	1,68
1424090_at	Sdcbp2	syndecan binding protein (syntenin) 2	1,68
1424562_a_at	Slc25a4	solute carrier family 25 (mitochondrial carrier, adenine nucleotide translocator), member 4	1,68
1425797_a_at	Syk	spleen tyrosine kinase	1,68
1426875_s_at	Srxn1	sulfiredoxin 1 homolog (S. cerevisiae)	1,68
1451272_a_at	Ube2f	ubiquitin-conjugating enzyme E2F (putative)	1,68
1451680_at	Srxn1	sulfiredoxin 1 homolog (S. cerevisiae)	1,68
1460232_s_at	Hsd3b2 /// Hsd3b3 /// Hsd3b6	hydroxy-delta-5-steroid dehydrogenase, 3 beta- and steroid delta-isomerase 2 /// hydroxy-delta-5-steroid dehydrogenase, 3 beta- and steroid delta-isomerase 3 /// hydroxy-delta-5-steroid dehydrogenase, 3 beta- and steroid delta-isomerase 6	1,68
1416481_s_at	Higd1a	HIG1 domain family, member 1A	1,74
1418253_a_at	Hspa4l	heat shock protein 4 like	1,74
1419103_a_at	Abhd6	abhydrolase domain containing 6	1,74
1424688_at	Creb3l3	cAMP responsive element binding protein 3-like 3	1,74
1426658_x_at	Phgdh	3-phosphoglycerate dehydrogenase	1,74

Table 16. List of all genes upregulated after UDCA treatment related to nontreated in normal mice

Affymetrix id	Gene name	Full name	Fold change
1427464_s_at	Hspa5	heat shock protein 5	1,74
1437621_x_at	Phgdh	3-phosphoglycerate dehydrogenase /// similar to 3-phosphoglycerate dehydrogenase	1,74
1448968_at	Ubfd1	ubiquitin family domain containing 1	1,74
1449348_at	Mpp6	membrane protein, palmitoylated 6 (MAGUK p55 subfamily member 6)	1,74
1450506_a_at	Isg20l1	interferon stimulated exonuclease gene 20-like 1	1,74
1435333_at	1110007M04Rik	RIKEN cDNA 1110007M04 gene	1,80
1449010_at	Hspa4l	heat shock protein 4 like	1,80
1452047_at	Cacybp	calcyclin binding protein	1,80
1422620_s_at	Ppap2a	phosphatidic acid phosphatase 2a	1,86
1422906_at	Abcg2	ATP-binding cassette, sub-family G (WHITE), member 2	1,86
1425351_at	Srxn1	sulfiredoxin 1 homolog (S. cerevisiae)	1,86
1424147_at	Ahsa1	AHA1, activator of heat shock protein ATPase homolog 1 (yeast)	1,87
1426510_at	LOC100044896 /// Sccpdh	saccharopine dehydrogenase (putative) /// similar to Saccharopine dehydrogenase (putative)	1,87
1450087_a_at	Nolc1	nucleolar and coiled-body phosphoprotein 1	1,87
1415800_at	Gja1	gap junction membrane channel protein alpha 1	1,93
1415909_at	Stip1	stress-induced phosphoprotein 1	1,93
1415964_at	Scd1	stearoyl-Coenzyme A desaturase 1	1,93
1435160_at	Ahsa2	AHA1, activator of heat shock protein ATPase homolog 2 (yeast)	1,93
1437992_x_at	Gja1	gap junction membrane channel protein alpha 1	1,93
1449493_at	Insl5	insulin-like 5	1,93
1416480_a_at	Higd1a	HIG1 domain family, member 1A	2,00
1417149_at	P4ha2	procollagen-proline, 2-oxoglutarate 4-dioxygenase (proline 4-hydroxylase), alpha II polypeptide	2,00
1417473_a_at	Ppcs	phosphopantothenoylcysteine synthetase /// similar to Phosphopantothenate--cysteine ligase	2,00
1417914_at	Rap2b	RAP2B, member of RAS oncogene family	2,00
1423138_at	Wdr4	WD repeat domain 4	2,00
1424367_a_at	Homer2	homer homolog 2 (Drosophila)	2,00
1425079_at	Tm6sf2	transmembrane 6 superfamily member 2	2,00
1425382_a_at	Aqp4	aquaporin 4	2,00
1427912_at	Cbr3	carbonyl reductase 3	2,00
1460179_at	Dnaja1	DnaJ (Hsp40) homolog, subfamily A, member 1	2,00
1417828_at	Aqp8	aquaporin 8	2,07
1418739_at	Sgk2	serum/glucocorticoid regulated kinase 2	2,07
1421063_s_at	Snrpn /// Snurf	small nuclear ribonucleoprotein N /// SNRPN upstream reading frame	2,07
1422075_at	Cdx2	caudal type homeo box 2	2,07
1419674_a_at	Dpep1	dipeptidase 1 (renal)	2,14

Table 16. List of all genes upregulated after UDCA treatment related to nontreated in normal mice

Affymetrix id	Gene name	Full name	Fold change
1426851_a_at	Nov	nephroblastoma overexpressed gene	2,14
1426852_x_at	Nov	nephroblastoma overexpressed gene	2,14
1427997_at	1110007M04Rik	RIKEN cDNA 1110007M04 gene	2,14
1450928_at	LOC100045546	similar to Id4	2,14
1452094_at	P4ha1	procollagen-proline, 2-oxoglutarate 4-dioxygenase (proline 4-hydroxylase), alpha 1 polypeptide	2,14
1452754_at	Creld2	cysteine-rich with EGF-like domains 2	2,14
1417273_at	Pdk4	pyruvate dehydrogenase kinase, isoenzyme 4	2,22
1423627_at	Nqo1	NAD(P)H dehydrogenase, quinone 1	2,22
1427347_s_at	Tubb2a	tubulin, beta 2a	2,22
1438945_x_at	Gja1	gap junction membrane channel protein alpha 1	2,29
1417936_at	Ccl9	chemokine (C-C motif) ligand 9	2,30
1428942_at	Mt2	metallothionein 2	2,30
1448231_at	Fkbp5	FK506 binding protein 5	2,37
1426657_s_at	Phgdh	3-phosphoglycerate dehydrogenase	2,38
1430388_a_at	Sulf2	sulfatase 2	2,38
1452260_at	Cidec	cell death-inducing DFFA-like effector c	2,38
1460645_at	Chordc1	cysteine and histidine-rich domain (CHORD)-containing, zinc-binding protein 1	2,38
1416125_at	Fkbp5	FK506 binding protein 5	2,46
1416288_at	Dnaja1	DnaJ (Hsp40) homolog, subfamily A, member 1	2,46
1415965_at	Scd1	stearoyl-Coenzyme A desaturase 1	2,55
1421041_s_at	Gsta1 /// Gsta2	glutathione S-transferase, alpha 1 (Ya) /// glutathione S-transferase, alpha 2 (Yc2)	2,55
1426225_at	LOC100047573 /// Rbp4	retinol binding protein 4, plasma /// similar to retinol binding protein	2,55
1418847_at	Arg2	arginase type II	2,64
1423550_at	Slc1a4	solute carrier family 1 (glutamate/neutral amino acid transporter), member 4	2,64
1425952_a_at	Gcg	glucagon	2,64
1426268_at	C130090K23Rik	RIKEN cDNA C130090K23 gene	2,64
1448683_at	Cyp2d26	cytochrome P450, family 2, subfamily d, polypeptide 26	2,64
1455069_x_at	Slc25a4	solute carrier family 25 (mitochondrial carrier, adenine nucleotide translocator), member 4	2,64
1416021_a_at	Fabp5	fatty acid binding protein 5, epidermal	2,73
1425260_at	Alb	albumin	2,73
1434449_at	Aqp4	aquaporin 4	2,73
1455106_a_at	Ckb	creatine kinase, brain	2,73
1435943_at	Dpep1	dipeptidase 1 (renal)	2,82
1422966_a_at	Tfrc	transferrin receptor	2,93
1434897_a_at	Slc25a4	solute carrier family 25 (mitochondrial carrier, adenine nucleotide translocator), member 4	2,93

Table 16. List of all genes upregulated after UDCA treatment related to nontreated in normal mice

Affymetrix id	Gene name	Full name	Fold change
1423259_at	Id4	inhibitor of DNA binding 4	3,03
1452661_at	Tfrc	transferrin receptor	3,03
1453836_a_at	Mgll	monoglyceride lipase	3,03
1421178_at	Mgat4c	mannosyl (alpha-1,3-)-glycoprotein beta-1,4-N-acetylglucosaminyltransferase, isozyme C (putative)	3,14
1437405_a_at	Igfbp4	insulin-like growth factor binding protein 4	3,24
1416022_at	Fabp5	fatty acid binding protein 5, epidermal	3,25
1427137_at	Ces5	carboxylesterase 5	3,25
1418069_at	Apoc2	apolipoprotein C-II	3,36
1425137_a_at	H2-Q10	histocompatibility 2, Q region locus 10	3,36
1450391_a_at	Mgll	monoglyceride lipase	3,36
1416529_at	Emp1	epithelial membrane protein 1	3,60
1422967_a_at	Tfrc	transferrin receptor	3,60
1419431_at	Ereg	epiregulin	3,73
1428722_at	Ckmt2	creatine kinase, mitochondrial 2	3,86
1426785_s_at	Mgll	monoglyceride lipase	4,00
1419559_at	Cyp4f14	cytochrome P450, family 4, subfamily f, polypeptide 14	4,14
1425993_a_at	Hsp110	heat shock protein 110	4,14
1429994_s_at	Cyp2c65	cytochrome P450, family 2, subfamily c, polypeptide 65	4,60
1423566_a_at	Hsp110	heat shock protein 110	4,76
1448964_at	S100g	S100 calcium binding protein G	4,76
1416808_at	Nid1	nidogen 1	4,92
1417745_at	Cpn1	carboxypeptidase N, polypeptide 1	5,10
1438841_s_at	Arg2	arginase type II	5,46
1424439_at	1810065E05Rik	RIKEN cDNA 1810065E05 gene	5,66
1418438_at	Fabp2	fatty acid binding protein 2, intestinal	6,73
1418486_at	Vnn1	vanin 1	7,21
1448741_at	Slc3a1	solute carrier family 3, member 1	7,21
1448377_at	Slpi	secretory leukocyte peptidase inhibitor	10,19
1450645_at	Mt4	metallothionein 4	10,20
1450682_at	Fabp6	fatty acid binding protein 6, ileal (gastrotropin)	10,82
1418655_at	B4galnt1	beta-1,4-N-acetyl-galactosaminyl transferase 1	13,93
1417802_at	1110032A04Rik	RIKEN cDNA 1110032A04 gene	16,00
1419498_at	Tmigd1	transmembrane and immunoglobulin domain containing 1	22,63
1418368_at	Retnlb	resistin like beta	38,05

Table 17. List of all genes downregulated after UDCA treatment related to nontreated in normal mice

Affymetrix id	Gene name	Full name	Fold change
1418207_at	Fxyd4	FXYD domain-containing ion transport regulator 4	0,21
1435853_at	9030605E09Rik	RIKEN cDNA 9030605E09 gene	0,21
1421225_a_at	Slc4a4	solute carrier family 4 (anion exchanger), member 4	0,22
1425398_at	LOC665622 /// RP23-38E20.1	H2b histone family, member A /// histone pseudogene	0,23
1435906_x_at	Gbp2	guanylate nucleotide binding protein 2	0,23
1417522_at	Fbxo32	F-box protein 32	0,25
1418240_at	Gbp2	guanylate nucleotide binding protein 2	0,28
1417991_at	Dio1	deiodinase, iodothyronine, type I	0,3
1418131_at	Samhd1	SAM domain and HD domain, 1	0,31
1419393_at	Abcg5	ATP-binding cassette, sub-family G (WHITE), member 5	0,31
1425233_at	2210407C18Rik	RIKEN cDNA 2210407C18 gene	0,31
1449409_at	Sult1c2	sulfotransferase family, cytosolic, 1C, member 2	0,31
1419479_at	Sectm1b	secreted and transmembrane 1B	0,32
1428014_at	Hist1h4h	histone cluster 1, H4h	0,32
1417590_at	Cyp27a1	cytochrome P450, family 27, subfamily a, polypeptide 1	0,33
1419478_at	Sectm1b	secreted and transmembrane 1B	0,33
1427056_at	Adamts15	a disintegrin-like and metallopeptidase (reprolysin type) with thrombospondin type 1 motif, 15	0,33
1450032_at	Slco2a1	solute carrier organic anion transporter family, member 2a1	0,33
1423439_at	Pck1	phosphoenolpyruvate carboxykinase 1, cytosolic	0,34
1452071_at	Slc4a4	solute carrier family 4 (anion exchanger), member 4	0,34
1419089_at	Timp3	tissue inhibitor of metalloproteinase 3	0,35
1422644_at	LOC100045042 /// Sh3bgr	SH3-binding domain glutamic acid-rich protein /// similar to putative SH3BGR protein	0,37
1448747_at	Fbxo32	F-box protein 32	0,37
1418606_at	Hoxd10	homeo box D10	0,38
1448250_at	9030425E11Rik	RIKEN cDNA 9030425E11 gene	0,38
1451547_at	Iyd	iodotyrosine deiodinase	0,38
1451791_at	Tfpi	tissue factor pathway inhibitor	0,38
1416179_a_at	Rdx	radixin	0,39
1416180_a_at	Rdx	radixin	0,39
1435866_s_at	Hist3h2a	histone cluster 3, H2a	0,39
1449568_at	Klb	klotho beta	0,39
1417689_a_at	Pdzk1ip1	PDZK1 interacting protein 1	0,4
1423405_at	Timp4	tissue inhibitor of metalloproteinase 4	0,4
1424854_at	Hist1h4i	histone cluster 1, H4i	0,4

Table 17. List of all genes downregulated after UDCA treatment related to nontreated in normal mice

Affymetrix id	Gene name	Full name	Fold change
1427221_at	Xtrp3s1	X transporter protein 3 similar 1 gene	0,4
1448236_at	Rdx	radixin	0,4
1435865_at	Hist3h2a	histone cluster 3, H2a	0,41
1416783_at	Tac1	tachykinin 1	0,42
1419040_at	Cyp2d22	cytochrome P450, family 2, subfamily d, polypeptide 22	0,42
1421221_at	Bcdo2	beta-carotene 9', 10'-dioxygenase 2	0,42
1422948_s_at	Hist1h4a, b, c, h, i, j, k, m	histone cluster 1, H4a, b, c, h, i, j, k, m	0,42
1424917_a_at	Wipi1	WD repeat domain, phosphoinositide interacting 1	0,42
1433756_at	S100pbp	S100P binding protein	0,42
1451359_at	Aytl2	acyltransferase like 2	0,42
1455531_at	Mfsd4	major facilitator superfamily domain containing 4	0,42
1460242_at	Cd55	CD55 antigen	0,42
1417160_s_at	Expi	extracellular proteinase inhibitor	0,43
1428209_at	Bex4	brain expressed gene 4	0,43
1426715_s_at	Slc46a1	solute carrier family 46, member 1	0,44
1451793_at	Klhl24	kelch-like 24 (Drosophila)	0,44
1418762_at	Cd55	CD55 antigen	0,45
1423104_at	Irs1	insulin receptor substrate 1	0,45
1426880_at	Etl4	enhancer trap locus 4	0,45
1435697_a_at	Pscdbp	pleckstrin homology, Sec7 and coiled-coil domains, binding protein	0,45
1436021_at	Mfsd4	major facilitator superfamily domain containing 4	0,45
1438385_s_at	Gpt2	glutamic pyruvate transaminase (alanine aminotransferase) 2	0,45
1448595_a_at	Bex1	brain expressed gene 1	0,45
1451538_at	Sox9	SRY-box containing gene 9	0,45
1455007_s_at	Gpt2	glutamic pyruvate transaminase (alanine aminotransferase) 2	0,45
1455477_s_at	Pdzk1ip1	PDZK1 interacting protein 1	0,45
1416332_at	Cirbp	cold inducible RNA binding protein	0,47
1418219_at	Il15	interleukin 15	0,47
1426714_at	Slc46a1	solute carrier family 46, member 1	0,47
1438164_x_at	Flot2	flotillin 2	0,47
1450584_at	Hoxd11	homeo box D11	0,47
1452492_a_at	Slc37a2	solute carrier family 37 (glycerol-3-phosphate transporter), member 2	0,47
1454930_at	Tbcel	tubulin folding cofactor E-like	0,47
1416723_at	Tcf4	transcription factor 4	0,48

Table 17. List of all genes downregulated after UDCA treatment related to nontreated in normal mice

Affymetrix id	Gene name	Full name	Fold change
1419656_at	Slc25a36	solute carrier family 25, member 36	0,48
1420993_at	B3gnt5	UDP-GlcNAc:betaGal beta-1,3-N - acetylglucosaminyltransferase 5	0,48
1422837_at	Scel	sciellin	0,48
1426951_at	Crim1	cysteine rich transmembrane BMP regulator 1 (chordin like)	0,48
1427008_at	Rnf43	ring finger protein 43	0,48
1438982_s_at	Flywch2	FLYWCH family member 2	0,48
1449459_s_at	Asb13	ankyrin repeat and SOCS box-containing protein 13	0,48
1449591_at	Casp4 /// LOC100044206	caspase 4, apoptosis-related cysteine peptidase /// hypothetical protein LOC100044206	0,48
1455065_x_at	EG667410 /// Gnpda1	glucosamine-6-phosphate deaminase 1 /// predicted gene, EG667410	0,48
1460203_at	Itpr1	inositol 1,4,5-triphosphate receptor 1	0,48
1417279_at	Itpr1	inositol 1,4,5-triphosphate receptor 1	0,5
1418014_a_at	B4galt1	UDP-Gal:betaGlcNAc beta 1,4- galactosyltransferase, polypeptide 1	0,5
1418394_a_at	Cd97	CD97 antigen	0,5
1419636_at	4833420G17Rik	RIKEN cDNA 4833420G17 gene	0,5
1419657_a_at	Slc25a36	solute carrier family 25, member 36	0,5
1426574_a_at	Add3	adducin 3 (gamma)	0,5
1426624_a_at	Ypel3	yippee-like 3 (Drosophila)	0,5
1428004_at	3300001G02Rik	RIKEN cDNA 3300001G02 gene	0,5
1429086_at	Grhl2	grainyhead-like 2 (Drosophila)	0,5
1429514_at	Ppap2b	phosphatidic acid phosphatase type 2B	0,5
1434372_at	AW112010	expressed sequence AW112010	0,5
1434776_at	Sema5a	sema domain, seven thrombospondin repeats (type 1 and type 1-like), transmembrane domain (TM) and short cytoplasmic domain, (semaphorin) 5A	0,5
1449187_at	Pdgfa	platelet derived growth factor, alpha	0,5
1451320_at	3110043J09Rik	RIKEN cDNA 3110043J09 gene	0,5
1451400_at	Gemin8	gem (nuclear organelle) associated protein 8	0,5
1452398_at	Plce1	phospholipase C, epsilon 1	0,5
1418149_at	Chga	chromogranin A	0,51
1415793_at	Pnpo	pyridoxine 5'-phosphate oxidase	0,52
1417962_s_at	Ghr	growth hormone receptor	0,52
1418366_at	Hist1h2ad, an, aa, h2aa2, 2ac	histone cluster 1h2ad, an, aa, h2aa2, 2ac	0,52
1418367_x_at	Hist1h2ad, an, aa, h2aa2, 2ac	histone cluster 1h2ad, an, aa, h2aa2, 2ac	0,52
1418780_at	Cyp39a1	cytochrome P450, family 39, subfamily a, polypeptide 1	0,52
1420961_a_at	Ivns1abp	influenza virus NS1A binding protein	0,52
1420973_at	Arid5b /// LOC100044968	AT rich interactive domain 5B (Mrf1 like) /// similar to modulator recognition factor 2	0,52
1421355_at	Tgm3	transglutaminase 3, E polypeptide	0,52

Table 17. List of all genes downregulated after UDCA treatment related to nontreated in normal mice

Affymetrix id	Gene name	Full name	Fold change
1421735_a_at	St8sia5	ST8 alpha-N-acetyl-neuraminide alpha-2,8-sialyltransferase 5	0,52
1425606_at	Slc5a8	solute carrier family 5 (iodide transporter), member 8	0,52
1448005_at	Sash1	SAM and SH3 domain containing 1	0,52
1448656_at	Cacnb3	calcium channel, voltage-dependent, beta 3 subunit	0,52
1451739_at	Klf5	Kruppel-like factor 5	0,52
1452870_at	Apaf1	apoptotic peptidase activating factor 1	0,52
1417196_s_at	Wwc2	WW, C2 and coiled-coil domain containing 2	0,53
1415935_at	Smoc2	SPARC related modular calcium binding 2	0,54
1417694_at	Gab1	growth factor receptor bound protein 2-associated protein 1	0,54
1418749_at	Psd3	pleckstrin and Sec7 domain containing 3	0,54
1420762_a_at	LOC100045903 /// Ybx2	Y box protein 2 /// similar to Y box protein 2	0,54
1426571_at	Tmem16a	transmembrane protein 16A	0,54
1433670_at	Emp2	epithelial membrane protein 2	0,54
1449109_at	Socs2	suppressor of cytokine signaling 2	0,54
1450344_a_at	Ptger3	prostaglandin E receptor 3 (subtype EP3)	0,54
1460367_at	Hbp1	high mobility group box transcription factor 1	0,54
1416724_x_at	Tcf4	transcription factor 4	0,55
1419039_at	Cyp2d22	cytochrome P450, family 2, subfamily d, polypeptide 22	0,55
1420747_at	LOC100044198 /// Ppnr	per-pentamer repeat gene /// hypothetical protein LOC100044198	0,55
1423635_at	Bmp2	bone morphogenetic protein 2	0,55
1424468_s_at	Phldb1	pleckstrin homology-like domain, family B, member 1	0,55
1426501_a_at	T2bp	Traf2 binding protein	0,55
1427050_at	5730420B22Rik	RIKEN cDNA 5730420B22 gene	0,55
1427345_a_at	Sult1a1	sulfotransferase family 1A, phenol-preferring, member 1	0,55
1427982_s_at	Syne2	synaptic nuclear envelope 2	0,55
1431182_at	Hspa8	heat shock protein 8	0,55
1434856_at	Ankrd44	ankyrin repeat domain 44	0,55
1438700_at	Fnbp4	formin binding protein 4	0,55
1448241_at	Gm2a	GM2 ganglioside activator protein	0,55
1449439_at	Klf7	Kruppel-like factor 7 (ubiquitous)	0,55
1450971_at	Gadd45b	growth arrest and DNA-damage-inducible 45 beta	0,55
1415803_at	Cx3cl1	chemokine (C-X3-C motif) ligand 1	0,57
1417066_at	Cabc1	chaperone, ABC1 activity of bc1 complex like (S. pombe)	0,57
1417686_at	Lgals12	lectin, galactose binding, soluble 12	0,57
1418507_s_at	Socs2	suppressor of cytokine signaling 2	0,57

Table 17. List of all genes downregulated after UDCA treatment related to nontreated in normal mice

Affymetrix id	Gene name	Full name	Fold change
1418748_at	Casp14	caspase 14	0,57
1423298_at	Add3	adducin 3 (gamma)	0,57
1424089_a_at	Tcf4	transcription factor 4	0,57
1424988_at	Mylip	myosin regulatory light chain interacting protein	0,57
1426799_at	Rab8b	RAB8B, member RAS oncogene family	0,57
1428289_at	Klf9	Kruppel-like factor 9	0,57
1429367_at	Wipi2	WD repeat domain, phosphoinositide interacting 2	0,57
1434149_at	Tcf4	transcription factor 4	0,57
1448145_at	Wwp2	WW domain containing E3 ubiquitin protein ligase 2	0,57
1449464_at	Kcnq1 /// LOC100044122	potassium voltage-gated channel, subfamily Q, member 1 /// similar to Potassium voltage-gated channel, subfamily Q, member 1	0,57
1450337_a_at	Nek8	NIMA (never in mitosis gene a)-related expressed kinase 8	0,57
1452148_at	Lrpap1	low density lipoprotein receptor-related protein associated protein 1	0,57
1455899_x_at	Socs3	suppressor of cytokine signaling 3	0,57
1460725_at	Xpa	xeroderma pigmentosum, complementation group A	0,57
1417848_at	Zfp704	zinc finger protein 704	0,59
1419033_at	2610018G03Rik	RIKEN cDNA 2610018G03 gene	0,59
1424351_at	Wfdc2	WAP four-disulfide core domain 2	0,59
1424544_at	Nrbp2	nuclear receptor binding protein 2	0,59
1424919_at	Erbb2	v-erb-b2 erythroblastic leukemia viral oncogene homolog 2, neuro/glioblastoma derived oncogene homolog (avian)	0,59
1425559_a_at	Acsm3	acyl-CoA synthetase medium-chain family member 3	0,59
1427915_s_at	LOC100045866 /// Tceb1	transcription elongation factor B (SIII), polypeptide 1 /// similar to elongation factor SIII p15 subunit	0,59
1428029_a_at	H2afv	H2A histone family, member V	0,59
1431055_a_at	Snx10	sorting nexin 10	0,59
1434148_at	Tcf4	transcription factor 4	0,59
1435221_at	---	Adult male corpora quadrigemina cDNA, RIKEN full-length enriched library, clone:B230341P20 product:inferred: forkhead box P1, full insert sequence	0,59
1437917_at	D530037H12Rik	RIKEN cDNA D530037H12 gene	0,59
1448409_at	Lrmp	lymphoid-restricted membrane protein	0,59
1448926_at	Hoxa5	homeo box A5	0,59
1450816_at	Polg2	polymerase (DNA directed), gamma 2, accessory subunit	0,59
1451526_at	Arhgap12	Rho GTPase activating protein 12	0,59
1452400_a_at	Hoxa11os	homeo box A11, opposite strand transcript	0,59
1415973_at	Marcks	myristoylated alanine rich protein kinase C substrate	0,6
1418265_s_at	Irf2	interferon regulatory factor 2	0,6
1422706_at	Tmepai	transmembrane, prostate androgen induced RNA	0,6
1417932_at	Il18	interleukin 18	0,61

Table 17. List of all genes downregulated after UDCA treatment related to nontreated in normal mice

Affymetrix id	Gene name	Full name	Fold change
1417971_at	Nrm	nurim (nuclear envelope membrane protein)	0,61
1421392_a_at	Birc3	baculoviral IAP repeat-containing 3	0,62
1421402_at	Mta3	metastasis associated 3	0,62
1422735_at	Foxq1	forkhead box Q1	0,62
1427318_s_at	Dysf /// Fer1l3	dysferlin /// fer-1-like 3, myoferlin (C. elegans)	0,62
1429173_at	Dnase1l1	deoxyribonuclease 1-like 1	0,62
1430527_a_at	Rnf167	ring finger protein 167	0,62
1436030_at	LOC100047857	similar to Cache domain containing 1	0,62
1437103_at	Igf2bp2	insulin-like growth factor 2 mRNA binding protein 2	0,62
1450881_s_at	Gpr137b	G protein-coupled receptor 137B	0,62
1450933_at	Pde7a	phosphodiesterase 7A	0,62
1451075_s_at	Ctdsp2	CTD (carboxy-terminal domain, RNA polymerase II, polypeptide A) small phosphatase 2	0,62
1456700_x_at	Marcks	myristoylated alanine rich protein kinase C substrate	0,62
1416274_at	Ctns	cystinosis, nephropathic	0,64
1418401_a_at	Dusp16	dual specificity phosphatase 16	0,64
1418501_a_at	Oxr1	oxidation resistance 1	0,64
1418581_a_at	Limk2	LIM motif-containing protein kinase 2	0,64
1419457_at	Rgnef	Rho-guanine nucleotide exchange factor	0,64
1421841_at	Fgfr3	fibroblast growth factor receptor 3	0,64
1429159_at	Itih5	inter-alpha (globulin) inhibitor H5	0,64
1433999_at	Slk	STE20-like kinase (yeast)	0,64
1434606_at	Erbb3	v-erb-b2 erythroblastic leukemia viral oncogene homolog 3 (avian)	0,64
1436031_at	Cachd1 /// LOC100047857	cache domain containing 1 /// similar to Cache domain containing 1	0,64
1438050_x_at	EG668383	predicted gene, EG668383	0,64
1448227_at	Grb7	growth factor receptor bound protein 7	0,64
1448335_s_at	Ccni	cyclin I	0,64
1448436_a_at	Irf1	interferon regulatory factor 1	0,64
1450044_at	Fzd7	frizzled homolog 7 (Drosophila)	0,64
1450223_at	Apaf1	apoptotic peptidase activating factor 1	0,64
1421088_at	Gpc4	glypican 4	0,66
1434931_at	Neo1	neogenin	0,66
1451687_a_at	Tcf2	transcription factor 2	0,66
1452060_a_at	Limk2	LIM motif-containing protein kinase 2	0,66

14 Curriculum Vitae

"For reasons of data protection, the Curriculum Vitae is not included in the online version"

15 Publications

Papers

S. Krishna-Subramanian, M.L. Hanski, C. Loddenkemper, B. Choudhary, B. Jebautzke, M. Zeitz, C. Hanski. *UDCA slows down intestinal cell proliferation by inducing high and sustained ERK phosphorylations*. **Submitted to Oncogene.**

R. Peiró-Jordán, S. Krishna-Subramanian, M.L. Hanski, J. Behrens, M. Zeitz, C. Hanski. *UDCA inhibits colon cancer cell proliferation by inhibiting cMyc expression.* **Manuscript in preparation.**

Posters

R. Peiró-Jordán, S. Krishna-Subramanian, M.L. Hanski, J. Behrens, M. Zeitz, C. Hanski. *Effects of Ursodeoxycholic acid treatment on colon cancer cell proliferation*. Falk Workshop: Mechanisms of Intestinal Inflammation (Dresden, 2007)

R. Peiró-Jordán, S. Krishna-Subramanian, M.L. Hanski, J. Behrens, M. Zeitz, C. Hanski. *Proliferation inhibition of colon cancer cells by UDCA: cellular response mechanisms*. Onkologie 2008; 31 (suppl.1) : 84

R. Peiró-Jordán, S. Krishna-Subramanian, M.L. Hanski, J. Behrens, M. Zeitz, C. Hanski. *UDCA targets S-phase and suppresses CDK2 and cyclin A expression: effects on colon cancer cell proliferation*. Z.Gastroenterol 2008; 46: 971

S. Krishna-Subramanian, C.Loddenkemper, M.L. Hanski, M. Zeitz, C. Hanski. *Ursodeoxycholic acid (UDCA) decreases the proliferation of normal intestinal epithelial cells in vivo and in vitro*. European Journal of Cancer Supplements 2008; 6: 38

S. Krishna-Subramanian, C.Loddenkemper, M.L. Hanski, M. Zeitz, C. Hanski. *Ursodeoxycholic acid inhibits proliferation of intestinal epithelial cells: role of EGF and ERK pathway*. European Journal of Cancer Supplements 2009; 7: 359

S. Krishna-Subramanian, C.Loddenkemper, M.L. Hanski, M. Zeitz, C. Hanski. *Ursodeoxycholic acid suppresses the transcription of genes responsible for proliferation in the normal intestinal epithelial cells in vivo and in vitro*. Z.Gastroenterol 2009; 47: 982

S. Krishna-Subramanian, B.Choudhary, M.L. Hanski, M. Zeitz, C. Hanski. *EGF and IGF-1 pathways are targeted by the chemopreventive agent ursodeoxycholic acid*. Onkologie 2010; 33(suppl.2): 39

S. Krishna-Subramanian, M.L. Hanski, M. Zeitz, C. Hanski. *High and persistent ERK phosphorylation induced by Ursodeoxycholic acid inhibits proliferation of intestinal epithelial cells*. European Journal of Cancer Supplements 2010; 8: 223

S. Krishna-Subramanian, M.L. Hanski, M. Zeitz, C. Hanski. *EGF-IGF-1 signal cross-talk: ERK regulates Irs-1 transcription*. Z.Gastroenterol 2010; 48 : 982